

การออกแบบรูปร่างพัลส์ที่เหมาะสมที่สุดสำหรับระบบอัลตราไวด์แบนด์ซึ่งมีโหม่งจิตเตอร์



นางสาววิไลพร แซ่ลี

สถาบันวิทยบริการ

จุฬาลงกรณ์มหาวิทยาลัย

วิทยานิพนธ์นี้เป็นส่วนหนึ่งของการศึกษาตามหลักสูตรปริญญาวิศวกรรมศาสตรดุษฎีบัณฑิต

สาขาวิชาวิศวกรรมไฟฟ้า ภาควิชาวิศวกรรมไฟฟ้า

คณะวิศวกรรมศาสตร์ จุฬาลงกรณ์มหาวิทยาลัย

ปีการศึกษา 2550

ลิขสิทธิ์ของจุฬาลงกรณ์มหาวิทยาลัย

AN OPTIMUM PULSE SHAPE DESIGN FOR ULTRA-WIDEBAND SYSTEMS WITH
TIMING JITTER

Miss Wilaiporn Lee

A Dissertation Submitted in Partial Fulfillment of the Requirements
for the Degree of Doctor of Philosophy Program in Electrical Engineering

Department of Electrical Engineering

Faculty of Engineering

Chulalongkorn University

Academic Year 2007

Copyright of Chulalongkorn University

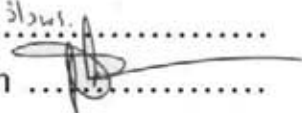
วิไลพร แซ่ลี: การออกแบบรูปร่างพัลส์ที่เหมาะสมที่สุดสำหรับระบบอัลตราไวด์แบนด์ซึ่งมี
 ไทมิงจิตเตอร์ (AN OPTIMUM PULSE SHAPE DESIGN FOR ULTRA-WIDEBAND
 SYSTEMS WITH TIMING JITTER) อ. ที่ปรึกษา: รศ. ดร.สมชาย จิตะพันธ์กุล,
 93 หน้า

อัลตราไวด์แบนด์ (ยูดับบิวบี) เป็นเทคโนโลยีใหม่ที่เสนอเพื่อแก้ไขปัญหาการขาดแคลน
 สเปกตรัมของสัญญาณวิทยุที่มีในปัจจุบัน โดยได้รับอนุญาตให้ใช้งานสเปกตรัมร่วมกับระบบ
 สัญญาณเดิม ก่อให้เกิดการรบกวนน้อยที่สุดหรือไม่เกิดการรบกวนเลย ปัญหาสำคัญ 2 ประการ
 ที่จะส่งผลกระทบต่อความสำเร็จในการสื่อสารระบบยูดับบิวบีคือ กำลังของพัลส์ส่งและผลของ
 ไทมิงจิตเตอร์ ตั้งแต่ปีค.ศ. 2002 ที่คณะกรรมการสื่อสารแห่งสหรัฐอเมริกา (เอฟซีซี) กำหนด
 ค่ามาตรฐานของกำลังแผ่ประสิทธิผลไอโซทรอปิก (อีไออาร์พี) สำหรับระบบยูดับบิวบี ปัญหา
 เรื่องรูปร่างสเปกตรัมของระบบยูดับบิวบีได้กลายเป็นปัญหาแฉกหน้าของงานวิจัย การรบกวน
 ของกำลังของพัลส์ส่งในช่วงความถี่เดียวกันต่อและจากระบบที่มีอยู่เดิม อาจจะมีผลต่อขีดของ
 ระบบยูดับบิวบีลง ปัญหาสำคัญอีกอย่างของระบบยูดับบิวบีคือ ผลของไทมิงจิตเตอร์ซึ่งเกิด
 จากความไม่เป็นอุดมคติของนาฬิกาในการสุ่มตัวอย่างของเครื่องรับที่มีอยู่ในปัจจุบัน ปัญหา
 ที่เกิดขึ้นนี้ส่งผลกระทบต่อความสัมพันธ์ของสัญญาณที่เครื่องรับและยังส่งผลกระทบต่อความสามารถในการ
 ตรวจจับสัญญาณของระบบยูดับบิวบี เนื่องจากความกว้างของยูดับบิวบีพัลส์สั้นมาก ความผิด
 พลาดทางเวลาเพียงเล็กน้อยสามารถส่งผลกระทบรุนแรงต่อประสิทธิภาพของเครื่องรับได้

ในวิทยานิพนธ์ฉบับนี้เสนอ เทคนิคใหม่ในการออกแบบพัลส์ที่เหมาะสมที่สุดสำหรับระบบ
 ยูดับบิวบีภายใต้การเกิดไทมิงจิตเตอร์ พัลส์ที่น่าเสนอมีพลังงานมากกว่าระดับสัญญาณรบกวน
 พื้นฐานและมีความทนทานต่อไทมิงจิตเตอร์ด้วย โดยพลังของพัลส์ที่น่าเสนอนี้ยังมีค่าพอดีกับ
 สเปกตรัมมาร์คสำหรับข้อจำกัดภายในอาคารของเอฟซีซี วิทยานิพนธ์ฉบับนี้ยังมีการนำเสนอ
 ค่าพารามิเตอร์ที่ใช้สำหรับกระบวนการออกแบบที่เหมาะสมที่สุดด้วย นอกจากนี้วิทยานิพนธ์ฉบับ
 นี้ได้นำเสนอการออกแบบพัลส์ที่ตั้งฉากกันเพื่อปรับปรุงความจุของระบบยูดับบิวบี การออก
 แบบพัลส์ที่ตั้งฉากกันนี้อยู่บนพื้นฐานของพัลส์ที่เหมาะสมที่สุด ดังนั้นทุกพัลส์ที่ตั้งฉากกันจะมี
 คุณสมบัติเหมือนกับคุณสมบัติของพัลส์ที่เหมาะสมที่สุดคือ ความหนาแน่นสเปกตรัมของพัลส์ที่
 ตั้งฉากกันนี้จะมีค่าตามสเปกตรัมมาร์คของเอฟซีซีและทนทานต่อไทมิงจิตเตอร์ นอกจากนี้
 แต่ละพัลส์ที่ตั้งฉากมีคุณสมบัติของความตั้งฉากซึ่งกันและกันด้วย

ผลการจำลองระบบแสดงให้เห็นถึงคุณประโยชน์หลายประการของพัลส์ที่น่าเสนอที่เหนือ
 กว่าพัลส์อื่นที่เสนอมาก่อนหน้า จากผลการจำลองระบบค่าผิดพลาดบิตน้อยที่สุดได้รับจากพัลส์
 ที่เหมาะสมที่สุดที่น่าเสนอเมื่อเกิดการผิดพลาดของไทมิงจิตเตอร์ที่อุณหภูมิห้อง สำหรับพัลส์ที่ตั้ง
 ฉากผลการทดลองได้ยืนยันคุณสมบัติการตั้งฉากซึ่งกันและกันของพัลส์ที่น่าเสนอและแสดงให้เห็น
 เห็นข้อดีของพัลส์ที่น่าเสนอดีกว่าพัลส์ยูดับบิวบีอื่นที่เสนอก่อนหน้า

ภาควิชา วิศวกรรมไฟฟ้า
 สาขาวิชา วิศวกรรมไฟฟ้า
 ปีการศึกษา 2550

ลายมือชื่อนิสิต 31001
 ลายมือชื่ออาจารย์ที่ปรึกษา 

##4871826621: MAJOR ELECTRICAL ENGINEERING

KEY WORD: UWB / Pulse shape design / FCC spectral masks / Timing jitter

WILAIORN LEE: AN OPTIMUM PULSE SHAPE DESIGN FOR ULTRA-WIDEBAND SYSTEMS WITH TIMING JITTER, THESIS ADVISOR: ASSOC. PROF. SOMCHAI JITAPUNKUL, Dr.Ing., 93 pp.

Ultra-wideband (UWB) technology offers a promising solution to the radio frequency (RF) spectrum drought by allowing new services to coexist with current radio systems with minimal or no interference. Two crucial keys to communications success of UWB systems are pulse transmission power and timing jitter effects. Since the Federal Communications Commission (FCC) published its standard for the limitation of effective isotropic radiation power (EIRP) for UWB systems in 2002, the problem of spectrum shaping for UWB systems came to the forefront of scientific discourse. The interference of pulse transmission power to and from existing systems operating over the same frequency may reduce the advantages of UWB systems. On the other hand, timing jitter which results from the presence of non-ideal sampling clocks in practical receivers causes distortion. This distortion affects the correlation of signals at the receiver and thereby reducing the signal detection ability of UWB systems. This is a serious problem because the UWB pulse duration is very short so only small timing misalignment can severely affect the performance of a correlation detector.

This dissertation presents a novel technique in designing the optimum pulse shape for UWB systems under the presence of timing jitter. The proposed pulse attains the adequate power to survive the noise floor and simultaneously provides good resistance to timing jitter. It also meets the power spectral mask restriction as prescribed by the FCC for indoor UWB systems. In addition, parameters of the proposed optimization algorithm are also investigated. Moreover, this study proposes a novel design of orthogonal pulses to improve the capacity of UWB systems. This orthogonal pulse design is based on the optimum pulse we propose. Therefore, all of the orthogonal pulses now have the same properties as the optimum proposed pulse. These properties include power spectral density (PSD) that meets the FCC spectral masks and simultaneously resists timing jitter. Additionally, each of the orthogonal pulses is mutually orthogonal to other pulses.

The simulation results have demonstrated several relevant merits of the optimum proposed pulse over the previously known pulses, namely the lowest bit error rate (BER) of the optimum proposed pulse is achieved in the system with the imperfect timing jitter at room temperature. For the orthogonal pulses, the simulation results confirm the orthogonality properties of the orthogonal proposed pulses and show the advantages of the novel design over others.

Department Electrical Engineering
 Field of study Electrical Engineering
 Academic year 2007

Student's signature Wilaiorn Lee

Advisor's signature Somchai Jitapunkul

Acknowledgements

This work contained in this dissertation represents the accumulation of three years of work made possible only by the collective support of family, friends, colleagues and mentors.

First and foremost, I would like to express my sincere gratitude to my advisor, Assoc. Prof. Dr. Somchai Jitapunkul who led me to this field and inspired my interest, for his support and inviable trust on my capabilities, especially at the difficult times. Without him, the goal could not have been achieved today.

My thanks also to the members of my dissertation committees, Assist. Prof. Dr. Chedsada Chinrungrueng, Assoc. Prof. Dr. Watit Benjapolkul, Assist. Prof. Dr. Nisachon Tangsangiumvisai, and Assist. Prof. Dr. Peerapol Yuvapoositanon for their suggestions and invaluable comments.

I would also like to thanks to Dr. Sangrawee Chaopricha for comprehensive reviews on my dissertation document, the Faculty Development Scholarship Program in Engineering with the Collaboration of AUN/SEED-Net and Cooperation Project between Department of Electrical Engineering and Private Sector for Research and Development.

Many thanks to Dr. Suwich Kunaruttanapruk for their very helpful comments on various aspects of my work and my all colleagues at DSPRL (Digital Signal Processing Research Laboratory) for academic documentary help, technical/theory information and programming/data information.

Finally, my life has been constantly fulfilled by love and support of my family. I am extremely grateful to my parents, Ngeg-hoh Lee, Hung-tiang Lee, for their love, caring and sacrifices, my father and mother for educating and preparing me for my future life since I was a kid, and my sister, Pehnwilai Lee, and my brothers, Sirhichai Lee and Suracharn Lee, for their love, caring and sacrifices. This work is dedicated to them.

Table of Contents

	Page
Abstract in Thai.....	iv
Abstract in English.....	v
Acknowledgements.....	vi
Table of Contents.....	vii
List of Tables.....	ix
List of Figures.....	x
Chapter	
I Introduction.....	1
1.1 Definition of UWB Systems.....	1
1.2 Development of UWB Systems.....	2
1.3 Literature Review.....	3
1.4 Objectives.....	9
1.5 Scope.....	9
1.6 Outline.....	10
II Basic Background and Related Topics.....	11
2.1 UWB Transmitters.....	11
2.1.1 UWB Modulation Schemes.....	12
2.1.1.1 On-Off Keying.....	12
2.1.1.2 Pulse-Amplitude Modulation.....	13
2.1.1.3 Pulse-Position Modulation.....	15
2.1.1.4 Biphase Modulation.....	16
2.1.1.5 Summary of UWB Modulation Methods.....	17
2.1.2 UWB Multiple Access Techniques.....	18
2.2 UWB Channel Models.....	20
2.3 UWB Receivers.....	24
2.3.1 RAKE Receivers.....	25
2.3.2 Transmit-reference Receivers.....	26
III UWB Pulse Shape Design.....	28
3.1 UWB Regulations.....	28
3.2 Gaussian Pulses.....	29
3.3 System Model.....	31
3.4 Relationship between the Autocorrelation and a PSD.....	34
3.5 Pulse Shape Optimization.....	36
3.6 Orthogonal Pulse Shape.....	39

Chapter	Page
IV The Experimental Results	41
4.1 Simulation Configuration	41
4.2 Effects of Timing Jitter on the Gaussian Derivative Pulses	41
4.3 Examples of the UWB Pulses Meeting the FCC Spectral Masks	45
4.3.1 The Scaled Monocycle Pulse	45
4.3.2 The Power Optimized Pulse	46
4.3.3 Optimum Pulse Shape Design	46
4.3.4 Parameters of the Proposed Pulse	52
4.4 Effects of Timing Jitter on the UWB Pulses Meeting the FCC Spectral Masks	55
4.4.1 RAKE Receivers	55
4.4.2 Transmitted-reference (TR) Receiver	60
4.5 The Orthogonal Pulses Design with Timing Jitter	65
4.6 Summary	75
V The Conclusions	77
5.1 Future Works	80
References	81
Appendices	90
Appendix A	91
Appendix B	92
Vitae	93

List of Tables

Table	Page
2.1 Advantages and disadvantages of the various modulation methods.	17
2.2 Parameter Settings for IEEE UWB Channel Models.	21
4.1 Comparisons of the mean correlation output (φ)	46
4.2 Summary of the BER comparison at room temperature.	76



สถาบันวิทยบริการ
จุฬาลงกรณ์มหาวิทยาลัย

List of Figures

Figure	Page
1.1 Narrowband versus UWB system	2
2.1 A general UWB transmitter block diagram.	12
2.2 On-off keying modulation	13
2.3 Pulse-amplitude modulation	14
2.4 Discrete spectral lines of periodic pulses	14
2.5 Pulse-position modulation	15
2.6 Smooth spectrum of PN time offsets	16
2.7 Biphase modulation	16
2.8 TH-PPM Modulation Examples	18
2.9 DS-BPAM Modulation Example	19
2.10 Impulse response of (a) CM1 (b) CM2	22
2.11 Impulse response of (a) CM3 (b) CM4	23
2.12 A general UWB receiver block diagram.	24
2.13 Block diagram of a typical RAKE receiver structure.	25
2.14 Block diagram of a transmit-reference system.	26
3.1 FCC spectral masks for indoor communications.	29
3.2 A Gaussian pulse, monocycle pulse, and doublet pulse in time domain.	30
3.3 A Gaussian pulse, monocycle pulse, and doublet pulse in frequency domain.	30
3.4 The desirable autocorrelation pulse and its corresponding PSD.	34
3.5 The desirable PSD pulse and its corresponding PSD.	34
3.6 BER versus Correlation output.	35
3.7 The UWB pulse design by the digital FIR filter.	36
4.1 Three Gaussian derivative pulses.	42
4.2 BER of binary PAM with different derivative Gaussian and timing error in AWGN.	43
4.3 BER of binary PAM with different derivative Gaussian and timing error in multipath channel.	43
4.4 BER of optimal PPM with different derivative Gaussian and timing error in AWGN.	44
4.5 BER of optimal PPM with different derivative Gaussian and timing error in multipath channel.	44
4.6 The scaled monocycle pulse and its PSD.	47
4.7 The autocorrelation of the scaled monocycle pulse.	47
4.8 The power optimized pulse and its PSD.	48
4.9 The autocorrelation of the power optimized pulse.	48
4.10 The scaled monocycle pulse compares with timing jitter PDF.	49
4.11 The proposed pulse and its PSD.	50
4.12 The autocorrelation of the proposed pulse.	50
4.13 Japan's preliminary UWB emission mask for indoor.	51
4.14 Europe's draft UWB emission mask.	51
4.15 The autocorrelation and the corresponding PSD of the proposed pulses that are generated with various WFNC values.	53

Figure	Page
4.16 The total pulse power of the proposed pulses versus the WFNC values.	54
4.17 BER versus the WFNC values.	54
4.18 BER comparison in a system with and without timing jitter (10 m Tx-Rx separation).	57
4.19 BER versus the jitter variance.	57
4.20 BER comparison in a system with and without timing jitter in AWGN channel (4 m Tx-Rx separation).	59
4.21 BER comparison in a system with and without timing jitter in CM2 channel (4 m Tx-Rx separation).	59
4.22 Placement of reference pulse in transmitted-reference receiver.	60
4.23 The BER of the STR receiver in AWGN channel.	62
4.24 The BER of the STR receiver in CM2 channel.	62
4.25 The BER of the ATR receiver in AWGN channel.	63
4.26 The BER of the ATR receiver in CM2 channel.	63
4.27 The BER of the R-ATR receiver in AWGN channel.	64
4.28 The BER of the R-ATR receiver in CM2 channel.	64
4.29 The 2 nd orthogonal pulse and its PSD.	66
4.30 The autocorrelation of the 2 nd orthogonal pulse.	66
4.31 The 3 rd orthogonal pulse and its PSD.	67
4.32 The autocorrelation of the 3 rd orthogonal pulse.	67
4.33 The 4 th orthogonal pulse and its PSD.	68
4.34 The autocorrelation of the 4 th orthogonal pulse.	68
4.35 The cross-correlation between the 1 st orthogonal pulse and the other pulses. .	69
4.36 The cross-correlation between the 2 nd orthogonal pulse and the other pulses. .	70
4.37 The cross-correlation between the 3 rd orthogonal pulse and the other pulses. .	71
4.38 The cross-correlation between the 4 th orthogonal pulse and the other pulses. .	72
4.39 The BER comparison of the four orthogonal pulses without timing jitter in AWGN channel.	73
4.40 The BER comparison of the four orthogonal pulses with timing jitter in AWGN channel.	74
5.1 The block diagram of two proposed techniques.	79

CHAPTER I

INTRODUCTION

The recent rapid growth in technology and the successful commercial deployment of wireless communications are significantly affecting our daily lives. As the demand for higher capacity, faster service, and more secure wireless connections increases, new enhanced technologies have to find their place in the overcrowded and scarce radio frequency (RF) spectrum. This is because every radio technology allocates a specific part of the spectrum; for example, the signals for TVs, radios, cell phones, and so on are sent on different frequencies to avoid interference to each other. As a result, the constraints on the availability of the RF spectrum become stricter with the introduction of new radio services. Ultra-wideband (UWB) technology offers a promising solution to the RF spectrum drought by allowing new services to coexist with current radio systems with minimal or no interference. This coexistence brings the advantage of avoiding the expensive spectrum licensing fees that providers of all other radio services must pay.

1.1 Definition of UWB Systems

UWB technology has become one of the fast growing research topics since the FCC approved in 2002 [1]. Currently, UWB technology is a promising candidate for the physical layer of the upcoming short range wireless network. UWB is used to refer to signal occupy fractional bandwidth greater than 20 % of the center frequency or more than 500 MHz of bandwidth in the 7.5 GHz band of spectrum between 3.1 GHz and 10.6 GHz. On the contrary, narrowband signals have fractional bandwidth less than 1 % of the center frequency.

The fractional bandwidth (FB) is defined as

$$FB = \frac{2(f_H - f_L)}{(f_H + f_L)} \quad (1.1)$$

where f_H and f_L are the upper and lower frequencies, respectively, measured at -10 dB below the peak emission point as shown in Figure 1.1.

The types of UWB signals can be categorized into two main categories: single band or impulse radio UWB (IR-UWB) [2–5] and multi-band or multicarrier UWB (MC-UWB) [6]. The IR-UWB systems are based on a very short pulse, which occupies a very broad bandwidth. Unlike conventional wireless communications systems, those are carrier based; UWB systems transmit information without translating it to a higher carrier frequency. This carrierless technique will greatly reduce the complexity and cost

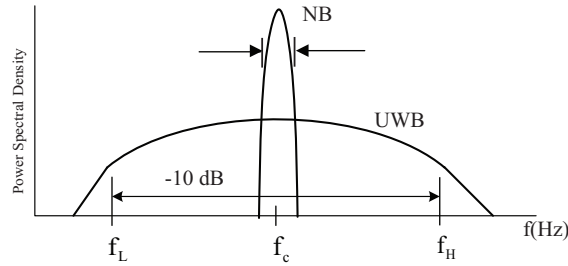


Figure 1.1 Narrowband versus UWB system

of the transceiver. On the other hand, the MC-UWB systems were based on multicarrier communications. The multicarrier techniques were first used in the late 1950s and early 1960s for higher data rate High frequency (HF) military communications. Since that time, orthogonal frequency division multiplexing (OFDM) has emerged as a special case of multicarrier modulation. OFDM is a multicarrier modulation with the minimum carrier spacing [7, 8]. OFDM subcarriers are separated apart by the reciprocal of the symbol duration. Spectra of each subcarrier are mutually overlapping. Therefore, higher spectral efficiency, compared with the conventional single carrier transmission, can be obtained from OFDM. Even though, OFDM techniques of multicarrier modulation can also satisfy the wide bandwidth requirement, the impulse based UWB systems remain the strong competence due to its simplicity. Therefore, this dissertation primarily focuses on impulse modulation.

1.2 Development of UWB Systems

In fact, UWB technology is not a new, it was originally discovered by Guglielmo Marconi in 1901 to transmit Morse code sequences across the Atlantic Ocean using spark gap radio transmitters. However, the benefit of a large bandwidth and the capability of implementing multi-user systems were never considered at that time. Approximately fifty years after Marconi, Harmuth at Catholic University of America, Ross and Robbins at Sperry Rand Corporation, and van Etten at the United States Air Force or USAF, Rome Air Development Center were some of the pioneers [9,10] who started the modern UWB communications from in time domain electromagnetic systems in the early 1960s. They all referred to the systems as baseband radio. During the same period, Los Alamos, an engineer at Lawrence Livermore National Laboratories (LLNL and LANL), and other engineers elsewhere performed some of the original research on pulse transmitters, receivers, and antennas.

However, a major breakthrough in the UWB communications occurred as a result of the development of the sampling oscilloscope by both Tektronix and Hewlett-Packard

in the 1960s. These sampling circuits provided a method to display and integrate UWB signals. Moreover, this research provided the simple circuits necessary for subnanosecond on baseband pulse generation. Cook and Bernfeld summarized Sperry Rand Corporation's developments in pulse compression, matched filtering, and correlation techniques in their book published in 1967. In 1972, Robbins invented a sensitive baseband pulse receiver as a replacement for the sampling oscilloscope. This invention led to the first patented design of the UWB communication systems by Ross at the Sperry Rand Corporation.

By the early 1970s, the basic designs for UWB radar and communication systems were developed with advances in electronic component technology. In 1974, Morey at the Geophysical Survey Systems Corporation commercialized the first ground-penetrating radar based on UWB. McEwan at LLNL developed the Micropower Impulse Radar (MIR) that provided compact, inexpensive and low power UWB systems for the first time in 1994. Around 1989, the United States Department of Defense (DOD or DoD) created the term *ultra wideband* to describe communication via the transmission and reception of impulses. The U.S. government has been and continues to be a major supporter of UWB research. The Federal Communications Commission (FCC) effort to authorize the use of UWB systems [1] spurred a great amount of interest and fear of UWB technology. In response to the uncertainty of how UWB systems and existing services could operate together, the U.S. government has sponsored several UWB interference studies

In 1993, Robert Scholtz at the University of Southern California presented a multiple access technique for UWB systems [11]. This technique allocates each user a unique spreading code that determines specific instances in time when the user is allowed to transmit. With a viable multiple access scheme, UWB systems become capable of supporting many fields like radar, point-to-point communications and wireless networks. For about the wireless network fields, a number of researchers in the late 1990s and early 2000s began investigations on UWB propagation in details. These propagation studies, and the channel models developed from the measurement results were culminated in a number of notable publications (Cassioli, Win, Scholtz, Molisch [2–4] and Foerster [5]).

1.3 Literature Review

This dissertation addresses two main problems of UWB systems: pulse transmission power and timing jitter tolerance. These problems are crucial keys to communications success. While there is a strong desire to maximize both of them, one must be trade off against the other. In the literature, much effort has been devoted to separately optimize each of them without considering the drawback to the other. Therefore, in this section, the relevant published research papers and proceedings are comprehensively reviewed.

When the FCC published its standard for the limitation of effective isotropic radiation power (EIRP) for UWB systems in 2002, the problem of spectrum shaping for UWB systems came to the forefront of scientific discourse. Moreover, the interference of

pulse transmission power to and from existing systems operating over the same frequency bands is crucial keys to communications success of UWB systems. This interference may reduce the advantages of UWB systems.

The conventional pulse, Gaussian 2^{nd} derivative pulse, is widely adopted in the investigation of UWB applications due to mathematical convenience and ease of generation [12,13]. Unfortunately, this pulse is not flexible enough to conform the FCC spectral masks. Thus, the Gaussian monocycle pulse must be modified and filtered to meet the FCC requirements [14–17]. One of the techniques to modified Gaussian monocycle is the method based on the linear combination of a number of Gaussian derivative pulses to form on single pulse that are introduced in [18,19]. In [19], W. Gao, R. Venkatesan and C. Li generated pulse using the combination of Gaussian derivative pulses from the 1^{st} to 15^{th} ones. The power spectral density (PSD) of this technique conforms the FCC spectral masks. However, this combination makes the implementation of the pulses very complicated.

In the literature, the pulse design techniques are categorized according to two criteria for a pulse design. Most of those works [20–50] consider the methods of obtaining pulse that meets the power spectral constraint of FCC masks. The other portion [51–55] devotes to the design of pulse that provides timing jitter tolerance. However, the later group spans only small number of works concerning with the optimal pulse design.

The pulse generation algorithms fitting the FCC masks can be grouped into three different techniques. Firstly, the most straight-forward method probably is the digital generation from sampled frequency response [20,21]. The implementation of this technique is prohibitively limited by the need of extremely high sampling rate digital to an analog (D/A) converter. Secondly, the method is based on linear combination of orthogonal pulse sets. The orthogonal pulse families are ranged from Prolate Spheroidal, Wavelet to Modified Hermite Pulse [22–43]. For the Prolate Spheroidal schemes, A. B. Parr, B. L. Cho and Z. Ding presented a pulse design algorithm for acquiring a set of orthogonal UWB impulse with limited time duration subject to a pre-selected frequency mask [22–24] in 2003. In addition, L. Yin and Z. Hongbo [25,26] proposed an optimized pulse design by using the Approximate Prolate Spheroidal Wave Functions (APSWF) in 2005. Their pulse meets the power spectral constrain and simple mathematical expression. Unfortunately, the mutual orthogonality of the pulses, which are generated using the prolate spheroidal function, are not preserved with the distortion of channel and the characteristics of antennas. Thus, this pulse design algorithm does not provide the orthogonality for received pulses which have notable impact on the performance of the correlation receiver [22–24]. Therefore, the new orthogonal pulse based on wavelet technique is proposed in [27–30] for a UWB pulse design that can maintain orthogonality at a receiver. Moreover, other linear combination pulse techniques such as Nyquist criteria or term of B-splines are proposed in [40–43]. These works offer a

design of pulses that meet the FCC spectral masks and have time-limit signals for no intersymbol interference (ISI).

A popular technique of the linear combination pulse is based on the modified Hermite polynomials (HP) that are proposed in [31–39]. Hermite pulses are orthogonal to one another; this orthogonality suggests that a variety of designs making use of simultaneous pulse transmission can be considered. Furthermore, these waveforms are well confined in both time and frequency, ensuring that all pulses have the same duration, which relates to achievable data rate, while maximizing frequency efficiency. Therefore, many works investigate the orthogonal UWB pulse using this method. In 2003, G. T. F. de Abreu, C. J. Mitchell and R. Kohno [31] presented orthogonal pulse of transmit waveform that are constructed as the combination of elementary Hermites with weighting coefficients derived by employing the Gram-Schmidt factorization. They originally established orthogonal pulse in UWB systems, but their pulses did not consider the condition of power spectral density limitation. In 2005, W. Hu and G. Zheng [33] proposed M-ary biorthogonal modulation based on orthogonal Hermite Pulse Shapes whose frequency response met the FCC standard. For the TH-PPM UWB system, J. G. Xing, Z. H. Bo and C. Wei [34] presented the design of a class of pulses that were based on Hermite functions. However, the high order of these pulses would be more susceptible to timing jitter. In 2007, X. L. Wu, X. J. Sha and N. T. Zhang [38] suggested a modified Hermite function based pulse shaping algorithm on the TH-PPM UWB system. The pulse duration presented in this study is shorter than orthogonal Hermite pulse in [34]. Unfortunately, frequency shifting and bandpass filters are required for the HP of order 0 or 1 and higher order HP, to satisfy the FCC spectral masks. High order HP pulses are susceptible to timing jitter and noise, and they also need bandpass filters to fit their PSD into the FCC mask [56].

The pulse design techniques, based on famous orthogonal pulse sets, gain from the rich knowledge of those pulse sets. However, these techniques are also difficult to implement due to the need of hundreds of pulse generators. This problem can even more severe if the pulse generator creates drifts or offsets during the generation process. Some authors suggested the digital implementation of such orthogonal pulse transformation [28]. However, the digital implementation of low duty cycle signals leads to the expensive hardware as in the case of D/A technique.

The last technique, the digital FIR filter solution, differs from the previous two methods because it does not aim to directly generate the desired pulse. On the other hand, it synthesizes the desired pulse by filtering the conventional input pulse, such as monocycle which was proposed in [44–50]. In 2003, X. Luo, L. Yang and G. B. Giannakis [46,47] proposed digital FIR filter design based on the Parks-McClellan (PM) algorithm for shaping UWB pulses under mask-fitting requirements [1]. The PM design utilizes the bandwidth (BW) and power allowed by the FCC spectral masks, and it can dynamically avoid narrow-band interference. However, trial-and-error may be required

to find suitable values for the implicit parameters in a PM design including the edge tolerances of the pass- and stop-bands, and the frequency weighting of the approximation error. In 2006, X. Wu, Z. Tian, T. N. Davidson and G. B. Giannakis [48, 49] introduced a globally optimal pulse design method based on semidefinite programming (SDP) to maximize the power utilization efficiency while complying with the spectral mask. The digital FIR filter technique was proposed to avoid the extremely high sampling rate implementation of the direct impulse optimization method. In addition, the direct pulse optimization also suffers from numerical instability because of the complicated optimization of very large number of variables. The optimization of FIR filter involves much smaller number of variables thus it is more attractive in the implementation perspective.

Apart from the pulse design problem, UWB systems are also very sensitive to a timing jitter. Timing jitter results from the presence of non-ideal sampling clocks in practical receivers. This distortion affects the correlation of signals at the receiver and thus the signal detection ability of UWB systems. Since UWB pulse duration is very short (in the range of a nanosecond), only small timing misalignment can severely affect the performance of a correlation detector. For the prior research on the performance of timing jitter, it can be separated into two forms - as uncorrelated (white timing jitter) and correlated (colored timing jitter).

The performance of UWB systems under white timing jitter has been extensively studied by many works [57–67]. In 2002, W. M. Lovelace and J. K. Townsend [57, 58] considered the effects of timing jitter performance of binary and orthogonal 4-ary PPM UWB communications. Moreover, they also investigated the tracking error performance on UWB systems. I. Guvenc and H. Arslan [59, 60] presented UWB systems performance by evaluating the degradation of the signal-to-noise ratio due to timing jitter. They present the BER performance of various modulation options for UWB systems such as PAM, PPM, OOK and BPSK. Moreover, they also consider another practical condition such as multipath, multiple access interference (MAI) and narrowband interference (NBI). In 2004, L. Mucchi, D. Marabissi, M. Ranaldi, E. Del Re, and R. Fantacci [61] compared the sensitivity to synchronization errors of the different multiple access techniques between the TH-PPM and the DS. Their results show that the TH technique overcomes DS when timing jitter occurs. In 2005, C. S. Sum, M. A. Rahman, S. Sasaki and J. Zhou [64] presented the impact of timing jitter on a DS-UWB system in AWGN and multipath channel. Investigation is performed in different Rake receivers (all-Rake and selective-Rake) and two types of timing jitter (uniformly and Gaussian distributed). In 2005, Z. Tian and G. B. Giannakis [65, 66] presented the BER sensitivity to epoch timing offset under different operating conditions, including frequency-flat fading channels, dense multipath fading channels, multiple access with and without time hopping, and various receiver types including sliding correlators and RAKE combiners. In 2006, N. V. Kokkalis, P. T. Mathiopoulos, G. K. Karagiannidis, and C. S. Koukourlis [67] also studied the performance of UWB under timing jitter. They

consider the BER performance of M-ary PPM which is not the same as that reported in [57, 58] in the presence of MUI. In addition, our work [68] investigated the effect of pulse shapes to timing jitter tolerance. The simulation results confirm that different pulses are the result of different level of immunity to timing jitter. The pulses having relatively flat autocorrelation function tend to be less sensitive to timing jitter.

On the other hand, the performances of UWB systems under colored timing jitter have been studied as follow. In 2004, P. B. Hor, C. C. Ko and W. Zhi [69,70] presented the BER performance of the pulse UWB system in the presence of colored timing jitter. They found that colored jitter degrades the BER performance more than white jitter and they are proposed a new jitter compensation scheme to improve the BER performance under colored jitter. In 2006, U. Onunkwo, Y. Li and A. Swami [71,72] investigated the impact of timing jitter on OFDM-based UWB systems and derived an exact expression for the ICI power due to timing jitter. For mathematical simplification, however, many works investigated timing jitter that has a normal distribution [57,58,61,67]. Thus, in this dissertation, we will use timing jitter modeled by the normal distributed random process.

Besides performance evaluation of timing jitter, the prior works in an attempt to alleviate the effect from timing jitter have been studied. These proposed methods can be categorized in two approaches: improve the timing synchronization accuracy and improve timing jitter involving the pulse shape. The first scheme which is techniques for improving the timing synchronization accuracy is proposed in [73–78]. In 2005, W. Zhang, Z. Bail, H. Shen, W. Liu and K. S. Kwak [73] proposed a virtual received waveform as integration of time-shifted version of conventional received waveform and the distribution of timing jitter. However, they neither clearly state the motivation of their virtual received waveform design nor show method in obtaining timing jitter distribution. The on-off keying modulation scheme is considered by Q. Li and W. S. Wong in [74]. A receiver is proposed to over-sampling the received waveform and the optimum threshold is determined by a version of Kiefer-Wolfowitz algorithm. The technique, proposed in [74], is difficult to apply to other popular modulation systems such as PPM or PAM. In 2006, S. Gezici, Z. Sahinoglu, H. Kobayashi and H. V. Poor proposed multi-user UWB systems that use multiple pulse waveforms [78]. For the conventional system that uses single pulse waveform, pulse with fast decaying autocorrelation function is desired in order to prevent interframe interference. However, such an autocorrelation function also results in a considerable decrease in the desired signal part of the receiver output in the presence of timing jitter [79,80]. In 2007, R. Merz, C. Botteron and P. A. Farine [81] estimated the BER performance for a UWB impulse radio in an AWGN transmission channel and with Gaussian jitter. They investigated the influence of the jitter on the received signal by assuming that the received pulses are combined to increase the SNR. Though, the timing synchronization accuracy is limited by the advancement of both algorithms and equipments. It seems to be impossible to perfectly synchronize the

timing in the near future.

The other approach that proposed by G. T. F. de Abreu and R. Kohno in 2005 to improve the robustness against timing jitter involves the pulse shape optimization [51,52]. In [51,52], the authors exploited the autocorrelation properties of the modified Hermite pulses to generate a pulse. Their works inherently lead to a relatively flat pulse. The pulse, obtained from the algorithm in [51,52], is a single polarized pulse with large time duration. Such pulse has narrow bandwidth, which does not efficiently utilize the allocated spectrum and violates the wide continuous bandwidth requirement. Moreover, Y. Chen and J. Chen and T. Lv [53, 54] proposed a novel technique that couples High Order Monocycle (HOM) with biphasic modulation (BPM) to achieve timing jitter-robust in UWB systems. However, the proposed technique finding high order monocycle pulse tends to lengthen the pulse duration, thereby reducing the data rate and system capacity as a result of [15]. In 2007, a new method for constructing UWB pulse based on Daubechies wavelets is proposed by L. Xin, A. B. Premkumar and A. S. Madhukumar [55]. The constructed pulse not only meets the FCC masks, but also provides good performance in the presence of timing jitter. However, the proposed pulse of this previous study has utilized low spectral mask and the high order tends to lengthen the pulse duration. This results of lengthening the pulse duration is the same as that yielded by using the technique in [53, 54].

In this dissertation, a novel pulse design technique is proposed for solving the two crucial problems in UWB systems. An optimal pulse design strategy jointly and simultaneously provides a good match to the FCC spectral masks and robustness to timing jitter. The digital FIR filter technique can be adopted in the proposed algorithm. The model of timing jitter as a normal distributed random variable with zero mean is applied in this dissertation. Moreover, the orthogonal pulses design for improving UWB capacity is also proposed. The orthogonal pulses are based on the optimum pulse design technique. Thus, each of the orthogonal pulse set provides the good utilization bandwidth and resists to timing jitter tolerance.

1.4 Objectives

The primary objective of this dissertation is to propose a novel technique in designing the optimum pulse shape for UWB systems under the presence of timing jitter. The proposed pulse attains the adequate power to survive the noise floor and simultaneously provides good robustness to timing jitter. It also meets the power spectral mask restriction as prescribed by the FCC for the indoor UWB systems. Moreover, the implementation of the proposed pulse and the essential parameters of the proposed optimization algorithm are also investigated.

Additionally, the orthogonal pulse design technique for improving UWB capacity is proposed. The orthogonal pulses algorithm is based on an optimum pulse shape technique. The orthogonal proposed pulses not only have robustness timing jitter properties and PSD conforming the FCC masks but also are orthogonal to one another. This orthogonality suggests that a variety of design making use of simultaneous pulse transmission can be considered.

1.5 Scope

As the optimum pulse shape for UWB systems under the presence of timing jitter investigated in the dissertation, the scope of the research works can be limited to the following:

1. Effects pulse shaping design and timing jitter on UWB systems.
2. A novel pulse shape technique that is jointly considers both factors between the pulse transmission power and timing jitter tolerance.
3. Parameters of the proposed optimization algorithm.
4. Performance of the proposed pulse and a comparative study of the proposed pulse with other techniques proposed by the authors in the past. The concerned issue includes bit error rate performance under with and without timing jitter.
5. Provision of the single proposed pulse to the multiple pulse sets that are mutually orthogonal.
6. Performance of the orthogonal proposed pulses technique and a comparative study of orthogonal proposed pulses with other pulse proposed previously.

1.6 Outline

For the rest of this dissertation, chapter II reviews, the basic knowledge of UWB systems including UWB transmitters, UWB channel models, and UWB receivers.

Chapter III presents the UWB regulations and the three well known Gaussian derivative pulses in order that the optimum pulse shape technique and its orthogonal pulse sets will be proposed.

In chapter IV, the effects of timing jitter on the three Gaussian derivative pulses are demonstrated. The 3 UWB pulses which are the scaled monocycle pulse, the power optimized pulse and the optimum proposed pulse are selected to be compared and discussed. In addition, parameters of the proposed optimization algorithm are described. The BER performances of the 3 UWB pulses are evaluated and the results are given in chapter IV.

Finally, the conclusion of this study along with recommendation for further research is presented in chapter V.



CHAPTER II

BASIC BACKGROUND AND RELATED TOPICS

In this chapter, the fundamental knowledge of the pulse based UWB systems is reviewed. The pulse based UWB systems consist of three important elements: transmitters, channels and receivers. The transmitters group the digital data stream into symbols and then they map these symbols onto analog waveforms. After that, the transmitters transmit them to the air through an antenna. The important parts of the transmitters include the modulation schemes and the multiple access methods. Additionally, the part of channels is one of the important elements. The channels represent the effects of traveling through space and include reflections and distortions as the electromagnetic pulses impinge on other objects. This dissertation considers the UWB channel model based on IEEE 802.15 that derives from the Saleh-Valenzuela. Finally, we discuss UWB receivers. The receivers collect the electromagnetic energy from the antenna, take the extremely weak signal, reconstruct the pulse shape, map the pulse shape to the appropriate symbols and then change them into the binary bit stream. Moreover, two types of general UWB receivers such as RAKE and transmit-reference receivers are reviewed in this dissertation.

2.1 UWB Transmitters

A block diagram of general UWB transmitters is shown in Figure 2.1. The UWB transmitter part can be divided into three important blocks [82]. The first block is bits to symbols. This block maps bits received from the binary data stream to symbols by using modulation and multiple access techniques. For modulation techniques, UWB systems enable various types of modulation to be employed, including on-off keying (OOK), pulse-amplitude-modulation (PAM), pulse-position-modulation (PPM), biphasic modulation (BPM). Consequently, the performance of different modulation schemes varies according to the type of the schemes [83,84]. Besides modulation methods, the multiple access schemes of UWB systems have two conventional methods: time-hopping spread spectrum impulse radio (TH-UWB) and direct sequence spread spectrum impulse radio (DS-UWB). In TH-UWB, when pulses are transmitted, the time hopping is determined based on a pseudorandom sequence. For DS-UWB, a pseudorandom sequence is used to spread the information bits, which are continuously transmitted. The works relative to improving the multiple access schemes are investigated in [85,86]. Moreover, the comparison between TH-UWB and DS-UWB has been studied in many works [87–90]. The results in [87] show that DS-UWB can better deal with multi-user interference than

TH-UWB on AWGN channels. However, this result is based on a single-user detector. With multi-user receivers such as MMSE detector, the performance difference between TH-UWB and DS-UWB systems seems to be almost negligible.

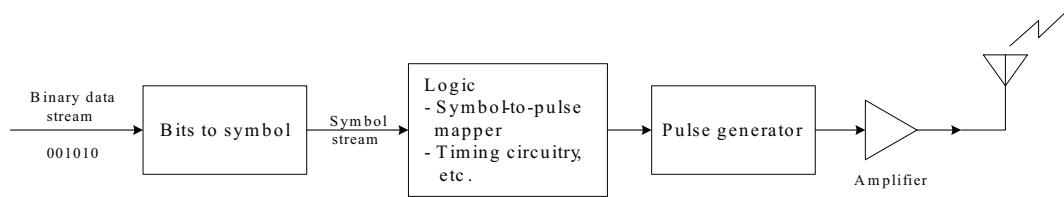


Figure 2.1 A general UWB transmitter block diagram.

The second block includes many parts such as symbol-to-pulse mapper, timing circuitry, etc. The symbols from the first block are then mapped to an analog pulse shape. Pulse shapes are generated by a pulse generator that is the last block. Precise timing circuitry which is crucial requires sending pulses out at intervals. If PPM is employed the timing must be even more precise, usually less than on pulse width. Pulses can then be optionally amplified before being passed to the transmitter. However, in general, a large gain is typically not needed to meet power spectral requirements and many are omitted.

2.1.1 UWB Modulation Schemes

In this section, we review the conventional UWB modulation methods and discuss the advantages or disadvantages of each technique. For UWB systems, the data modulation is typically done using pulse-modulation techniques in the time domain. The choice of modulation method can affect a number of design parameters in the UWB systems development such as data rate, robustness to interference and noise and transceiver complexity that directly impacts the overall size and cost of the system.

2.1.1.1 On-Off Keying

The on-off keying (OOK) is the simplest technique of the UWB modulation. The transmission of a pulse represents a data bit “1” and its absence represents a data bit “0”. Figure 2.2 shows an example of the OOK modulation technique in the UWB communication systems.

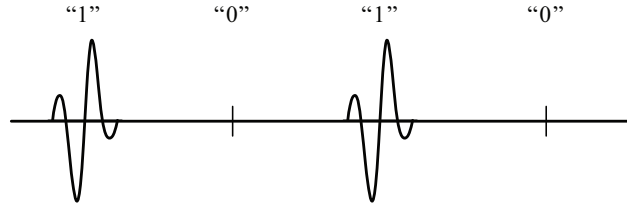


Figure 2.2 On-off keying modulation

The general signal model, $s(t)$, for an OOK modulated signal can be represented by

$$s(t) = \sum_{n=1}^N b_n \cdot P(t - nT) \quad (2.1)$$

where N is the maximum number of transmitted bits, $b_n \in [0, 1]$ represents the n^{th} data bit, $P(t)$ is the UWB pulse and T is the pulse repetition period.

The main advantages of the OOK modulation are simplicity and low implementation cost. The OOK transmitter is quite uncomplicated. This technique can use a simple RF switch that turns on and off to represent data. This way, the OOK modulation allows the transmitter to idle while transmitting a bit “0” and thus save power. However, this modulation scheme has several disadvantages in UWB systems. The OOK modulation is highly sensitive to noise and interference: an unwanted signal can be detected as a false data bit “1”. Moreover, the difficult task of UWB synchronization becomes even more challenging for the OOK modulation if a stream of zeros is transmitted. Therefore, the OOK technique is not a popular modulation technique for UWB systems.

2.1.1.2 Pulse-Amplitude Modulation

The pulse-amplitude modulation (PAM) encodes the data bits based on different levels of power (amplitude) in short-duration pulses. In this modulation technique, a pulse with higher amplitude represents a data bit “1” and a pulse with lower amplitude represents a data bit “0”. Figure 2.3 shows an example of the PAM for the UWB communications.

The general signal model for the PAM signals is given by

$$s(t) = \sum_{n=1}^N A_{b_n} \cdot P(t - nT) \quad (2.2)$$

where A_{b_n} is the specific power level for each user’s data bits, N is the maximum number of transmitted bits, $P(t)$ is the UWB pulse, $b_n \in [0, 1]$ represents the n^{th} data bit, and T is the pulse repetition period. As shown in (2.2), the PAM and the OOK

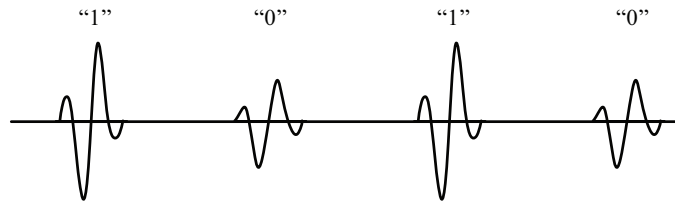


Figure 2.3 Pulse-amplitude modulation

signal models are very similar, except for the existence of the amplitude parameter, A_{b_n} , in the PAM model, which represents the different amplitudes considered for a UWB pulse data transmission.

The advantage of the PAM modulation is also simplicity. It is simple because the PAM generation requires pulses with only one polarity to represent data. On the contrary, the first disadvantage of the PAM modulation is noise immunity. Although PAM pulses are less sensitive to noise than the OOK modulated pulses, attenuation in wireless channels can convert them to the OOK case. Furthermore, because of the periodicity of transmitted pulses, some discrete lines will be present on the PSD of the PAM pulses. These discrete lines can cause harmful interference to other narrowband and wideband signals sharing the frequency spectrum with UWB systems. Figure 2.4 illustrates such discrete spectral lines on the PSD of periodic pulses.

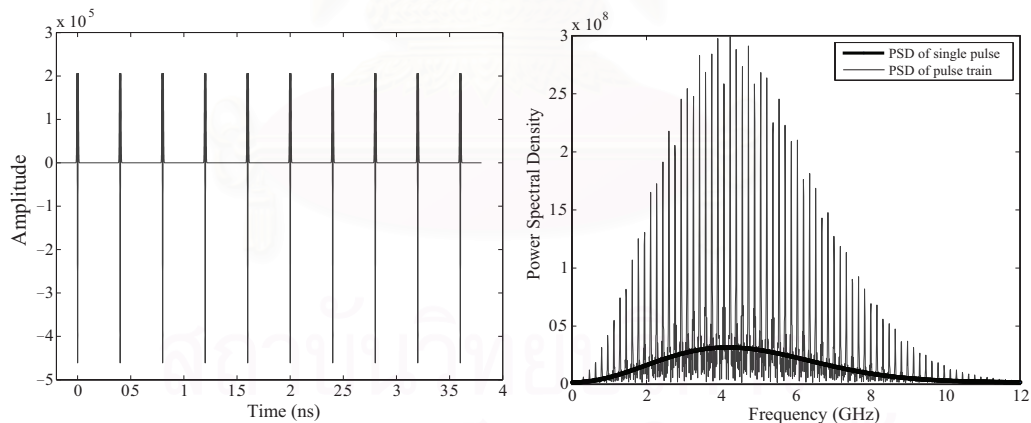


Figure 2.4 Discrete spectral lines of periodic pulses

The discrete power spectral lines can interfere with the conventional radio services and the UWB signals. Therefore, it's quite important to avoid the discrete spectral lines. One method to overcome these spectral lines is to “dither” the transmitted signal by adding a random offset to each pulse and removing the common spectral components [82]. However, the random offset of this technique is unknown at the receiver, making it extremely difficult to acquire and track the transmitted the UWB signal. An-

other method with similar random properties, but using a known sequence, is to use *pseudo-random noise* (PN) codes. For more information on this technique, we will describe it at the end of the next subsection.

2.1.1.3 Pulse-Position Modulation

The pulse-position modulation (PPM) is pseudo-randomly encoded based on the position of the transmitted pulse trains by shifting the pulses in a predefined window in time. Compared to the OOK and the PAM pulses, the PPM signals are more immune to false detection due to channel noise. This is because the pulses that represent the data bits in the PPM have the same amplitude, so the probability of detecting a false data bit is reduced. A version of the PPM represents a data bit “0” by not shifting with respect to a specific reference point in time; it represents a data bit “1” by a pulse advancing the same reference point as shown in Figure 2.5.

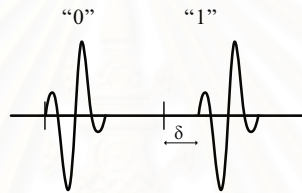


Figure 2.5 Pulse-position modulation

The general signal model for the PPM signals is given by

$$s(t) = \sum_{n=1}^N P(t - nT - b_n\delta) \quad (2.3)$$

where δ is the modulation index that provides a time shift to represent digital bits, N is the maximum number of transmitted bits, $P(t)$ is the UWB pulse, $b_n \in [0, 1]$ represents the n^{th} data bit, and T is the pulse repetition period.

The disadvantage of the PPM scheme is its sensitivity to timing synchronization. Because data bits are recovered exclusively based on their exact position in time, timing uncertainties, such as jitter and drift, can degrade their performance significantly. For instance, timing uncertainties can cause synchronization errors that result in increased MAI in multiple-access channels. Further, the strict timing synchronization of narrow UWB pulses prior to the correlation process in the PPM receivers requires very fast (on the order of gigahertz) analog-to-digital converters (ADCs). Moreover, multipath distortions can stretch the pulses and cause them to overlap; thus detection becomes challenging of the pulse positions in the PPM systems.

For the discrete spectral lines problem, another method to overcome this problem is to use PN codes to add an offset to the PPM signal [82]. Since these codes are

known and easily reproducible at the receiver, the problem for the receiver becomes mostly acquisition of the signal, but tracking makes it much easier. Moreover, the use of a PN time shift has other benefits besides just reducing the spectral lines. Since the PN code is a channel code it can be used as a multiple access method to separate users in a similar manner to the code division multiple access (CDMA) scheme. By shifting each pulse at a pseudo-random time interval the pulses appear to be white background noise to users with a different PN code. Furthermore, the use of the PN code makes data transmission more secure in a hostile environment. The impact of the PN time offsets on energy distribution in the frequency domain is illustrated in Figure 2.6.

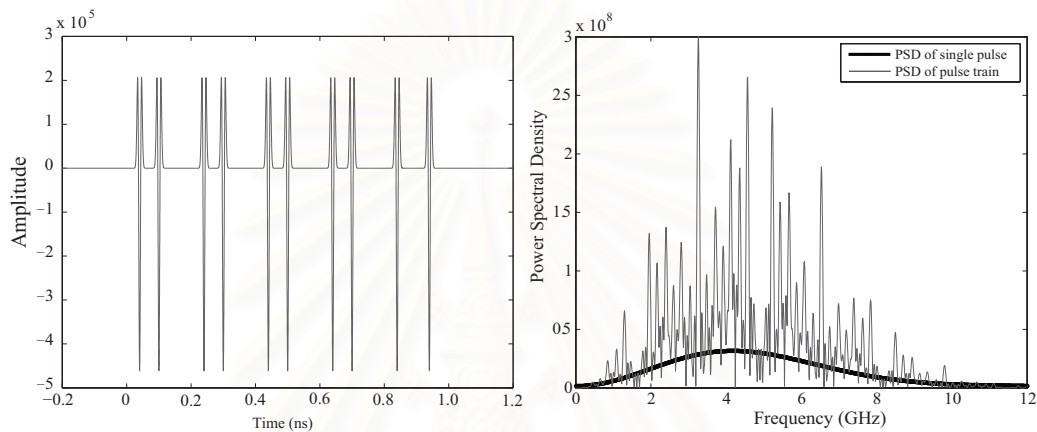


Figure 2.6 Smooth spectrum of PN time offsets

2.1.1.4 Biphase Modulation

The biphase modulation (BPM) employs the polarity of the pulse changes to represent digital data bits. Figure 2.7 demonstrates the biphase modulation for the UWB pulses.

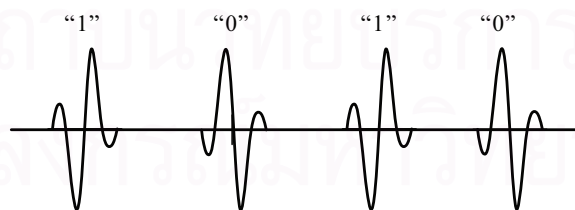


Figure 2.7 Biphase modulation

The general signal model for the biphase modulation is given by

$$s(t) = \sum_{n=1}^N b_n P(t - nT) \quad (2.4)$$

where N is the maximum number of transmitted bits, $P(t)$ is the UWB pulse, $b_n \in [-1, 1]$ represents the n^{th} data bit, and T is the pulse repetition period.

The first advantage of the biphase modulation is less susceptible to distortion because the difference between the two pulse levels is twice the pulse amplitude. Another advantage of biphase modulation is that the change in polarity can remove the discrete spectral lines in the pulse's PSD, because changing the polarity of pulses produces a zero mean [91]. However, for a stream of data, accurate timing between the two transmitters is of great importance.

2.1.1.5 Summary of UWB Modulation Methods

In this subsection, we conclude the discussion of the modulation methods for the UWB communications with Table 2.1 which summarizes the advantages and disadvantages of each of the modulation methods [82].

Table 2.1 Advantages and disadvantages of the various modulation methods.

Modulation methods	Advantages	Disadvantages
OOK	Simplicity	Binary only, noise immunity
PAM	Simplicity	Noise immunity
PPM	Simplicity	Fine time resolution needed
BPM	Simplicity, efficiency	Binary only

2.1.2 UWB Multiple Access Techniques

In this section, we describe the typical multiple-access methods for the UWB communications systems. The multiple-access techniques are needed to perform the channelization for multiple users because several users transmit information simultaneously and independently over a shared channel. For the impulse-radio UWB, two common multiple access (MA) techniques are employed such as time-hopping (TH) technique and direct-sequence (DS) technique. Both of the methods are typically applied to the modulation schemes previously discussed.

First of all, the TH technique can be applied to all of the modulation schemes, where each user is assigned a time-hopping sequence. This sequence reduces collisions in the communication system by assigning each user a unique time shift pattern. Each receiver can detect a signal during its own unique hopping pattern, mitigating interference. The mathematical representation for the k^{th} user's transmit signal is given as [13]:

$$y_{(k)}(t) = \sum_{j=-\infty}^{\infty} s(t - jT_f - c_j^{(k)}T_c - \delta b_{[j/N_s]}^{(k)}) \quad (2.5)$$

where s is the transmitted baseband pulse waveform, T_f is the pulse repetition time, $c_j^{(k)}$ is the time-hopping sequence, T_c is the duration of the time delay bins, $b_j^{(k)}$ is the data sequence, N_s is the number of pulses in any given binary symbol and δ is the modulation index.

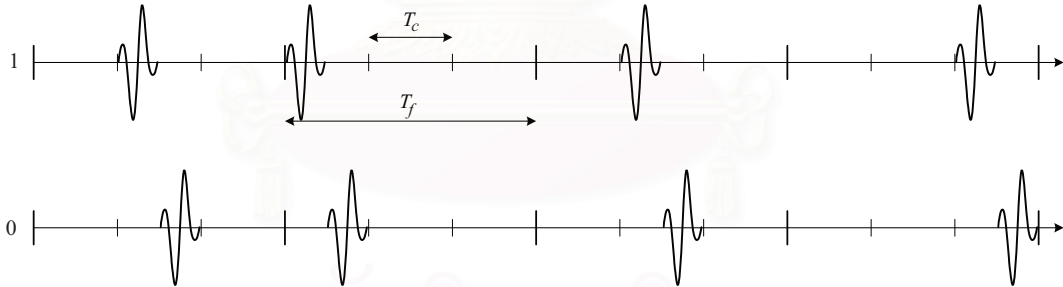


Figure 2.8 TH-PPM Modulation Examples

An example of pulse trains for binary data bit “1” and “0” is demonstrated in Figure 2.8, in which the first pulse train is transmitting binary bit “1”, and the second pulse train is sending binary bit “0”. The only difference between the two is that all pulses in pulse train 0 are delayed a little bit comparing to the pulses in pulse train 1.

The direct sequence (DS) is the other form of MA commonly used with the impulse-radio UWB, although it is typically limited to OOK, Binary PAM and biphas modulation schemes. The idea is to modulate an antipodal pseudo-random noise (PN) sequence, which is unique at the time of communication. Therefore, a minimal amount of interference occurs with other users as they are assigned with different PN codes that have good autocorrelation and cross-correlation properties. The transmitted DS-UWB waveform is defined as [92]:

$$y^{(k)}(t) = \sum_{i=-\infty}^{\infty} \sum_{n=0}^{N_r-1} b_i^{(k)} a_n^{(k)} s(t - iT_r - nT_c) \quad (2.6)$$

where s is the transmitted baseband pulse waveform, N_r is the spread spectrum processing gain, $b_j^{(k)}$ is the modulated data symbols for the k^{th} user, $a_n^{(k)}$ is the k^{th} user spreading chips, T_r is the bit period and T_c is the chip period.

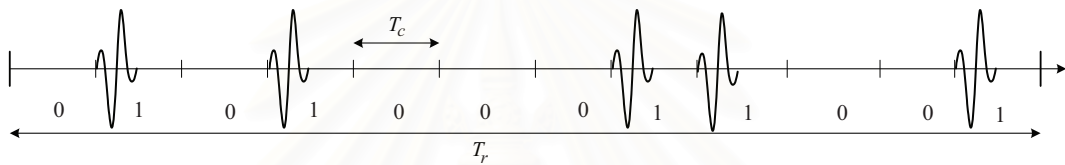


Figure 2.9 DS-BPAM Modulation Example

An example of the direct sequence binary amplitude modulation (DS-BPAM) is demonstrated in Figure 2.9, where data bit “1” is spread into a binary sequence of 010100011001.

2.2 UWB Channel Models

Based on the clustering phenomenon observed in several channel measurements, the IEEE 802.15 [93] task group adopted an UWB channel model derived from the Saleh-Valenzuela model [94] with a couple of slight modifications. Specifically, the multipath model is described by the discrete time impulse response below:

$$h(t) = X \sum_{l=0}^L \sum_{k=0}^K \alpha_{k,l} \delta(t - T_l - \tau_{k,l}) \quad (2.7)$$

where $\alpha_{k,l}$ is the path gain coefficient of the k^{th} path within the l^{th} cluster, T_l is the arrival time of the first path of the l^{th} cluster, $\tau_{k,l}$ is the delay of the k^{th} path within the l^{th} cluster relative to the first path arrive time T_l and X is the log-normal shadowing coefficient.

Clearly, we have $\tau_{0,l} = 0$ by definition. To proceed, we further define the following two arrival rates: Λ is cluster arrival rate and λ is ray arrival rate, i.e., the arrival rate of path within a cluster.

Now, the distribution of the T_l and $\tau_{k,l}$ can be characterized by

$$p(T_l | T_{l-1}) = \Lambda e^{-\Lambda(T_l - T_{l-1})}, \quad l > 0 \quad (2.8)$$

$$p(\tau_{k,l} | \tau_{k-1,l}) = \lambda e^{-\lambda(\tau_{k,l} - \tau_{k-1,l})}, \quad k > 0 \quad (2.9)$$

i.e., the inter-cluster arrival time is exponentially distributed with rate Λ and the inter-ray arrival time is exponentially distributed with rate λ .

The channel gain coefficient $\{\alpha_{k,l}\}$ is defined as follows:

$$\alpha_{k,l} = p_{k,l} \xi_l \beta_{k,l} \quad (2.10)$$

where $p_{k,l}$ is equally probable of ± 1 to account for the signal inversion due to reflections, ξ_l reflects the fading associated with the l^{th} cluster and $\beta_{k,l}$ corresponds to the fading associated with the k^{th} ray of the l^{th} cluster. With the mean energy of the first path of the first cluster being denoted by Ω_0 , the mean energy of $\alpha_{k,l}$ is given by [93]:

$$\text{E} [|\alpha_{k,l}|^2] = \text{E} [|\xi_l \beta_{k,l}|^2] = \Omega_0 e^{-(T_l/\Gamma)} e^{-(\tau_{k,l}/\gamma)} \quad (2.11)$$

where Γ is the cluster decay factor and γ is the ray decay factor. The distribution of the path gain magnitude $|\alpha_{k,l}|$ is assumed to be log-normally distributed:

$$20 \log_{10} (\xi_l \beta_{k,l}) \sim N(\mu_{k,l}, \sigma_1^2 + \sigma_2^2), \quad (2.12)$$

where σ_1 is the standard deviation of the cluster log-normal fading (in dB) and σ_2 is the standard deviation of the ray log-normal fading (in dB). From (2.11) and (2.12), we obtain:

$$\mu_{k,l} = \frac{10 \ln \Omega_0 - 10T_l/\Gamma - 10\tau_{k,l}/\gamma}{\ln 10} - \frac{\ln 10 (\sigma_1^2 + \sigma_2^2)}{10} \quad (2.13)$$

Finally, with a standard deviation of σ_x in dB, the log-normal shadowing term X is characterized by

$$20 \log_{10} X \sim N(0, \sigma_x^2). \quad (2.14)$$

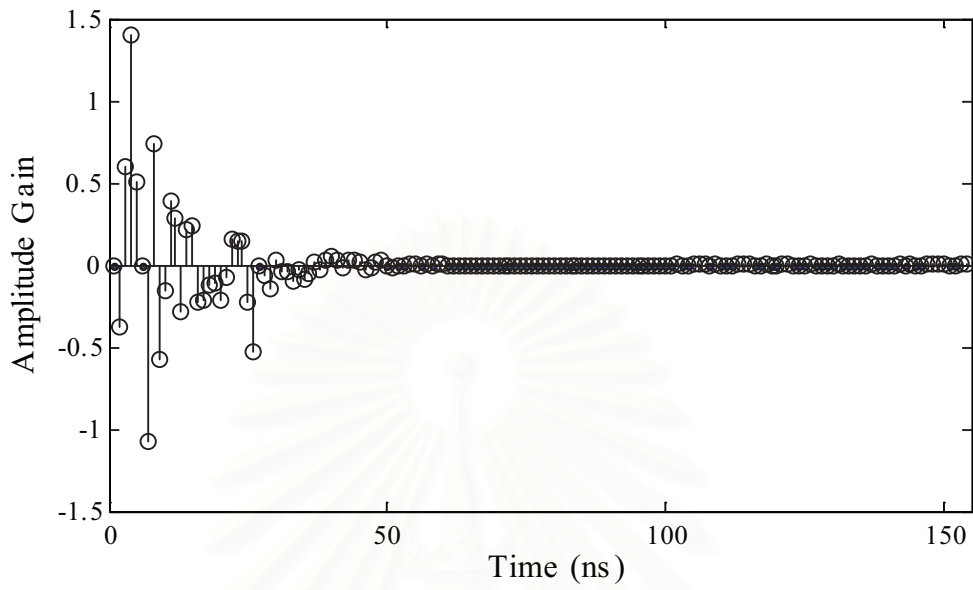
Since we can capture the total multipath energy in term X , the total energy contained in the terms $\{\alpha_{k,l}\}$ is normalized to unity for each realization.

In IEEE 802.15 working group, the UWB channel is further classified into four models. Channel model 1 (CM1) represents Line-Of-Sight (LOS) and distance from 0 to 4 m UWB channel, while channel model 2 (CM2) represents Non-Line-Of-Sight (NLOS) and distance from 0 to 4 m UWB channel. Distance from 4 m to 10 m and NLOS UWB channel is modeled as CM3 and distance over 10 m NLOS UWB channels are all classified into the extreme model CM4. The simulation parameters setting for all the four channel models are listed in Table 2.2 [93].

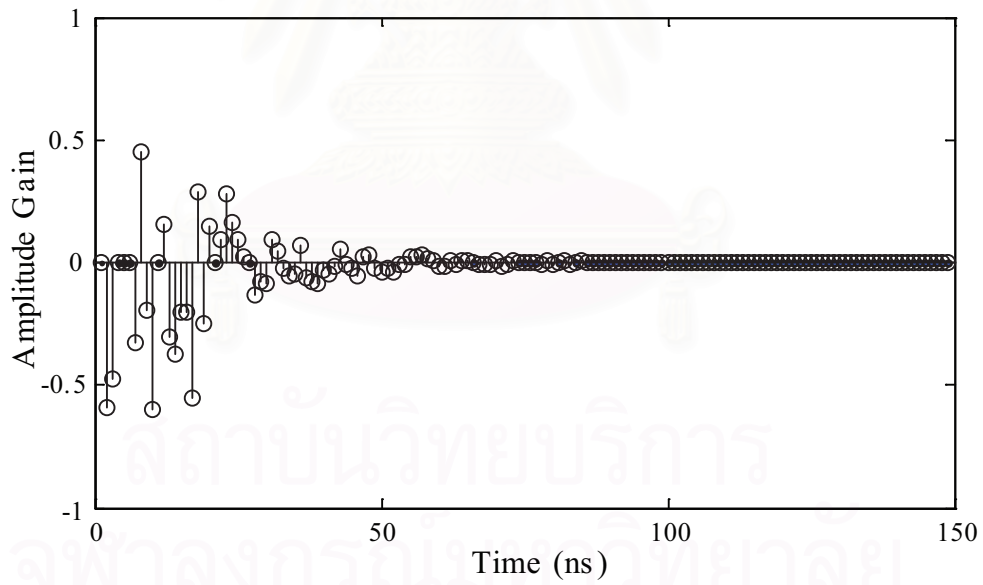
Table 2.2 Parameter Settings for IEEE UWB Channel Models.

Scenario	Λ (1/ns)	λ (1/ns)	Γ (ns)	γ (ns)	σ_1 (dB)	σ_2 (dB)	σ_3 (dB)
CM1 LOS (0-4 m)	0.0233	2.5	7.1	4.3	3.3941	3.3941	3
CM2 NLOS (0-4 m)	0.4	0.5	5.5	6.7	3.3941	3.3941	3
CM3 NLOS (4-10 m)	0.0667	2.1	14	7.9	3.3941	3.3941	3
CM4 Extreme NLOS	0.0667	2.1	24	12	3.3941	3.3941	3

With the exact channel parameters listed in Table 2.2, the UWB channels for all the four channel scenarios are simulated using the Saleh-Velenzuela model. The simulated channel impulse responses for CM1, CM2, CM3 and CM4 are shown in Figures 2.10(a), 2.10(b), 2.11(a) and 2.11(b), respectively.

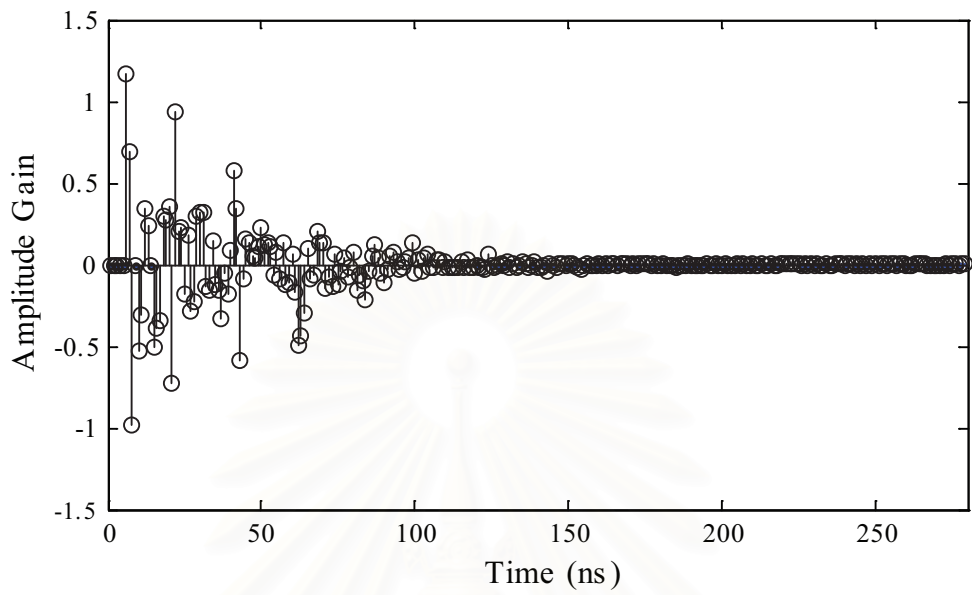


(a)

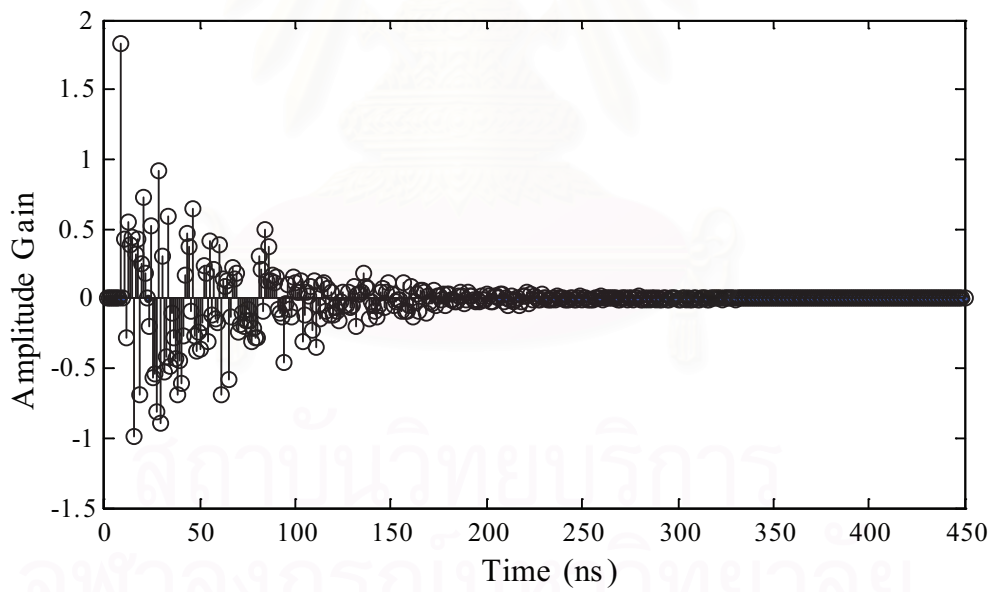


(b)

Figure 2.10 Impulse response of (a) CM1 (b) CM2



(a)



(b)

Figure 2.11 Impulse response of (a) CM3 (b) CM4

2.3 UWB Receivers

A general UWB receiver block diagram is shown in Figure 2.12. The receiver performs the inverse operation of the transmitter to recover the data. As shown in the Figure 2.12, the first block of the receiver includes many parts such as acquisition, tracking, demapping pulse shapes-to-symbols, etc. This block performs the functions of detection or acquisition to locate the required pulses amongst the other signals and then to continue tracking these pulses to compensate for any mismatch between the clocks of the transmitter and the receiver. The second block is pulse generation that generates the template pulse for the use of detecting the received signals of a first block. The last block is a symbol to bits. This block converses an analog pulse shape to the binary data stream.

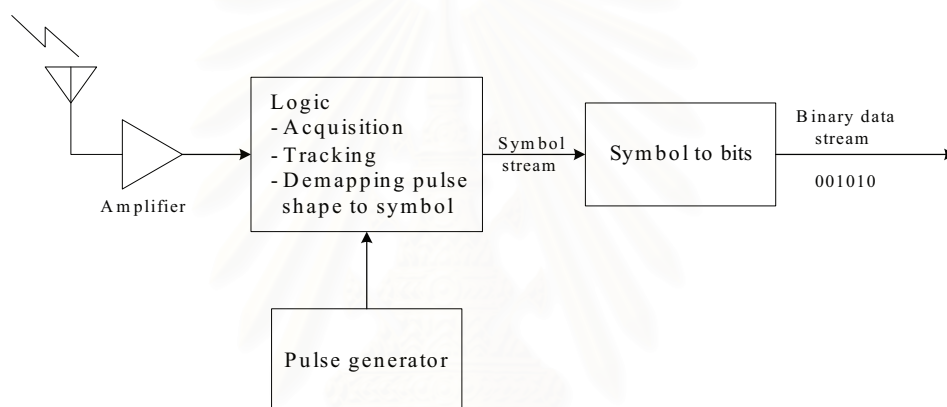


Figure 2.12 A general UWB receiver block diagram.

The most common UWB receiver design includes threshold/energy detectors, correlation detectors, RAKE and transmit-reference (TR) receivers. The threshold/energy detectors are simple to implement. However, this receiver is a trade-off between the simplicity and the performance. The correlation receiver is a matched filter system and it can provide the optimum detection SNR if the template waveform exactly matches the time and shape of the incoming waveform. However, this receiver has high complexity from the match filter structure. RAKE receivers are a bank of correlators. Each finger of the RAKE is synchronized to a multipath component. Most of early receiver research focused on RAKE type of receivers. Recently due to the difficulty and complexity from stringent timing synchronization requirement and energy capture of multipaths, suboptimal TR (also called autocorrelation) receivers attract significant attentions. Next we will look into the ideas of the RAKE and the TR receiver structures, and compare their advantages and disadvantages.

2.3.1 RAKE Receivers

For AWGN channels, the typically optimum receiver is a correlator (i.e. match filter) receiver. The local receiver generated template waveform is perfectly synchronized and correlated with the incoming pulse train, which is only distorted by AWGN noise.

For impulse-radio UWB systems, the UWB transmissions can resolve many paths and are thus rich in multipath diversity. RAKE receivers can be used to exploit the diversity by constructively combining the separable received multipath components. It consists sub-receivers each of which delays to tune into the individual multipath components. Each branch of the RAKE receivers is a correlator (match filter) that collects coherent received signal energy independently. The output of each finger is combined in order to make the most use of the different transmission characteristics of each transmission path. This can very well result in higher signal-to-noise ratio (SNR, also known as E_b/N_0) in a multipath environment.

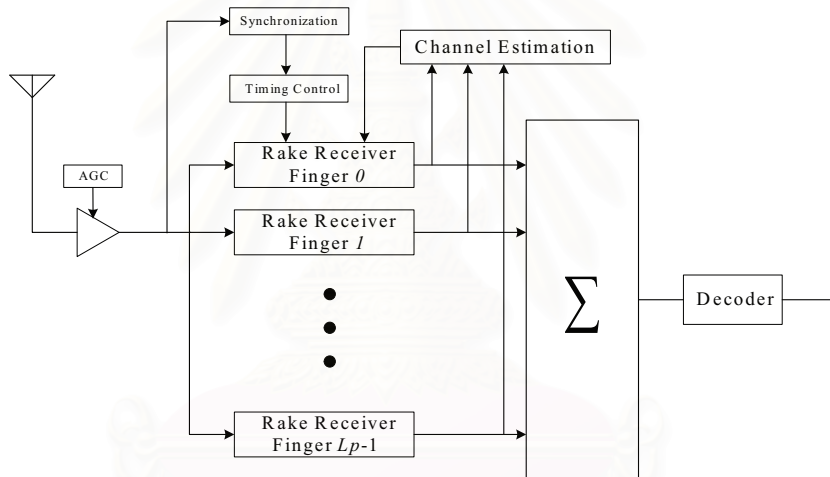


Figure 2.13 Block diagram of a typical RAKE receiver structure.

Figure 2.13 [95] shows the receiver block diagram, which consists of L_p correlators/fingers to collect the received signal energy from the L_p strongest paths having excess delays $\{\tau_l\}_{l=0}^{L_p-1}$. The l^{th} correlator, $l = 0, 1, 2, \dots, L_p - 1$, is to correlate the received signal with the receiver locally generated reference signal delayed by τ_l . The output of the correlators can be linearly combined in different ways to form the decision variable. The maximal ratio combining (MRC) approach provides optimal performance, with the prerequisite of accurate channel information at the receiver. As accurate channel information are not available, equal gains combining (EGC) and some other methods could be selected.

2.3.2 Transmit-reference Receivers

From the previous subsection, we know that the coherent RAKE receivers offer optimal performance that rely on enough fingers to accurately capture all or a significant part of resolvable multipath components (MPCs) [96,97]. In a pulse based UWB system, the number of resolvable paths could reach tens to over a hundred in typical indoor propagation environments [98], which impose technical hurdles as well as implementation difficulties. In order to capture a considerable portion of the signal energy scattered in multipath components, a conventional RAKE-based digital receiver not only has to sample and operate at a minimum of hundreds of MHz to even multi-GHz clock rates, but also requires an impractically large number of RAKE fingers. In addition, realizing optimal RAKE reception performance requires accurate channel and timing knowledge, which is quite challenging to obtain as the number of resolvable paths grows. The received pulse shapes of resolvable multipath are distorted differently due to diffraction, which make it suboptimal to use line-of-sight signal waveform as the correlation template in RAKE reception. Since these issues are unique to the UWB pulsed radios, an optimal RAKE receiver design becomes either ineffective or very complicated.

For these reasons, TR receivers (also called autocorrelation receivers) have drawn significant attention in recent years [99,100]. As a suboptimal, low-complexity alternative, TR receivers offer better multipath capture capability at much lower hardware complexity than RAKE receivers. TR encodes the data in the phase difference of the two pulses of a pulse pair. The first pulse in that pair does not carry information, but serves as a reference pulse; the second pulse is modulated by the data and is referred to as the data pulse. The two pulses are separated by a fixed delay. It can be easily shown that the receiver can demodulate this signal by simply multiplying the received signal with a delayed version of itself. The simple TR transceiver structure is shown by the block diagram in Figure 2.14 [95].

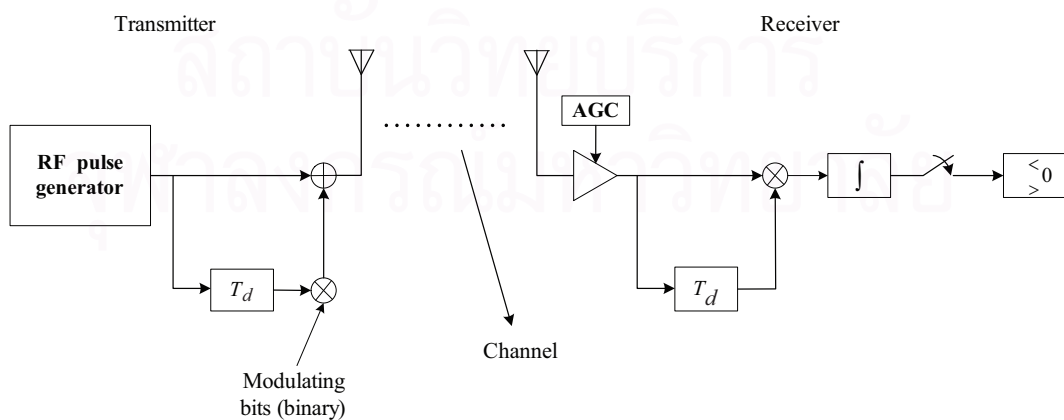


Figure 2.14 Block diagram of a transmit-reference system.

In a slow fading environment, TR collects multipath energy efficiently without requiring multipath tracking or channel estimation. Analog autocorrelation also alleviates the burden on A/D converters, thus lowering the power consumption by interface circuits in the UWB regime. However, TR autocorrelators entail several drawbacks and usually show worse performance than coherent RAKE receivers: the use of reference pulses increases transmission overhead and reduces data rate, which results in reduced transmission power efficiency; the bit error rate (BER) performance is limited by the noise term in the reference signal [100]. Finally, the performance of TR receivers relies on the implementation of accurate analog delay lines which can save and delay the reference waveforms for up to tens of nanoseconds. This is still a big challenge to current circuit technology.



สถาบันวิทยบริการ
จุฬาลงกรณ์มหาวิทยาลัย

CHAPTER III

UWB PULSE SHAPE DESIGN

This chapter presents a novel technique in designing the optimum pulse and the orthogonal pulses under the presence of timing jitter to improve the performance of UWB systems. Moreover, it describes the key idea and the foundation of this technique. The proposed pulses attain the adequate power to meet the FCC spectral masks and simultaneously provide good resistance to the timing jitter. First of all, we review the UWB regulations prescribed by the FCC. And then, we show the conventional UWB pulses that have been widely adopted since the early stage of UWB applications. Moreover, we discuss the UWB system model used in this study and the relationship between the autocorrelation and a PSD. Later, the novel pulse optimization technique, which jointly considers both pulse power and timing jitter resistance, is demonstrated. Finally, we investigate the orthogonal pulses based on the optimum proposed pulse.

3.1 UWB Regulations

In February 2002, the FCC amended the Part 15 rules to allow operation of devices incorporating UWB technology in the frequency band of 3.1 - 10.6 GHz [1]. Devices must operate within this 7.5 GHz of unlicensed spectrum and be designed to coexist with other allocated radio systems in an uncontrolled environment. The FCC rules ensure that UWB emission levels are exceedingly small, with very low PSD. The Equivalent Isotropically Radiated Power (EIRP) limit is -41 dBm/MHz. The total emitted power over several gigahertz of bandwidth is a fraction of a milliwatt. The spectrum mask of the UWB signal is shown in Figure 3.1.

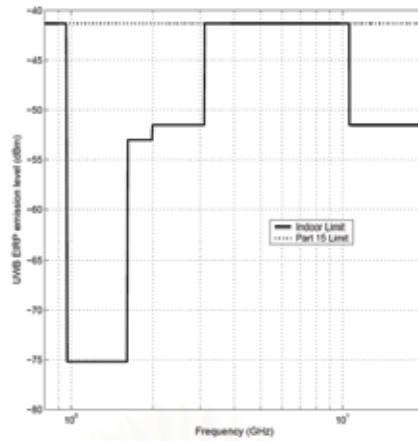


Figure 3.1 FCC spectral masks for indoor communications.

3.2 Gaussian Pulses

In most the UWB literature, three types of the UWB pulses are usually employed; they are a Gaussian pulse, Gaussian monocycle, and Gaussian doublet. The Gaussian pulse has a shape of the Gaussian distribution. It is worth to note that the Gaussian pulses remains the Gaussian distribution when it passes through any linear systems. A general formula of the Gaussian pulse is shown in (3.1). The Gaussian monocycle is the first derivative of the Gaussian pulse and the Gaussian doublet is the second derivative of the Gaussian pulse. The general formulas for the Gaussian monocycle and the Gaussian doublet are shown in (3.2) and (3.3) respectively.

$$y_1(t) = K_1 e^{-\left(\frac{t}{\tau_g}\right)^2} \quad (3.1)$$

$$y_2(t) = K_2 \left(\frac{-2t}{\tau_g^2}\right) e^{-\left(\frac{t}{\tau_g}\right)^2} \quad (3.2)$$

$$y_3(t) = K_3 \left(\frac{-2}{\tau_g^2}\right) \left(1 - \frac{2t^2}{\tau_g^2}\right) e^{-\left(\frac{t}{\tau_g}\right)^2} \quad (3.3)$$

where τ_g is a time-scaling factor, $K_1 = \sqrt{E/\sqrt{\pi/2}}$, $K_2 = \sqrt{\tau_g E/\sqrt{\pi/2}}$, and $K_3 = \tau_g \sqrt{\tau_g E/3\sqrt{\pi/2}}$ are the amplitude constant with E being the desired energy of $y_1(t)$, $y_2(t)$ and $y_3(t)$, respectively. The three pulses, i.e., the Gaussian pulse, monocycle pulse, and doublet pulse, are compared in time domain in Figure 3.2. In all three cases, $\tau = 50$ ps is assumed. It can be seen that the Gaussian pulse has no zero crossing point, the monocycle pulse has one zero crossing, and the doublet pulse has two zero crossings.

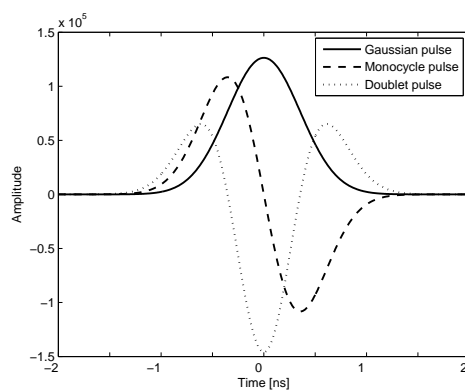


Figure 3.2 A Gaussian pulse, monocycle pulse, and doublet pulse in time domain.

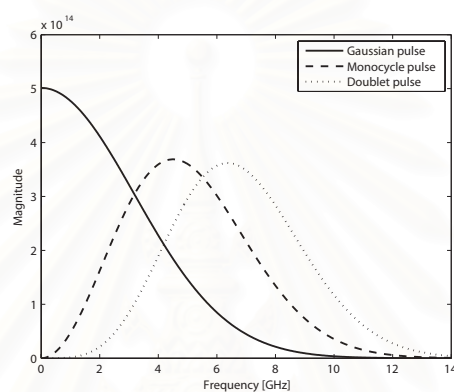


Figure 3.3 A Gaussian pulse, monocycle pulse, and doublet pulse in frequency domain.

The power spectral density (PSD) of the three pulses are examined side by side in Figure 3.3. The PSD of the Gaussian pulse centers at zero frequency. The power density spectrum centers of monocycle and doublet pulse are skewed to higher frequency, and the doublet pulse is more skewed than the monocycle pulse.

สถาบันวิทยบริการ
จุฬาลงกรณ์มหาวิทยาลัย

3.3 System Model

In UWB systems, every information symbol is conveyed over a train of N_f repeated basic pulses, with one pulse per frame of frame duration T_f . Each pulse $p(t)$ is limited to an ultra-short duration T_p at the nanosecond scale ($T_p \ll T_f$, and hence occupies an ultra-wideband. The equivalent symbol signature waveform is $p_s(t) := \sum_{n=0}^{N_f-1} p(t - c_n T_c - n T_f)$ of symbol duration $T_s := N_f T_f$, where the sequence $\{c_n\}_{n=0}^{N_f-1}$ represents the user-specific pseudo-random time-hopping (TH) code with $c_n T_c \ll T_f$, $\forall n \in [0, N_f - 1]$. Let $b_k \in \{\pm 1\}$ be independent and identically distributed (i.i.d) binary data symbols with energy ε_s spreading over N_f frames. Focusing on pulse amplitude modulation (PAM), we express the transmitted PAM UWB waveform as:

$$u(t) = \sqrt{\varepsilon_s/N_f} \sum_k b_k p_s(t - k T_s). \quad (3.4)$$

The power spectral density (PSD) of $u(t)$ is then given by

$$\phi_{uu}(f) = \frac{\varepsilon_s}{N_f T_s} |P_s(f)|^2 \quad (3.5)$$

where $P_s(f)$ is the Fourier transform (FT) of $p_s(t)$, whose spectrum depends not only on $p(t)$, but also on the TH code $\{c_n\}_{n=0}^{N_f-1}$. Specially, $P_s(f)$ can be expressed as

$$P_s(f) = P(f) \sum_{n=0}^{N_f-1} e^{-j2\pi f n T_f} e^{-j2\pi f c_n T_c} \quad (3.6)$$

where $P(f)$ is the FT of $p(t)$. Eq. 3.5 now becomes

$$\phi_{uu}(f) = \frac{\varepsilon_s}{T_s N_f} |P(f)|^2 \left| \sum_{n=0}^{N_f-1} e^{-j2\pi f (n T_f - c_n T_c)} \right|^2 \quad (3.7)$$

when the TH code $\{c_n\}_{n=0}^{N_f-1}$ is independent and uniformly distributed over $[0, N_c - 1]$ with integer values, $\phi_{uu}(f)$ can be approximated as [47]:

$$\phi_{uu}(f) \approx \varepsilon_s \frac{|P(f)|^2}{T_f}. \quad (3.8)$$

It is observed that the spectral shape of $p(t)$ determines the power spectrum of a UWB transmitter. Hence, the UWB pulse design problem is equivalent to designing the basic pulse $p(t)$ to meet all of the system requirements.

In this dissertation, we consider the characteristics of a UWB pulse under the presence of background noise and timing jitter. Non-overlapping time slot is allocated to each user so that the UWB pulses of different users cannot interfere with each other. As a result, a multi-user system can be regarded as a simple single user system. Since the UWB pulse has extremely short duration, most of the significant multipath components are more than pulse duration apart. Therefore, we can simplify the system model by

neglecting the distortion due to multipath. This simplification is similar to what other researchers have done [51,52]. Even though, the technique developed from the simplified model will be suboptimal for the multipath channels, it does not require the knowledge of channel information, which facilitates the generalized pulse design for any channels. In fact, we can integrate the channel information into the pulse design by pre-compensating the channel distortion to the optimized pulse.

Assuming an antipodal pulse amplitude modulation (PAM) over an additive white Gaussian noise (AWGN) channel, the received signal, corresponding to the n^{th} binary codeword, is given by

$$r_n(t) = \alpha_n b_n p(t) + w_n(t) \quad (3.9)$$

where α_n is a path loss factor, b_n is the n^{th} binary data bit, $p(t)$ is a UWB pulse waveform with duration T_p , and $w_n(t)$ is a noise term, modeled as a zero mean normal distributed random process with variance σ_n^2 .

The decision statistic is given by a correlator, which multiplies the received signal by a pulse waveform and then integrates the output from that process. The sampled signal at an output of the correlator is given by

$$\begin{aligned} y_n(t) &= \int_0^{T_p} r_n(t) p(t + \tau) dt \\ &= \int_0^{T_p} \alpha_n b_n p(t) p(t + \tau) dt \\ &\quad + \int_0^{T_p} w_n(t) p(t + \tau) dt \\ &= \alpha_n b_n \delta(\tau) + \tilde{w}_n \end{aligned} \quad (3.10)$$

where τ is a timing jitter. Timing jitter is modeled as a normal distributed random process with zero mean and variance σ_τ^2 [57, 59, 68]. As indicated in [72], the *root-mean-square* (RMS) of timing jitter, σ_τ , typically ranges from 10 to 150 ps in the UWB receivers. It should be noted that, even though, we assume timing jitter as a normal distributed random variable, our proposed algorithm can modify other timing jitter models as well. The $\delta(\tau) = \int_0^{T_p} p(t) p(t + \tau) dt$ is a pulse autocorrelation value at the delay τ and \tilde{w}_n is a normal distributed random process with zero mean and variance $\tilde{\sigma}_n^2 = \sigma_n^2 \left| \int_0^{T_p} p(t + \tau) dt \right|^2$.

Information bit is detected by comparing the decision statistic to a zero threshold. Using (3.10), we can express the probability of error or bit error rate (BER) for a given timing jitter τ' as

$$P_e(\tau = \tau') = \begin{cases} Q\left(\frac{\alpha_n \delta(\tau')}{\sqrt{N_0/2}}\right) & ; \delta(\tau') \geq 0 \\ 1 - Q\left(\frac{\alpha_n \delta(\tau')}{\sqrt{N_0/2}}\right) & ; \delta(\tau') < 0 \end{cases} \quad (3.11)$$

where $Q(\cdot)$ is the complementary cumulative distribution function of the unit normal random variable, and N_0 is the noise power spectral density.

Among several factors, having an effect on the probability of error, it is only a pulse shape that we can control. For the systems with perfect timing synchronization (i.e. $\tau' = 0$), $\delta(\tau')$ will be at its maximum non-negative value. In this case, a pulse shape should intuitively be designed to achieve maximum power under the spectrum mask constrain. Unfortunately, a realistic system tends to undergo the timing misalignment situation. Therefore, a more complicated pulse shape optimization technique is needed.

The overall probability of error is obtained by averaging (3.11) over the probability density function (PDF) of timing jitter

$$P_e = \frac{1}{\sqrt{2\pi\sigma_\tau^2}} \int_{-\infty}^{\infty} P_e(\tau) e^{-\frac{\tau^2}{2\sigma_\tau^2}} d\tau \quad (3.12)$$

3.4 Relationship between the Autocorrelation and a PSD

From the BER expression in (3.11), it is seen that the most important characteristic of the UWB pulse is its autocorrelation function ($\delta(\tau')$). The desirable autocorrelation function should have large positive value over a wide range of timing jitter delay as depicted in Figure 3.4. Since the autocorrelation function is directly related to a PSD through the Fourier transform, the wide shape autocorrelation function should normally have a narrow shape PSD. As a consequence, the pulse with a desired autocorrelation function may not efficiently utilize the allocated spectrum. An example of pulse with the desired PSD is shown in Figure 3.5. It is observed that the pulse of Figure 3.5 has the narrow shape autocorrelation function. Such pulse waveform is susceptible to the timing jitter.

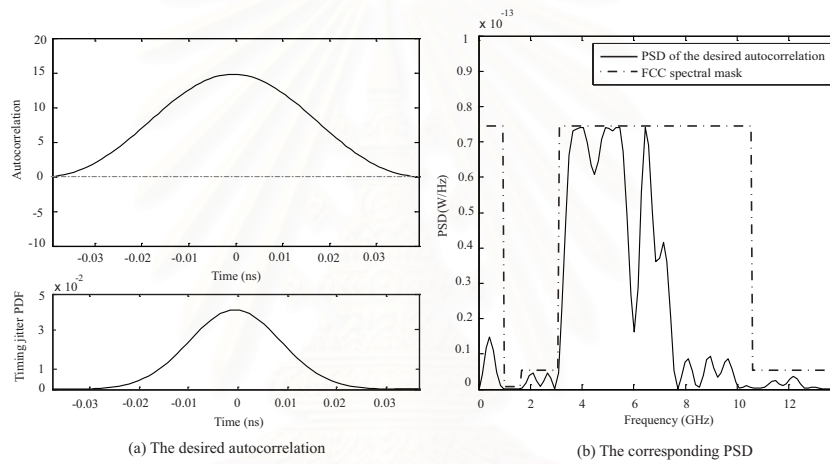


Figure 3.4 The desirable autocorrelation pulse and its corresponding PSD.

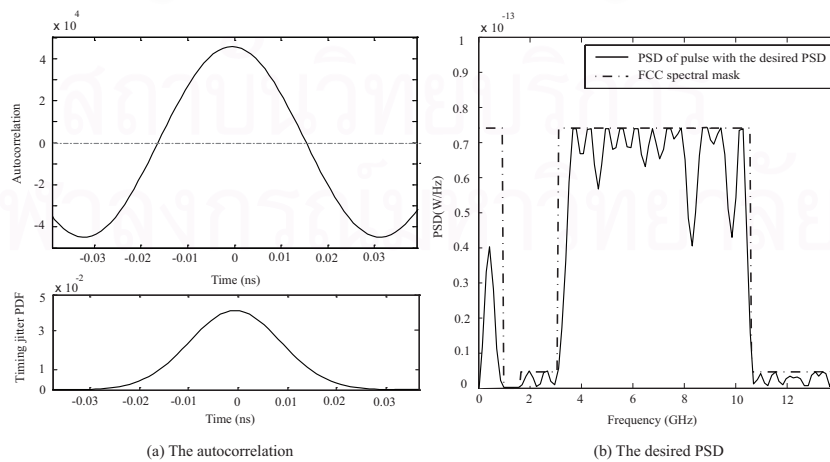


Figure 3.5 The desirable PSD pulse and its corresponding PSD.

The relationship between the correlator output value and the BER at various levels of noise power is depicted in Figure 3.6. From Figure 3.6, we can notice that the BER is not a linear function of the correlator output value. For a low noise power case, we can observe a very steep slope of the BER on the transition area between the positive and negative correlator output values. A small negative correlator output value can even result in the extremely high BER (BER approaches 1). At the same time, a very large positive correlator output value is not needed because only a small positive correlator output value can give the almost error-free level. It should be noted that the BER in Figure 3.6 is obtained under the offset correlator condition. Therefore, the BER values can be higher than 0.5 especially in the case that the correlator gives negative output. For example, the reader may consider the case that the timing aligned correlator gives output value of A but the timing mismatch alters the correlator output to $-B$. In this case, the timing mismatched output is no longer reliable and if there is no background noise, it can result in a completely wrong decision.

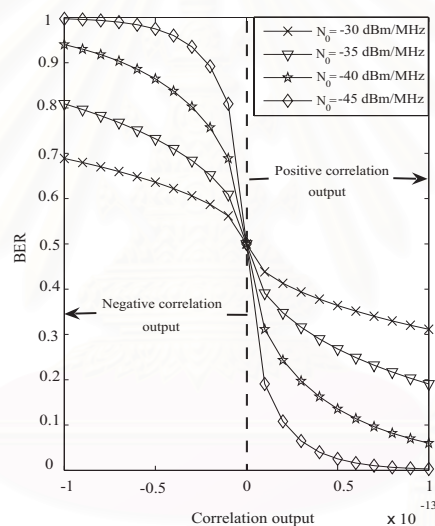


Figure 3.6 BER versus Correlation output.

3.5 Pulse Shape Optimization

In this section, a novel pulse optimization technique, which jointly considers both pulse power and timing jitter resistance, is proposed [101]. The proposed pulse attains the adequate power to survive the noise floor and simultaneously provides good robustness to timing jitter. The proposed pulse also meets the power spectral mask restriction as prescribed by the FCC for the indoor UWB systems.

According to the literature, the direct optimization of a pulse waveform experiences several obstacles such as excessive optimization variables, requirement of high speed digital to an analog (D/A) converter, and implementation difficulty [20–43]. In order to avoid such disadvantages, we indirectly generate the pulse by feeding an arbitrary pulse waveform into an N -tap finite impulse response (FIR) filter as shown in Figure 3.7. The input pulse can be any pulses that are easily generated. The resultant pulse is described by

$$p(t) = \sum_{k=0}^{N-1} x[k] q(t - kT_0) \quad (3.13)$$

where $x[k]$ is the k^{th} tap coefficient, T_0 is filter tap delay, $q(t)$ is an input pulse. In this dissertation, the well-known Gaussian monocycle pulse is selected as the input pulse. The picture of the Gaussian monocycle pulse is illustrated in Figure 4.6.

We define the Fourier transform of $p(t)$, $x[k]$, and $q(t)$ as $P(f)$, $X(e^{j2\pi fT_0}) := \sum_{k=0}^{N-1} x[k]e^{-j2\pi f kT_0}$ and $Q(f)$, respectively. The power spectrum of the UWB pulse can be formulated as

$$S_p(f) = S_q(f) S_x(f) \quad (3.14)$$

where $S_p(f) := |P(f)|^2$ is the power spectrum of $p(t)$,
 $S_q(f) := |Q(f)|^2$ is the power spectrum of $q(t)$,
 $S_x(f) := |X(e^{j2\pi fT_0})|^2$ is the power spectrum of $x[k]$.

Imposing the FCC regulations, the UWB pulse $p(t)$ must be designed so that, $S_p(f) \leq S_{FCC}(f)$ or equivalently $S_x(f) \leq S_{FCC}(f)/S_q(f)$, where $S_{FCC}(f)$ is the regulatory mask function. In this dissertation, we choose the FCC as a regulatory

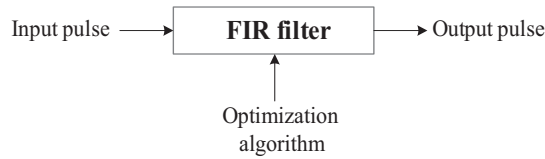


Figure 3.7 The UWB pulse design by the digital FIR filter.

body and we adopt its spectrum mask in our simulation. However, our optimization scheme does not limit to only the FCC spectral masks. Any other spectrum regulations can be employed to our algorithm. The examples of our algorithm constrained by FCC and other regulations are given in the next chapter. A set of filter coefficients $\{x[k]\}_{k=0}^{N-1}$ and a set of autocorrelation samples of $x[k]$, i.e., $r[m] = \sum_k x[k]x[k+m]$, can be combined into a vector form as follows: $\mathbf{x} := [x[0], x[1], \dots, x[N-1]]^T$ and $\tilde{\mathbf{r}} = [r[0], r[1], \dots, r[N-1]]^T$, respectively. Where bold lower case letters denote column vectors and $(\cdot)^T$ denotes transposition.

We further define

$$\mathbf{v}(f, N) = [1, e^{j2\pi f T_0}, e^{j2\pi f 2T_0}, \dots, e^{j2\pi f (N-1)T_0}]^T \quad (3.15)$$

$$\tilde{\mathbf{v}}(f, N) = [1, \cos(2\pi f T_0), \cos(2\pi f 2T_0), \dots, \cos(2\pi f (N-1)T_0)]^T \quad (3.16)$$

where $\mathbf{v}(f, N)$ and $\tilde{\mathbf{v}}(f, N)$ form the basis of complex-phase and linear-phase components, respectively. Now, the frequency response and the power spectrum form of $x[k]$ can be given by

$$X(e^{j2\pi f T_0}) = \mathbf{v}^H(f, N) \mathbf{x} \quad (3.17)$$

$$\begin{aligned} S_x(f) &= |X(e^{j2\pi f T_0})|^2 = \text{Re}(e^{j2\pi f T_0}) \\ &= \tilde{\mathbf{v}}^T(f, N) \tilde{\mathbf{r}} \end{aligned} \quad (3.18)$$

where $\text{Re}(\cdot)$ denotes the real part and $(\cdot)^H$ represents Hermitian transposition.

From the discussion in Section 3.4, the desired pulse should have large positive autocorrelation for all timing jitter delays. With careful consideration regarding the severity of a negative correlator output, the desired pulse should also have as less negative autocorrelation value as possible. Since the timing jitter is a random variable, we have to consider a mean autocorrelation value over timing jitter PDF. Finally, the pulse's PSD must be restricted to the FCC spectral masks. These circumstances can be translated into the following constrained optimization formulations:

$$\text{Objective :} \quad \max_{\mathbf{x}} \{\varphi\} \quad (3.19)$$

$$\text{Subjected to :} \quad \tilde{\mathbf{v}}^T(f, N) \tilde{\mathbf{r}} \leq \frac{S_{FCC}(f)}{S_q(f)} \quad (3.20)$$

where φ is a mean correlation output which is given as:

$$\varphi = \frac{1}{\sqrt{2\pi\tilde{\sigma}_\tau^2}} \int_{-\infty}^{\infty} g_{\mathbf{x}}(\tau) e^{-\frac{\tau^2}{2\tilde{\sigma}_\tau^2}} d\tau \quad (3.21)$$

where $\tilde{\sigma}_\tau^2$ is a target timing jitter variance for an optimization purpose, and $g_{\mathbf{x}}(\tau)$ is the weighted autocorrelation function of the synthesized pulse. $g_{\mathbf{x}}(\tau)$ is defined as

$$g_{\mathbf{x}}(\tau) = \begin{cases} \delta_{\mathbf{x}}(\tau), & \text{for } \delta_{\mathbf{x}}(\tau) \geq 0 \\ G \cdot \delta_{\mathbf{x}}(\tau), & \text{for } \delta_{\mathbf{x}}(\tau) < 0 \end{cases} \quad (3.22)$$

where $\delta_{\mathbf{x}}(\tau)$ is the autocorrelation function of the pulse generated by a filter with coefficients value \mathbf{x} and G is a weight factor for negative correlation (WFNC). The WFNC is presented to stress the significance of the negative correlator output.



สถาบันวิทยบริการ
จุฬาลงกรณ์มหาวิทยาลัย

3.6 Orthogonal Pulse Shape

In this section, the orthogonal pulses design technique is proposed. This technique can be used additionally for improving the UWB pulse system capacity. For the orthogonal pulses design, we look at two pulses $p_i(t)$ and $p_j(t)$ that are generated by two different sets of filter coefficients \mathbf{x}_i and \mathbf{x}_j each of length N . Cross-correlation between $p_i(t)$ and $p_j(t)$ is defined as

$$C_{i,j}(\tau) = \int_0^{T_p} p_i(t)p_j(t+\tau)dt \quad (3.23)$$

If the autocorrelation function of $q(t)$ is denoted $R_q(\tau) = \int_0^{T_q} q(t)q(t+\tau)dt$, substituting (3.13) in (3.23) results in

$$C_{i,j}(\tau) = \mathbf{x}_i^T \mathbf{R}_q(\tau) \mathbf{x}_j. \quad (3.24)$$

Here, $\mathbf{R}_q(\tau)$ is the $N \times N$ Toeplitz matrix of $R_q(\tau)$: $\mathbf{R}_q(\tau) = [R_q(\tau + (i-j)T_s)]_{N \times N}$.

As in [35, 46–50], orthogonality among radiated pulses is defined as zero cross-correlation for a zero time shift. From (3.24), these two waveforms must be orthogonal when they have to satisfy the following constraint:

$$C_{i,j}(0) = \mathbf{x}_i^T \mathbf{R}_q(0) \mathbf{x}_j = 0, \text{ for } i = 1, 2, \dots, (j-1).$$

For the first step, we design the first pulse $p_1(t)$ subject to the scheme that is proposed in Section 3.5. Subsequent pulses $p_k(t)$, $k = 2, \dots, j$, are then designed one by one to fit into the desired spectral mask, as well as to be orthogonal to all previously designed pulses. This approach can be formulated and shown below:

$$\text{Objective :} \quad \max_{\mathbf{x}_j} \{\varphi\} \quad (3.25)$$

$$\text{Subjected to :} \quad \tilde{\mathbf{v}}^T(f, N) \tilde{\mathbf{r}}_j \leq \frac{S_{FCC}(f)}{S_q(f)} \quad (3.26)$$

$$\mathbf{x}_i^T \mathbf{R}_q(0) \mathbf{x}_j = 0 \quad (3.27)$$

where φ is a mean correlation output which is given as:

$$\varphi = \frac{1}{\sqrt{2\pi\tilde{\sigma}_\tau^2}} \int_{-\infty}^{\infty} g_{\mathbf{x}_j}(\tau) e^{-\frac{\tau^2}{2\tilde{\sigma}_\tau^2}} d\tau \quad (3.28)$$

where $\tilde{\sigma}_\tau^2$ is a target timing jitter variance for an optimization purpose, and $g_{\mathbf{x}_j}(\tau)$ is the weighted autocorrelation function of the synthesized pulse. $g_{\mathbf{x}_j}(\tau)$ is defined as

$$g_{\mathbf{x}_j}(\tau) = \begin{cases} \delta_{\mathbf{x}_j}(\tau), & \text{for } \delta_{\mathbf{x}_j}(\tau) \geq 0 \\ G \cdot \delta_{\mathbf{x}_j}(\tau), & \text{for } \delta_{\mathbf{x}_j}(\tau) < 0 \end{cases} \quad (3.29)$$

where $\delta_{x_j}(\tau)$ is the autocorrelation function of the pulse generated by a filter with coefficients value x_j .

In order to solve the optimization problem of Section 3.5 and the orthogonal pulse sets in this section, we adopt the available generalized non-linear optimization package in MATLAB. The MATLAB's optimization package, which is used in our simulations, is based on a Sequential Quadratic Programming algorithm [102]. In this method, a Quadratic Programming (QP) subproblem is solved at each major iteration. An estimate of the Hessian of the augmented Lagrangian is updated at each iteration using the BFGS formula. Line searches are used, and the QP subproblem is solved using an active set solution strategy. Even though the optimization process consumes much computation and time, it is only a one time calculation that can be done offline. The continuous frequency spectrum constraint is sampled to enable the numerical optimization. It should be noted that the objective function is not a convex function. The efficiency of the optimization depends on variable initialization. To compensate the local minima, we need to run a large number of optimization with different initial variable values and select only the best solution.

Our optimization algorithm requires the knowledge of the timing jitter statistics, which may not be available. However, we will demonstrate in the simulation that the pulse, obtained from inaccurate timing jitter information, can still have relatively good performance.

CHAPTER IV

THE EXPERIMENTAL RESULTS

In this chapter, we present the experimental results of the proposed technique. First of all, we consider the effects of the timing jitter on the conventional UWB pulses. And then, the performances of the optimum proposed pulse compared to the other previously known pulses in various environments are discussed. Finally, we show the examples of the orthogonal pulses that have the same necessary properties as the optimum proposed pulse.

4.1 Simulation Configuration

In our simulation, a non-overlapping time slot is allocated to each user so that the UWB pulses of different users cannot interfere with each other. As a result, a multi-user system can be regarded as a simple single user system. We further select the symbol duration (T_s) = 80 ns, the frame duration (T_f) = 20 ns and the number of frames per symbol (N_f) = 4. The TH spreading code $\{c_k\}_{k=0}^{N_f-1}$ is randomly generated taking values in $\{0, 1, 2, \dots, N_f - 1\}$.

The bit error rate (BER) performances in this dissertation are evaluated through the computer simulations. Two receiver types including RAKE and TR receivers are used in our simulations. For the RAKE receivers, perfect knowledge of the channel is provided. Two channel models such as AWGN and multipath channel are investigated in our experiment. The multipath channel model, “CM2” [93], based on NLOS (0-4 m) channel measurements is adopted due to a trade-off between LOS (0-4 m) and LOS (4-10 m). From the experimental measurements [103], a 70-dB path loss is expected for a 4-m Tx-Rx separation. Therefore, we assume 70-dB path loss in our simulations. For the imperfect time synchronized case, we assume timing jitter as a normal distributed random variable and its timing jitter variance is $\sigma_\tau^2 = 4.7187 \times 10^{-22} \text{ s}^2$ or 21.72 ps of RMS value.

4.2 Effects of Timing Jitter on the Gaussian Derivative Pulses

The main objective of this section is to investigate the impact of different order derivation of Gaussian pulses to the timing error [68]. Additionally, we also consider the effects of timing jitter on the TH-PAM and TH-PPM modulation schemes in AWGN and CM2 channel models.

The conventional waveforms, which often employ in UWB systems, are three well known Gaussian derivative pulses. The time domain of three Gaussian derivative pulses that are normalized to unitary energy and their autocorrelation are plotted and shown in Figures 4.1. From Figure 4.1(b), the higher derivative orders of Gaussian pulses are more widely shape of autocorrelation. In this sense, we can conclude that the lowest derivative Gaussian pulse causes the most resistance to timing jitter effects.

Figures 4.2 and 4.3 show the BER of the PAM modulation in AWGN and CM2 channel models, respectively. It can be seen that all of the Gaussian derivative pulses have the same probability of error when no timing jitter exists. Moreover, the BER of the imperfect timing synchronization shows that the Gaussian pulses with higher derivative orders are more sensitive to timing jitter than those with lower derivative orders. Hence, timing jitter limits the use of pulses with high derivative orders. In Figures 4.4 and 4.5, the BER of the PPM modulation under the AWGN and CM2 channel models is presented. From these figures, similar results as in the case of the PAM modulation can be observed. In the perfect timing jitter, three Gaussian derivative pulses have the same BER value, but the lower derivative orders are more enduring to timing jitter effects when the timing error occurs.

Finally, when we consider the BER under different modulation schemes, we can conclude that the TH-PAM systems provide a lower the BER than the TH-PPM systems do in all cases.

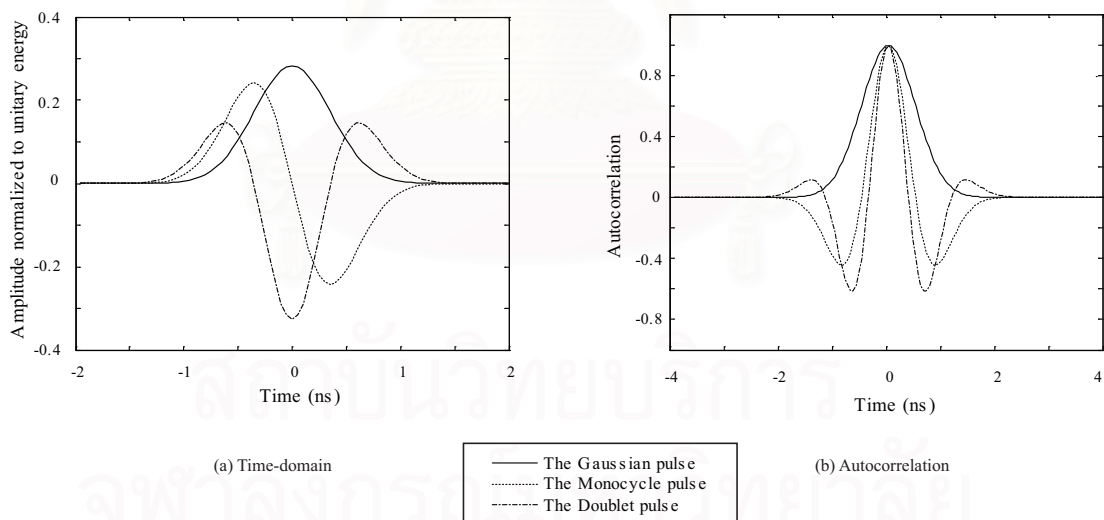


Figure 4.1 Three Gaussian derivative pulses.

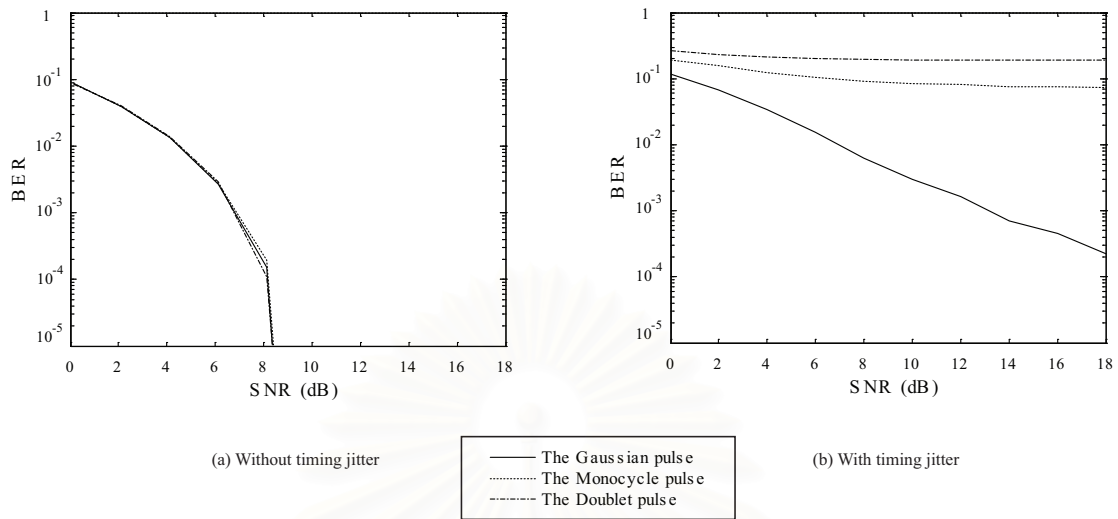


Figure 4.2: BER of binary PAM with different derivative Gaussian and timing error in AWGN.

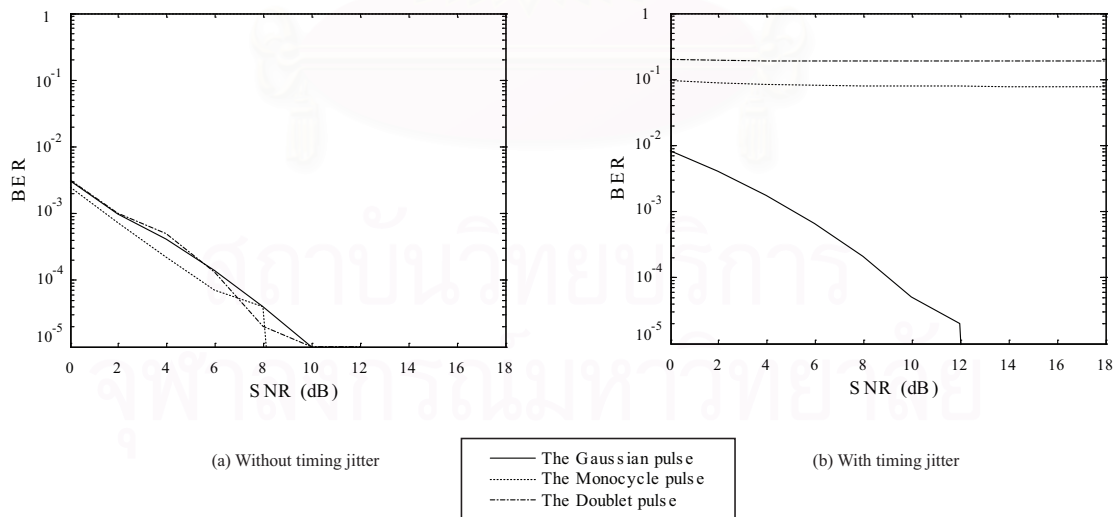


Figure 4.3: BER of binary PAM with different derivative Gaussian and timing error in multipath channel.

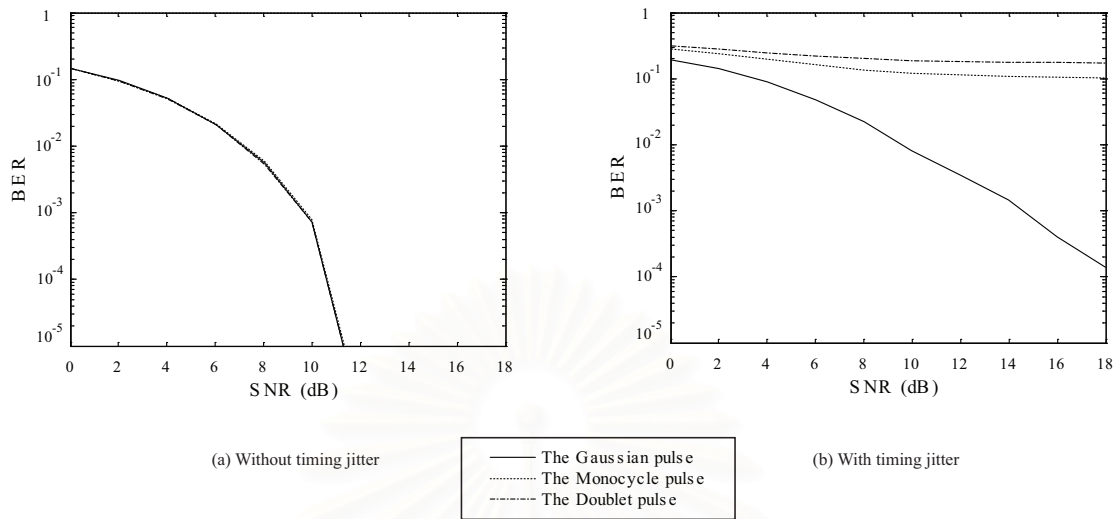


Figure 4.4: BER of optimal PPM with different derivative Gaussian and timing error in AWGN.

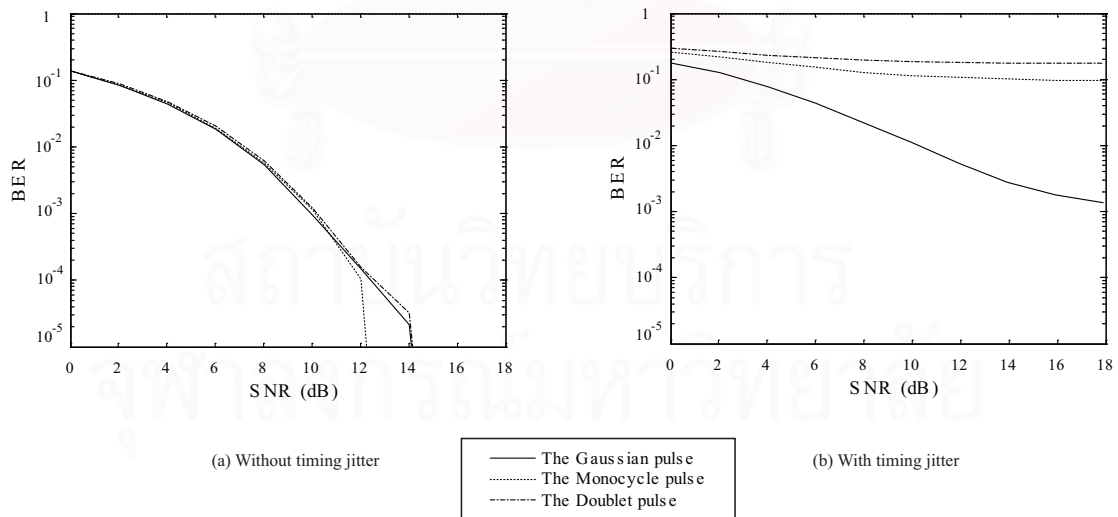


Figure 4.5: BER of optimal PPM with different derivative Gaussian and timing error in multipath channel.

4.3 Examples of the UWB Pulses Meeting the FCC Spectral Masks

In this section, we compare the performance of 3 UWB pulses families: the scaled monocycle pulse, the power optimized pulse [49], and the proposed pulse. All of the pulses have the PSD that meets the constraint of the FCC spectral masks. Firstly, we show 3 UWB pulses in the time domain, the corresponding PSD and the autocorrelation compared with the probability density function (PDF) of timing jitter. Next, the BER performances of these UWB pulses in various environments are considered and discussed.

In our simulations, the power optimized pulse [49] and the proposed pulse are obtained by optimizing the pulse shaping FIR filter, having $N = 55$ equally spaced taps. Each tap is spaced by $T_0 = 0.001$ ns and the frame duration is $T_f = 20$ ns. The input pulse for the optimization processes is the Gaussian monocycle pulse, which is scaled in order to comply with FCC regulations. The Gaussian monocycle pulse is selected for the input pulse because of its simplicity in generation.

4.3.1 The Scaled Monocycle Pulse

According to the literature, the conventional pulse, Gaussian 2^{nd} derivative pulse, is widely adopted in the investigation of the UWB applications due to mathematical convenience and ease of generation [12, 13]. Unfortunately, a PSD of the Gaussian monocycle pulse does not match the FCC spectral masks. Thus, the Gaussian monocycle pulse must be modified and filtered to meet the FCC requirements [14–17]. Referring to Figure 4.6, we show the scaled monocycle pulse whose corresponding PSD conforms the FCC spectral masks. In this case, we choose the time-scaling factor and amplitude constant of (3.2) so that its peak frequency response can be located at $1/(4\tau_g) = 6.85$ GHz and the pulse has unit energy.

The scaled monocycle pulse and its PSD are presented in Figure 4.6(a) and Figure 4.6(b), respectively. From Figure 4.6(b), it is apparent that the scaled monocycle pulse fails to utilize the allocated spectrum band in an energy-efficient manner. Figure 4.7 shows the autocorrelation of the scaled monocycle pulse and its closer view plotted along with timing jitter PDF. From Figure 4.7, we can observe that the scaled monocycle pulse has similar autocorrelation characteristics as the desired autocorrelation in Figure 3.4. Therefore, we can expect that the scaled monocycle pulse is robust to timing jitter.

4.3.2 The Power Optimized Pulse

The power optimized pulse is initiated by X. Wu and Z. Tian and T. N. Davidson and G. B. Giannakis [49]. This pulse design technique has been introduced to maximize the power utilization efficiency while complying with the spectral mask.

The power optimized pulse and its PSD are illustrated in Figures 4.8(a) and 4.8(b), respectively. From Figure 4.8(b), the PSD of the power optimized pulse is appreciatively fitted the FCC spectral masks. The autocorrelation of the power optimized pulse and its magnified view are depicted in Figure 4.9. From Figure 4.9, the autocorrelation of the power optimized pulse is less than zero for many delay values. These negative autocorrelation output values have adverse effect on BER as earlier discussed in Figure 3.6. Therefore, we can foresee the susceptibility of the power optimized pulse to timing jitter. The simulation results, later in this section, will clearly support this observation.

4.3.3 Optimum Pulse Shape Design

The proposed pulse is optimized from (3.19) and (3.20). We set the WFNC symbol equal to 10^5 and assume the jitter variance $\tilde{\sigma}_\tau^2 = \sigma_{\tau_0}^2 = 4.7187 \times 10^{-22} \text{ s}^2$. Figure 4.10 compares timing jitter PDF with the scaled monocycle pulse duration.

The proposed pulse and the corresponding PSD are plotted and shown in Figures 4.11(a) and 4.11(b), respectively. From Figure 4.11(b), the PSD of the proposed pulse is quite fitted the FCC spectral masks. Even though the PSD of the proposed pulse is not as close to the FCC spectral masks as the power optimized pulse (Figure 4.8(b)), it is far better than the scaled monocycle pulse (Figure 4.6(b)). Figure 4.12 shows the autocorrelation and its magnified view of the proposed pulse. We see that the autocorrelation of the proposed pulse has the desired properties as presented in Figure 3.4. Therefore, we can expect the good robustness of the proposed pulse to the timing jitter.

Table 4.1 compares the mean correlation output values (φ) from (3.19) of various pulse types. From Table 4.1 evidently shows that our proposed pulse has the highest mean correlation output value among all the considered pulses.

Table 4.1 Comparisons of the mean correlation output (φ)

Pulse types	φ
The scaled monocycle pulse	4.53×10^{-30}
The power optimized pulse	2.94×10^{-16}
The proposed pulse: WFNC = 10^5	2.80×10^{-14}

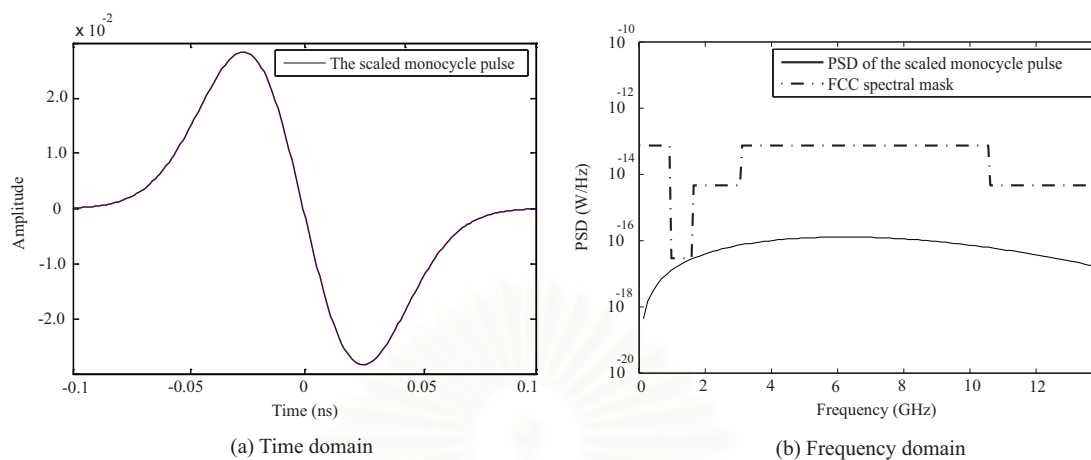


Figure 4.6 The scaled monocycle pulse and its PSD.

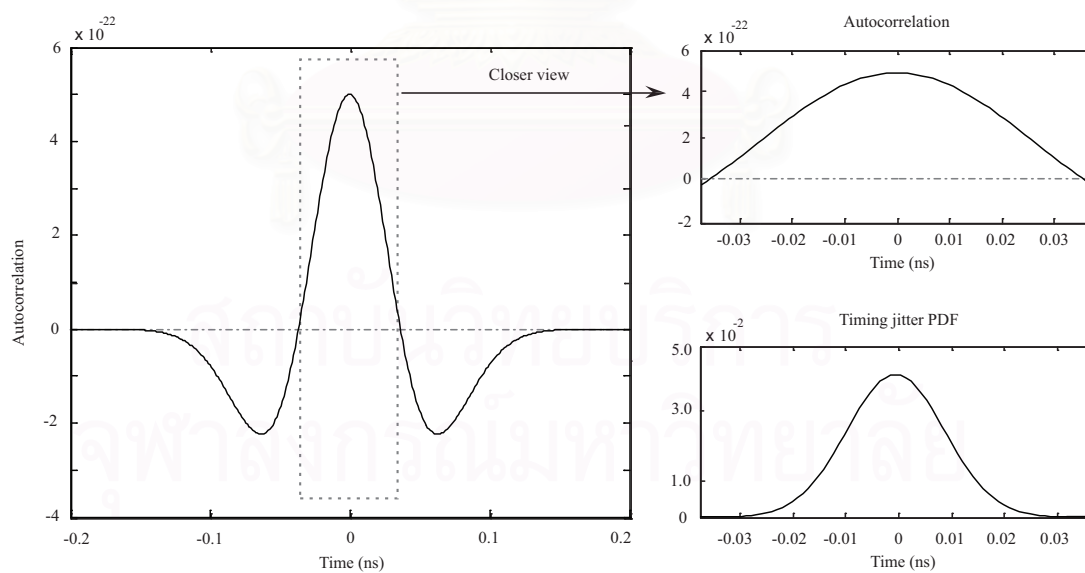


Figure 4.7 The autocorrelation of the scaled monocycle pulse.

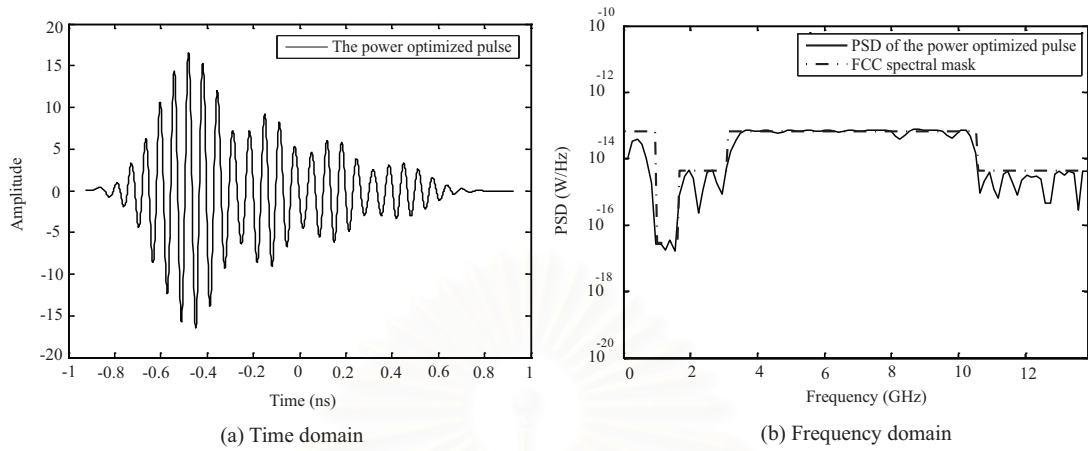


Figure 4.8 The power optimized pulse and its PSD.

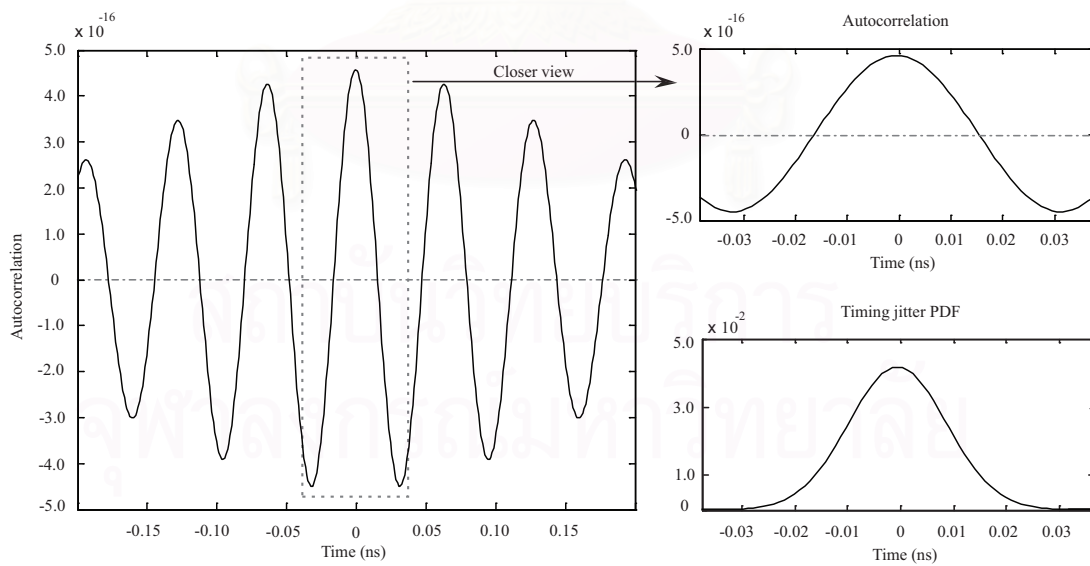


Figure 4.9 The autocorrelation of the power optimized pulse.

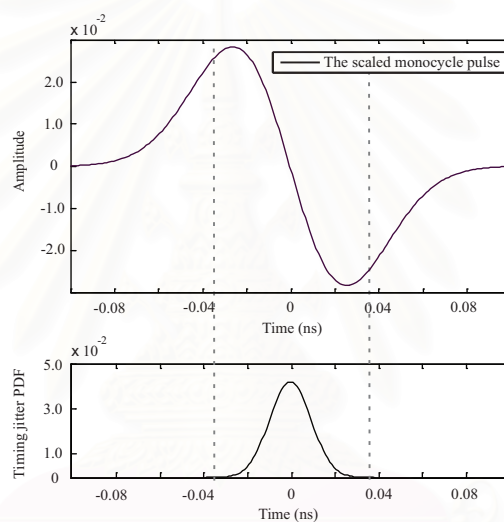


Figure 4.10 The scaled monocycle pulse compares with timing jitter PDF.

สถาบันวิทยบริการ
จุฬาลงกรณ์มหาวิทยาลัย

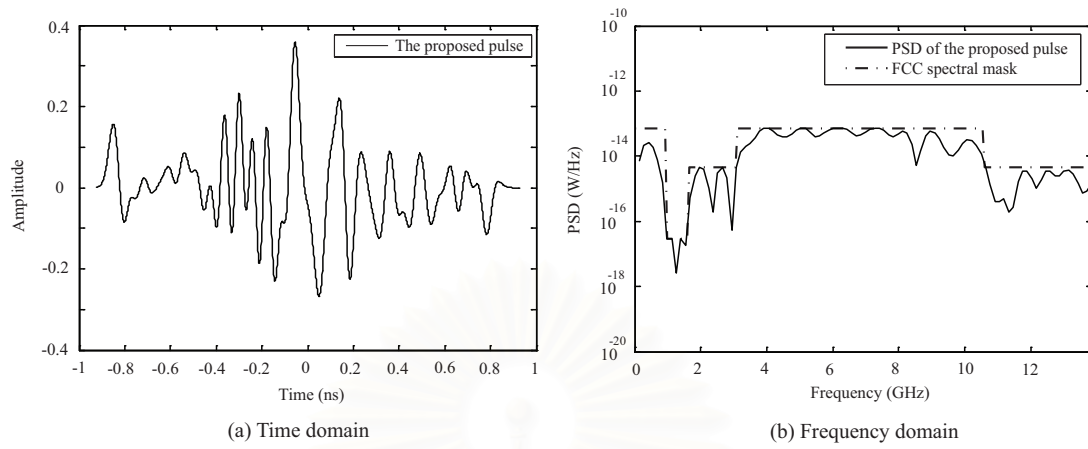


Figure 4.11 The proposed pulse and its PSD.

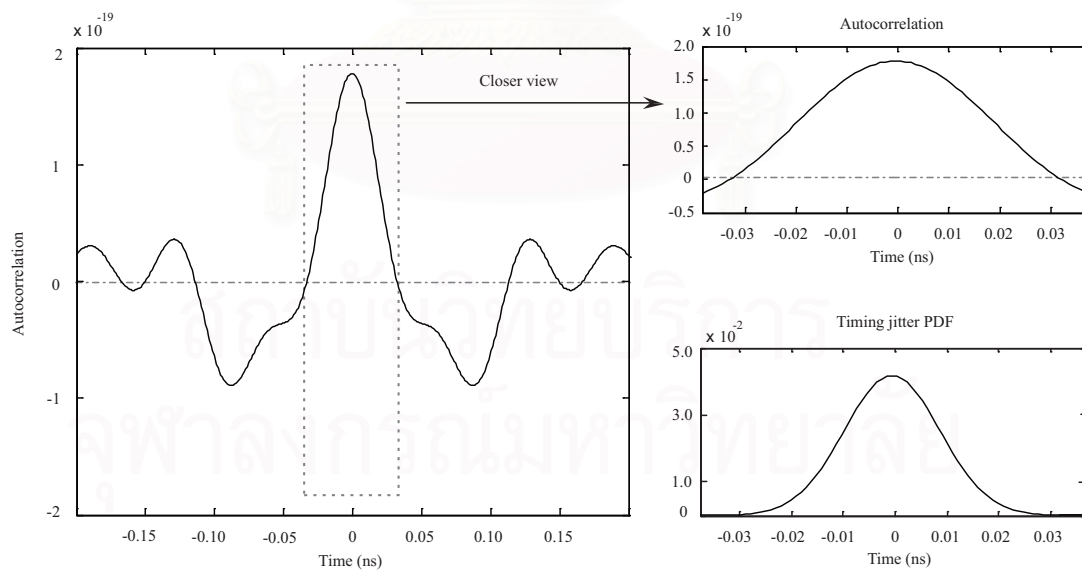
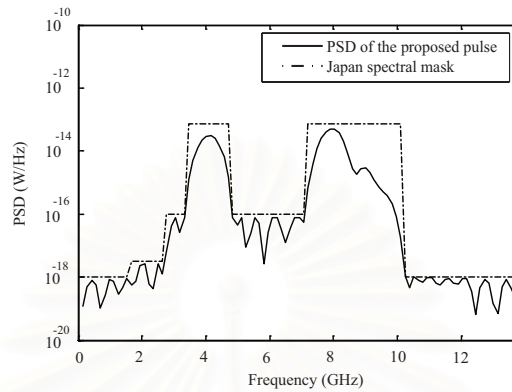


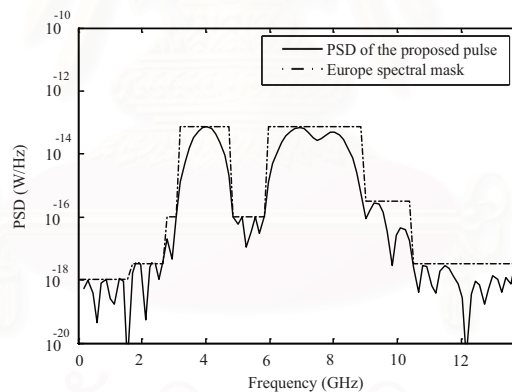
Figure 4.12 The autocorrelation of the proposed pulse.

Additionally, we demonstrate the spectrum of pulses obtained from our algorithm under other spectral masks [104]. Figure 4.13 shows the preliminary indoor transmission mask of Japan that was released in August 2005. Figure 4.14 presents the Europe or Electronic Communication Commission (ECC)'s draft of emission limits for generic UWB device in band below 10.6 GHz.



(b) Frequency domain

Figure 4.13 Japan's preliminary UWB emission mask for indoor.



(b) Frequency domain

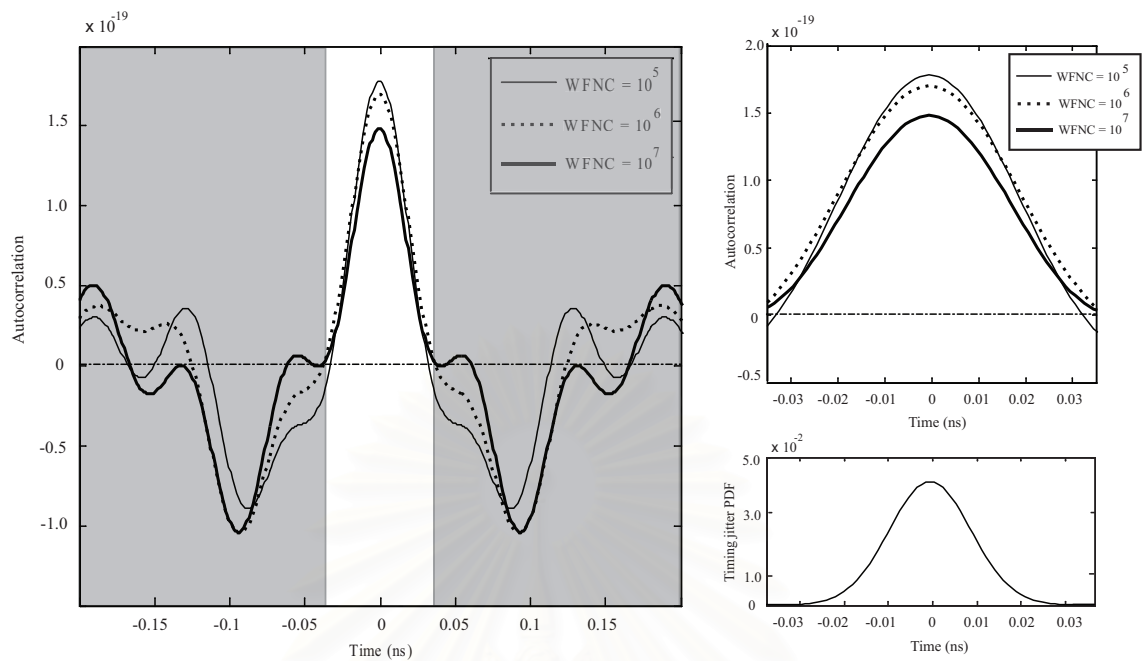
Figure 4.14 Europe's draft UWB emission mask.

4.3.4 Parameters of the Proposed Pulse

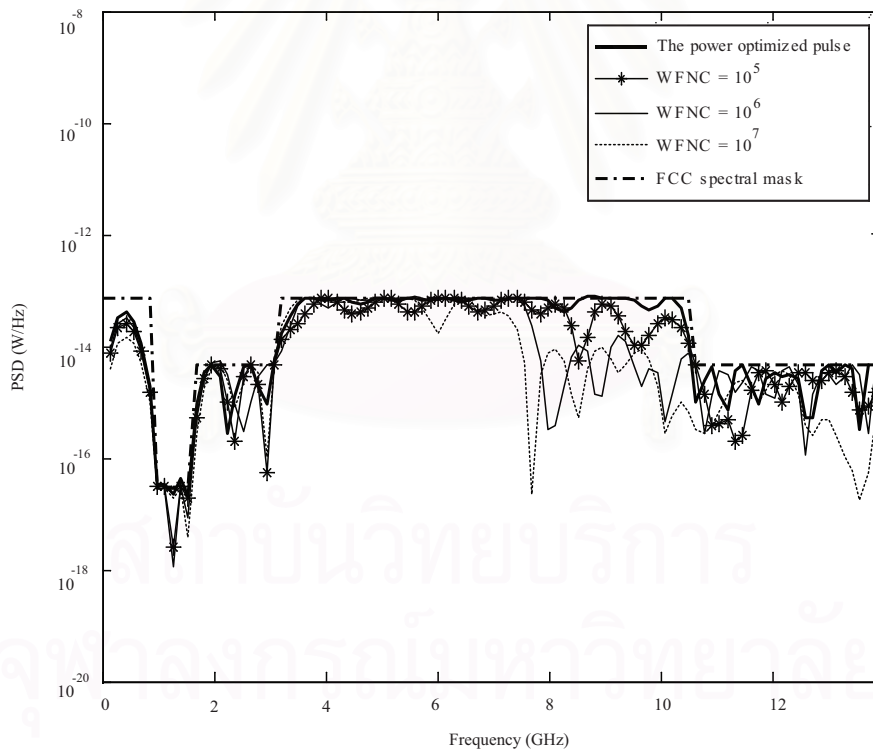
In this subsection, we show the method we used in finding the parameters of the proposed optimization algorithm. The WFNC is the importance variable for generating the proposed pulse.

Figures 4.15(a) and 4.15(b) compare the autocorrelation and the PSD of the proposed pulses, which are generated by using various WFNC values. From Figure 4.15(a), a higher WFNC value shapes the autocorrelation of the pulse to be less negative within the significant timing jitter span, which is denoted by an un-shaded region. With WFNC equal to 10^6 , the autocorrelation of the optimized pulse is positive for all important delay values. However, a high WFNC value has a draw back as shown in Figure 4.15(b). A higher WFNC value results in the optimized pulse, whose PSD more deviates from the FCC spectral masks. The relationship between the WFNC value and power of the optimized pulse is shown in Figure 4.16.

Figure 4.17 displays the BER of UWB systems using the proposed pulses that are generated by various WFNC values. The BER is calculated by assuming the jitter variance $\sigma_{\tau}^2 = \sigma_{\tau_0}^2$. The obtained results show that an appropriate WFNC value can improve the system performance. As earlier discussed, the WFNC can be seen as a trade-off parameter between pulse power and timing jitter tolerance. For a high noise PSD environment, a larger WFNC value leads to a pulse that has better robustness to timing jitter but weaker pulse power. In such a case, excessive WFNC can worsen the BER. In contrast, the BER is dominated by timing jitter in a low noise PSD environment. Under such a situation, the gain from larger WFNC is noticeable. Apart from the trade-off issue, it should also be noted that the numerical optimization algorithm becomes unstable at a very large WFNC value. In order to avoid an undesired optimization response and ensure a good performance over broad range of noisy environment, the WFNC values of 10^5 and 10^6 are considered appropriate.



(a) The autocorrelation



(b) The corresponding PSD

Figure 4.15: The autocorrelation and the corresponding PSD of the proposed pulses that are generated with various WFNC values.

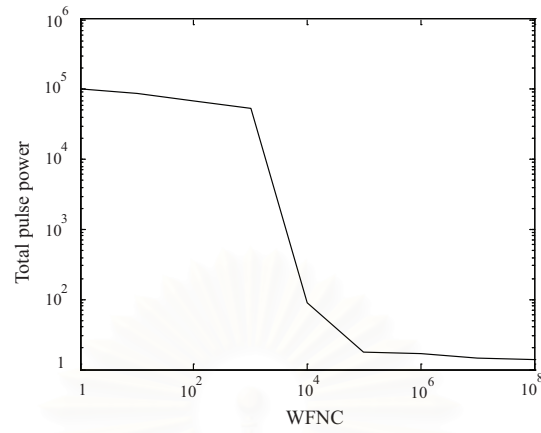


Figure 4.16 The total pulse power of the proposed pulses versus the WFNC values.

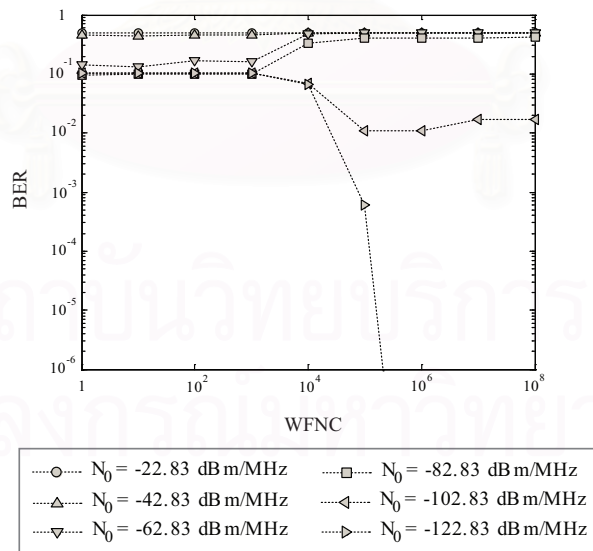


Figure 4.17 BER versus the WFNC values.

4.4 Effects of Timing Jitter on the UWB Pulses Meeting the FCC Spectral Masks

In this section, we describe our evaluated on the proposed optimization pulse against the other previously known pulses using the BER simulation. Two receiver types are used in our simulation. For the RAKE receivers, we assume that the receiver knows the channel information for detection data. For the transmitted-reference (TR) receiver, the performances and three placements of reference pulse are considered and compared.

4.4.1 RAKE Receivers

In this subsection, we first consider the BER simulation by using the RAKE receivers. According to the FCC regulations, UWB systems are focused on a short range communication (0-10 m). We simulate the experimental results under two distance cases. The first case study is 10 m Tx-Rx separation which is the longest distance of UWB systems that can work. From the experimental measurements [103], an 80-dB path loss is expected for a 10 m range. Thus, we assume 80-dB path loss in our simulations in this first case. The other case is 4 m duration of Tx-Rx. We compare two channel models: AWGN and CM2 in this second distance case. From the channel characteristics presented in Table. 2.2, the CM2 channel model represents NLOS and distance from 0 to 4 m UWB channel. Thus, the path loss of this case will be changed to 70-dB [103].

The BER versus the noise power spectral density for the system without timing jitter of 10 m Tx-Rx separation is plotted and shown in Figure 4.18(a). According to the results shown in Figure 4.18(a), the scaled monocycle pulse has the worst BER among all the considered pulses. It cannot be operated if the noise power spectral density is greater than -125 dBm/MHz. The noise power spectral density (N_0) is conventionally given by $N_0 = kT_0 \cdot F \cdot L$ where T_0 is a temperature in Kelvin, $k = 1.38 \times 10^{-23}$ J/K is Boltzmann's constant, $F = 6$ dB is a noise figure, and $L = 5$ dB is a link margin. At room temperature, $T_0 = 300$ K, the noise power spectral density is $N_0 = -102.83$ dBm/MHz. Moreover, if we consider the BER of the scaled monocycle pulse, we may conclude that the scaled monocycle pulse is not suitable for UWB communication. For a timing jitter free environment, the power optimized pulse exhibits the best performance.

Figure 4.18(b) shows the BER of the system with jitter variance $\sigma_r^2 = \sigma_{r_0}^2$. As observed from the results, the sensitivity of the power optimized pulse to timing jitter is confirmed. Timing jitter introduces an irreducible error floor to both the power optimized pulse and the proposed pulse. However, the error floor of the proposed pulse is much lower than that of the power optimized pulse. The proposed pulse is slightly overwhelmed by the power optimized pulse in the extremely strong noise PSD case. At room temperature, the proposed pulse outperforms the power optimized pulse by more

than 5 dB. It should be noted that the scaled monocycle pulse becomes the best pulse when the noise PSD is very low. In such almost noise free environment, the weak power monocycle pulse can survive the background noise and enjoy its good autocorrelation characteristics.

The proposed optimization algorithm requires knowledge of a timing jitter variance, which is normally unknown. Figure 4.19 shows the BER of the pulse, which is obtained by assuming timing jitter variance $\tilde{\sigma}_\tau^2 = \sigma_{\tau_0}^2$, in the systems with various timing jitter variance values. It is seen that the proposed pulse can outperform the power optimized pulse over a broad range of an actual timing jitter variance, although the proposed pulse is generated by an inexact timing jitter variance value.



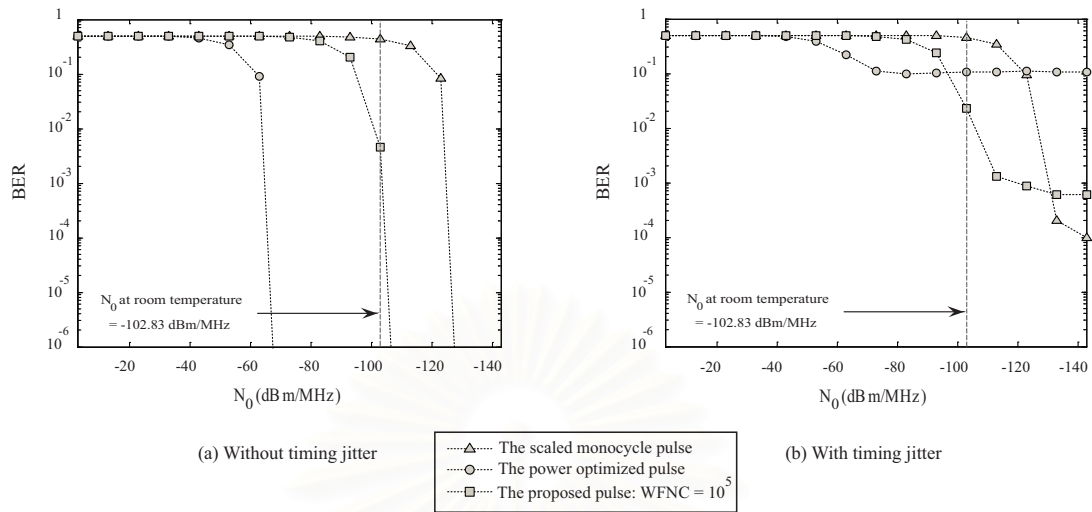


Figure 4.18: BER comparison in a system with and without timing jitter (10 m Tx-Rx separation).

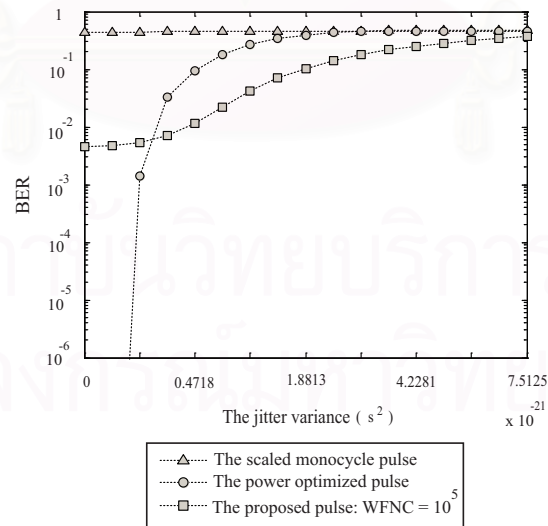


Figure 4.19 BER versus the jitter variance.

Next, we describe the comparison among the 3 UWB pulses in AWGN and CM2 channel models in 4 m Tx-Rx separation. Figure 4.20(a) shows the BER comparison of the 3 UWB pulses when no timing jitter exists in the AWGN channel. Accordingly, it is evident that the power optimized pulse demonstrates the best performance. The pulse obtained from our proposed algorithm is inferior to the power optimized pulse. However, there is no significant performance difference between the proposed pulse and the power optimized pulse at the operating temperature.

Figure 4.20(b) shows the BER performance when timing jitter occurs in the AWGN channel. It can be seen that the BER of the proposed pulse is about 20 dB lower than the error floor of the power optimized pulse. It should be noted that at room temperature N_0 in Figure 4.20 does not consider the implementation loss. In the presence of implementation loss, the N_0 will increase (the N_0 line will shift to the left). However, it can be seen from Figure 4.20 that, with a 15 dBm/MHz increase in N_0 , our proposed pulse can still provide the best BER. For the scaled monocycle pulse, the BER of this pulse at room temperature still cannot work because of the low efficient utilization of bandwidth (BW) of the scaled monocycle pulse.

For the CM2 channel model, the BER performances of 3 UWB pulses are show in Figure 4.21. As a result, the BER of this channel model is lower than the AWGN channel for all cases. Figure 4.21(b) shows the BER performance with timing jitter. We can observe that the BER of the proposed pulse of this channel model can be improved for 5 dB when comparing to the BER of the proposed pulse in AWGN channel. Unfortunately, the BER performance of the power optimized pulse cannot be changed. Thus, the comparison confirms that the proposed pulse has better performance than the power optimized pulse under timing jitter environment.

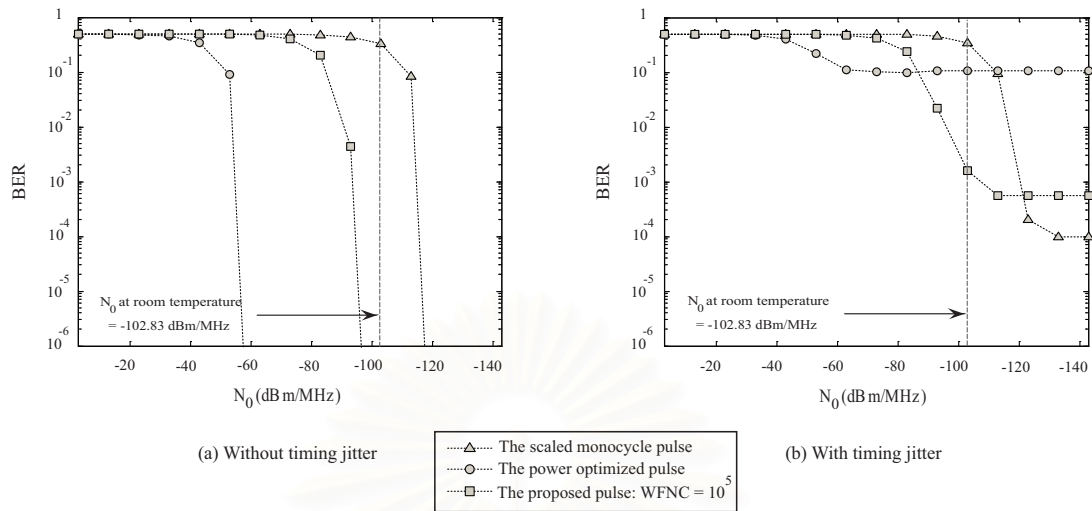


Figure 4.20: BER comparison in a system with and without timing jitter in AWGN channel (4 m Tx-Rx separation).

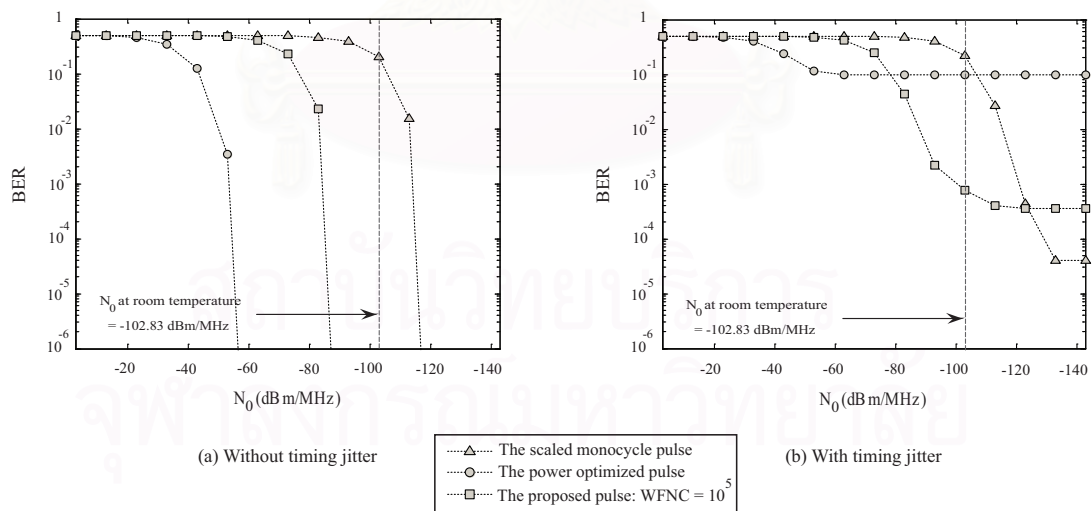


Figure 4.21: BER comparison in a system with and without timing jitter in CM2 channel (4 m Tx-Rx separation).

4.4.2 Transmitted-reference (TR) Receiver

In this subsection, we describe our evaluation on the proposed pulse against the other previously known pulses in UWB systems using a TR receiver. Nowadays, the TR receiver has drawn significant attention because this receiver type has low complexity and can collect multipath energy without requiring multipath tracking or channel estimation.

In this dissertation, three placements of a reference pulse including a simple transmitted reference (STR), an average transmitted reference (ATR) and a random average transmitted reference (R-ATR) receiver are considered. Firstly, the STR technique [105] is shown in Figure 4.22(a). This scheme generates two adjacent pulses. The first pulse that does not carry information is a reference pulse. The other pulse is modulated by the data and is referred to as the data pulse. The two pulses are separated by a fixed delay. It can be easily shown that the receiver can demodulate this signal by simply multiplying the received signal with a delay version of itself.

Secondly, an ATR method [105] is presented in Figure 4.22(b). All of reference pulses are sent to the receiver before the data information. The ATR receiver averages all the received reference pulses to reduce the noise in the reference waveform and then data detection proceeds with the reduced noise reference. The ATR receiver usually has higher complexity and better performance than the STR receiver.

In addition, the R-ATR technique is shown in Figure 4.22(c). This method is similar to the ATR scheme. However, the reference pulses are sent by a random sequence. At the receiver, the several reference pulses are also averaged for clean up the correlator template.

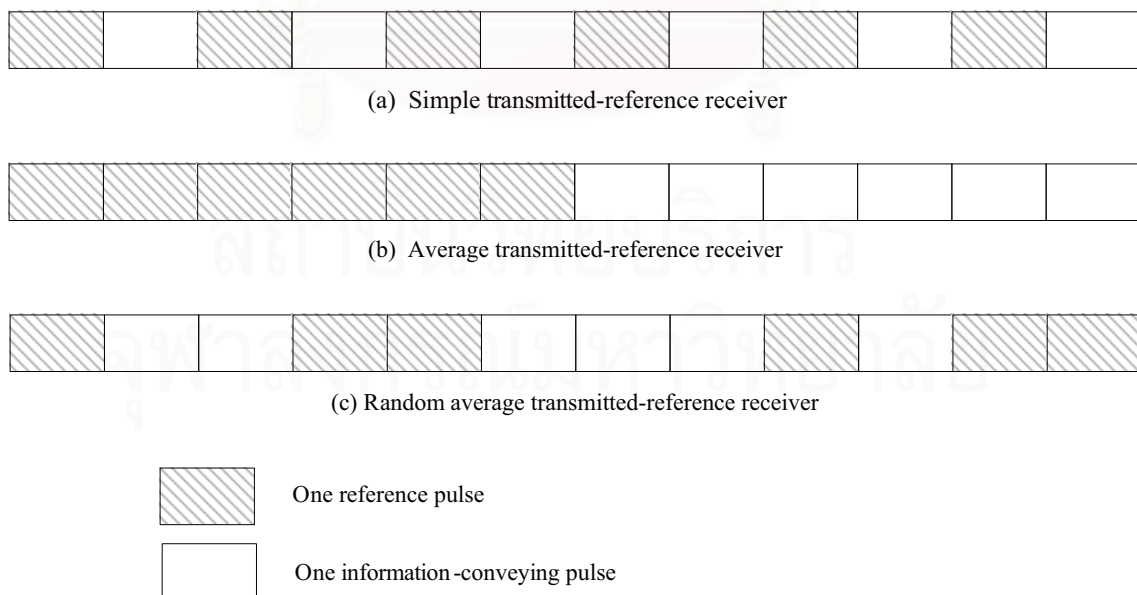


Figure 4.22 Placement of reference pulse in transmitted-reference receiver.

Figures 4.23 and 4.24 show the BER of the STR in the AWGN and CM2 channel models, respectively. The drawback of the STR receiver is the noisy reference template. Therefore, the weak power pulses cannot correctly detect. In the AWGN channel, we can observe that the BER of the scaled monocycle pulse and the proposed pulse at room temperature cannot operate. For the CM2 channel model, the performance of the BER of three comparison pulses we compare is improved. For no timing jitter exists, the power optimized pulse has also the best performance. On the contrary, the proposed pulse has a better performance than the power optimized pulse at the room temperature when timing jitter occurs. For the scaled monocycle pulse, the BER performance cannot operate because the very low power of the monocycle pulse cannot survive the noisy template waveform.

The BER of the ATR and R-ATR receivers in the AWGN channel are presented in Figures 4.25 and 4.27, respectively. In these receivers, the reference pulses are averaged in order to clean up the noises. Therefore, the weak power pulse can work in these receiver types. As a result, the BER of the proposed pulse at room temperature can operate with and without timing jitter. For the system with the timing jitter, the proposed pulse has the BER approximately 10 dB lower than the error floor of the power optimized pulse. Figures 4.26 and 4.28 reveal the BER in CM2 channel model of the ATR and R-ATR receivers, respectively. In this system, the proposed pulse has the BER approximately 15 dB lower than the power optimized pulse.

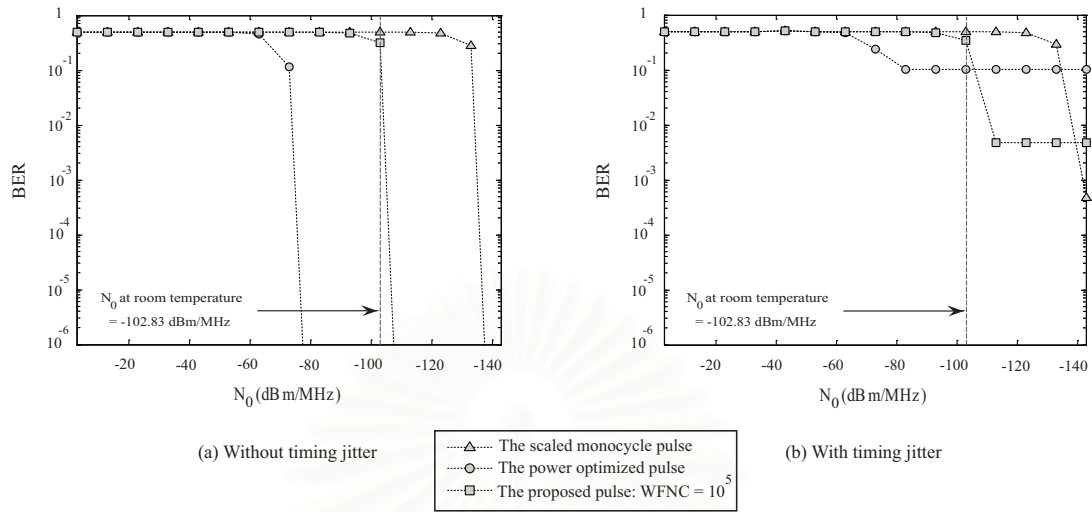


Figure 4.23 The BER of the STR receiver in AWGN channel.

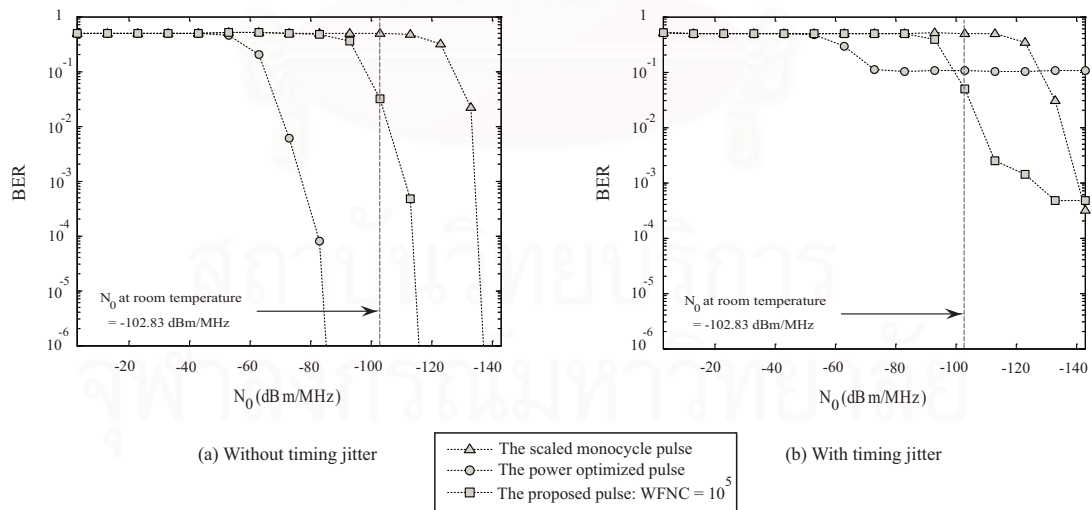


Figure 4.24 The BER of the STR receiver in CM2 channel.

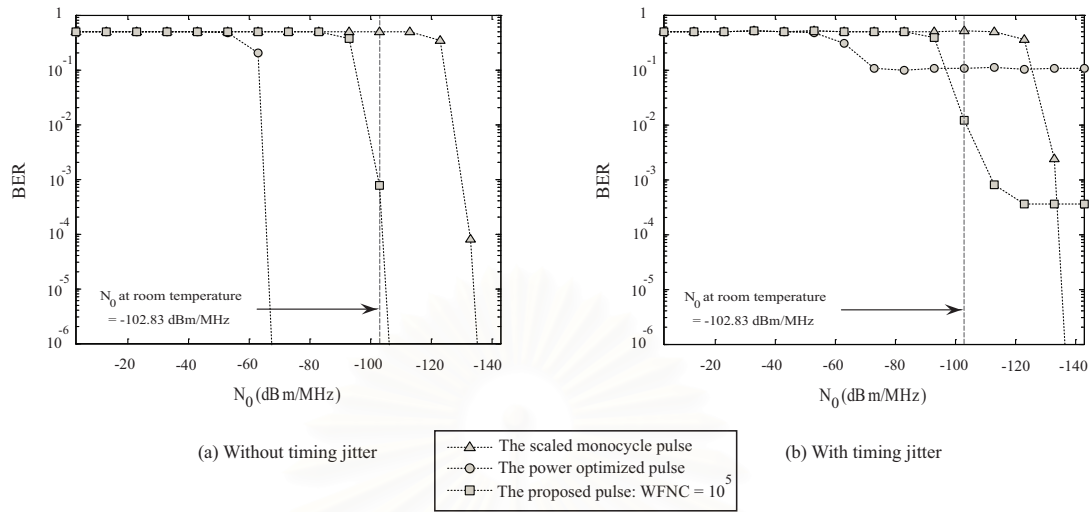


Figure 4.25 The BER of the ATR receiver in AWGN channel.

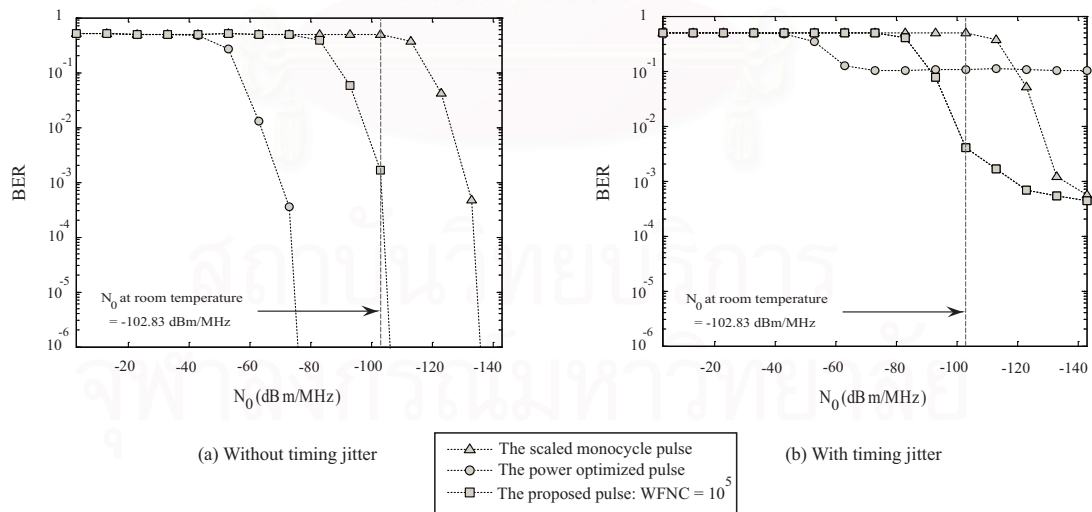


Figure 4.26 The BER of the ATR receiver in CM2 channel.

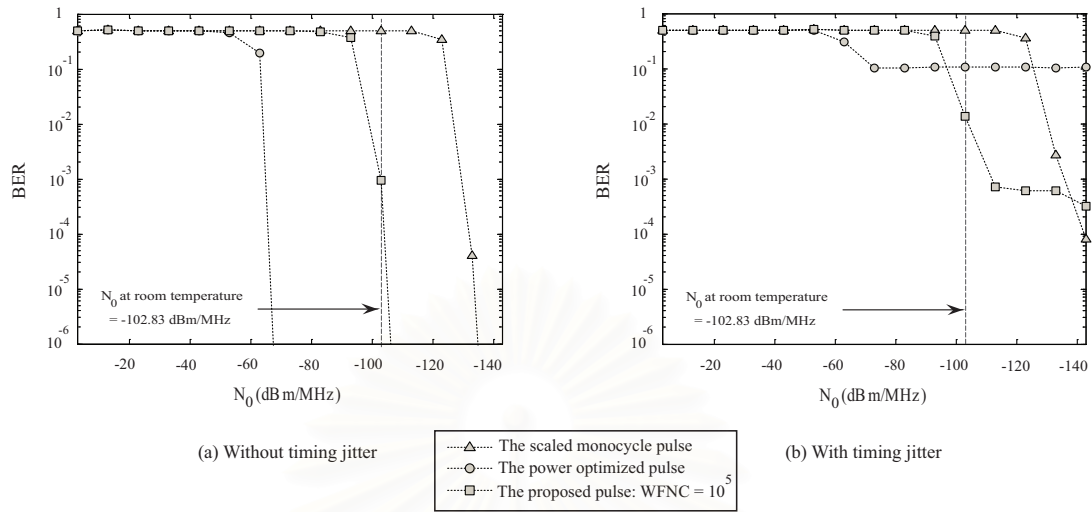


Figure 4.27 The BER of the R-ATR receiver in AWGN channel.

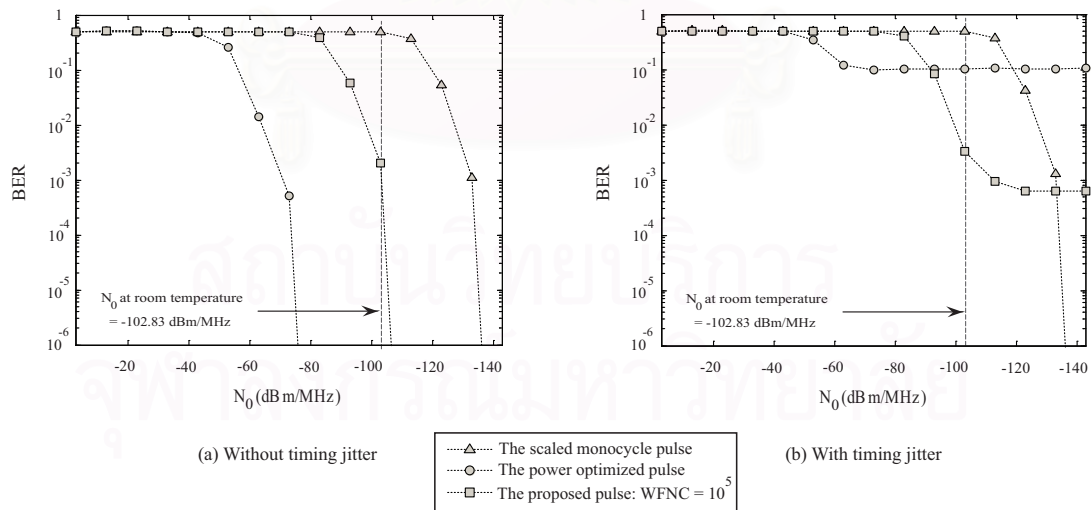


Figure 4.28 The BER of the R-ATR receiver in CM2 channel.

4.5 The Orthogonal Pulses Design with Timing Jitter

In this section, we demonstrate four examples of orthogonal pulses described in Section 3.6. The initial pulse of the orthogonal pulses set is the optimum proposed pulse shown in Figure 4.11; hereon, we call it the 1st orthogonal pulse. The other orthogonal pulses (2nd, 3rd and 4th orthogonal pulse) can generate from (3.25) and (3.26). For this technique, we set the WFNC value of all orthogonal pulses equal to 10^5 .

The time domain and its corresponding PSD of the 1st orthogonal pulse shown in Figure 4.11 and the autocorrelation comparing with the PDF timing jitter were presented in Figure 4.12. Additionally, the time domain and the corresponding PSD of the 2nd, 3rd and 4th orthogonal pulses are plotted and shown in Figures 4.29, 4.31 and 4.33, respectively. We can see that the PSD of these pulses conform the FCC spectral masks. Furthermore, the autocorrelation of the 2nd, 3rd and 4th orthogonal pulses that compare with the PDF timing jitter are demonstrated in Figures 4.30, 4.32 and 4.34, respectively. The autocorrelation of these pulses has less negative value within the significant timing jitter span. In this sense, we can conclude that all orthogonal pulses can resist timing jitter.

The cross-correlation is used to verify the orthogonality properties. Figure 4.35 shows the cross-correlation of the 1st orthogonal pulse to the other orthogonal pulses. According to this figure, the cross-correlation pulse between the 1st orthogonal pulse and the other orthogonal pulses especially at zero time is lower than the autocorrelation value of 1st orthogonal pulse. In this case, the mutual orthogonality between the 1st orthogonal pulse and the other orthogonal pulses is confirmed. For other orthogonal pulses, the cross-correlation of each pulse, 2nd, 3rd and 4th, is plotted and shown in Figures 4.36, 4.37 and 4.38, respectively.

The BER used in comparing the performance of four orthogonal pulses is shown in Figures 4.40. We evaluate these pulses in AWGN channel by using RAKE receivers in 4 m Tx-Rx separation. When no timing jitter exists, the values of BER of the four orthogonal pulses are closely similar and, at room temperature, the proposed orthogonal pulses can operate. For the imperfect timing jitter, the values of BER of the orthogonal proposed pulses are lower than that of the power optimized pulse. Therefore, we can conclude that all of the orthogonal pulses not only robustness timing jitter properties and have the PSD conforming the FCC masks but also are orthogonal to one another. This orthogonality suggests that a variety of design making use of simultaneous pulse transmission be considered.

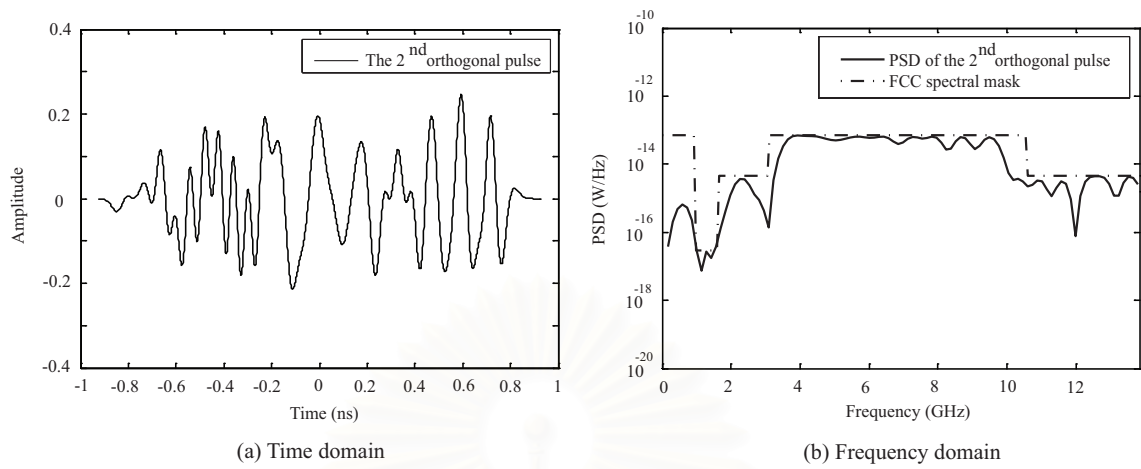


Figure 4.29 The 2nd orthogonal pulse and its PSD.

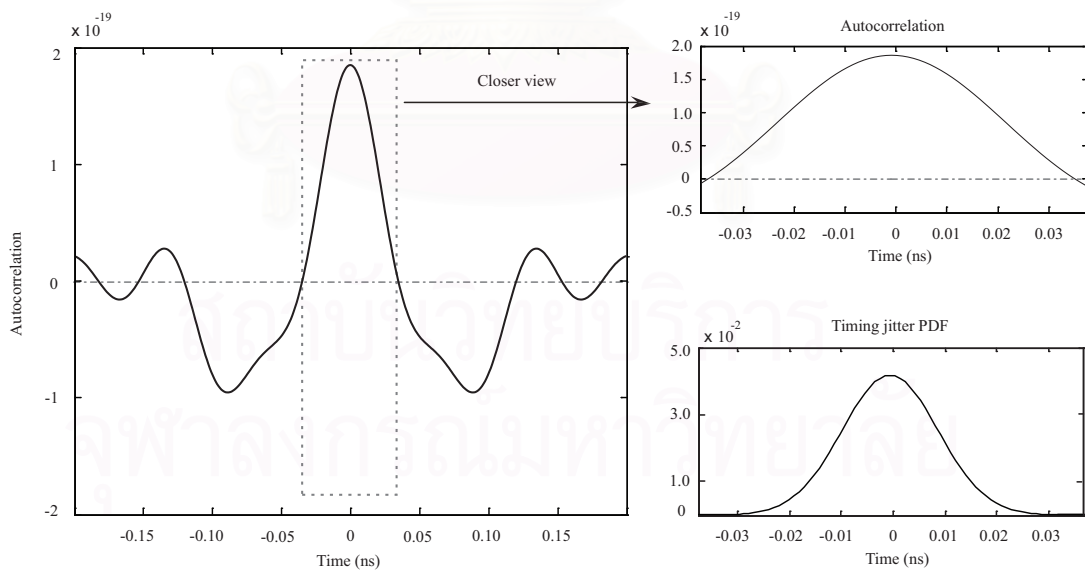


Figure 4.30 The autocorrelation of the 2nd orthogonal pulse.

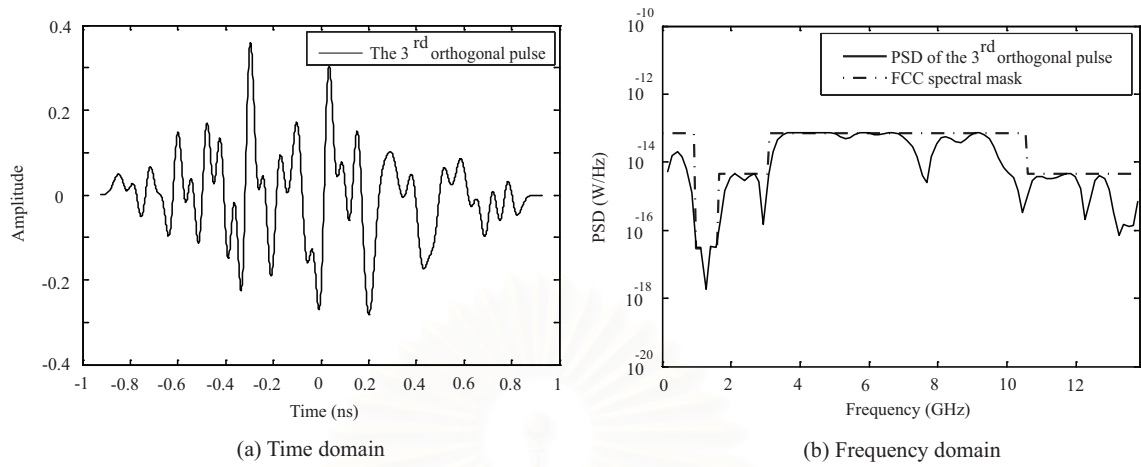


Figure 4.31 The 3rd orthogonal pulse and its PSD.

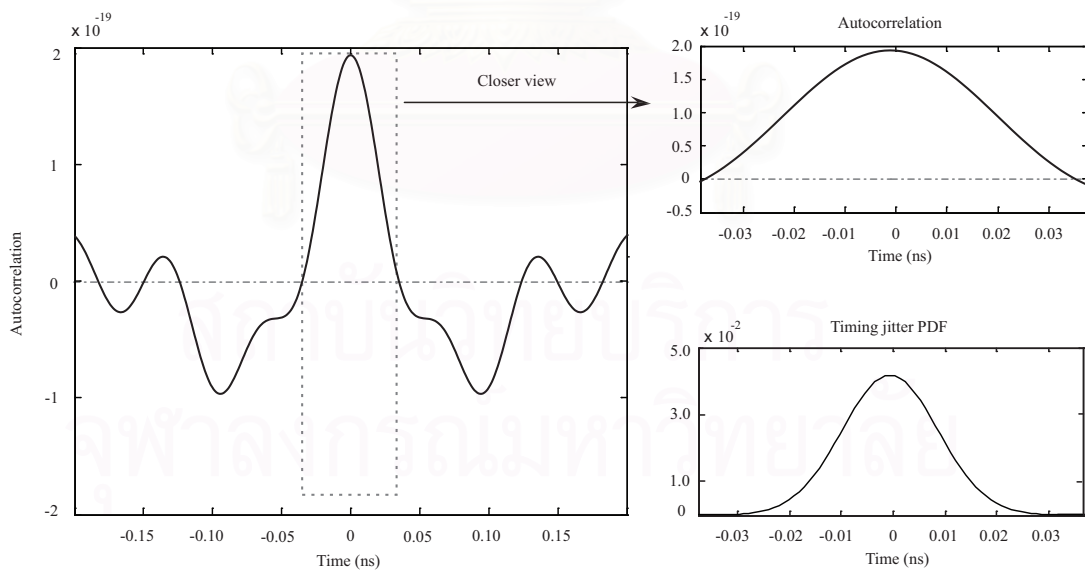


Figure 4.32 The autocorrelation of the 3rd orthogonal pulse.

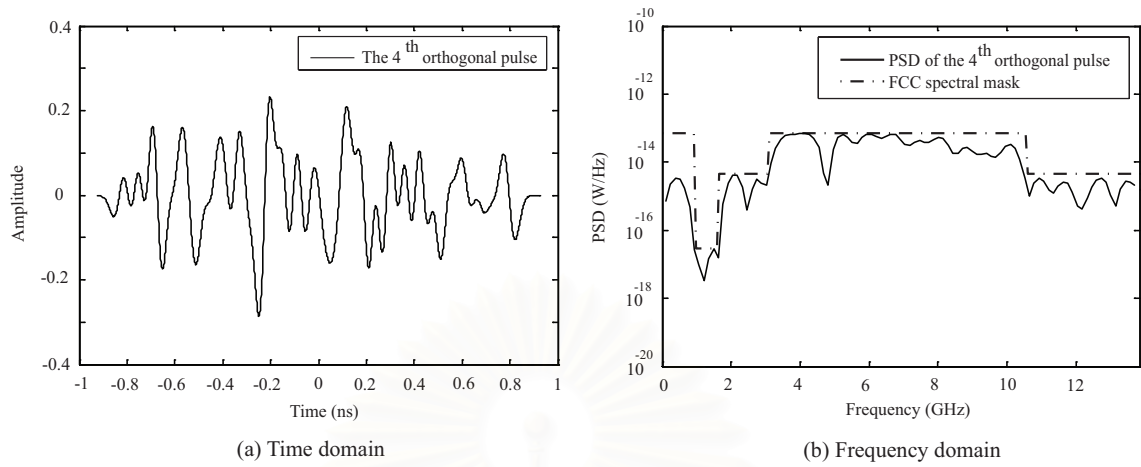


Figure 4.33 The 4th orthogonal pulse and its PSD.

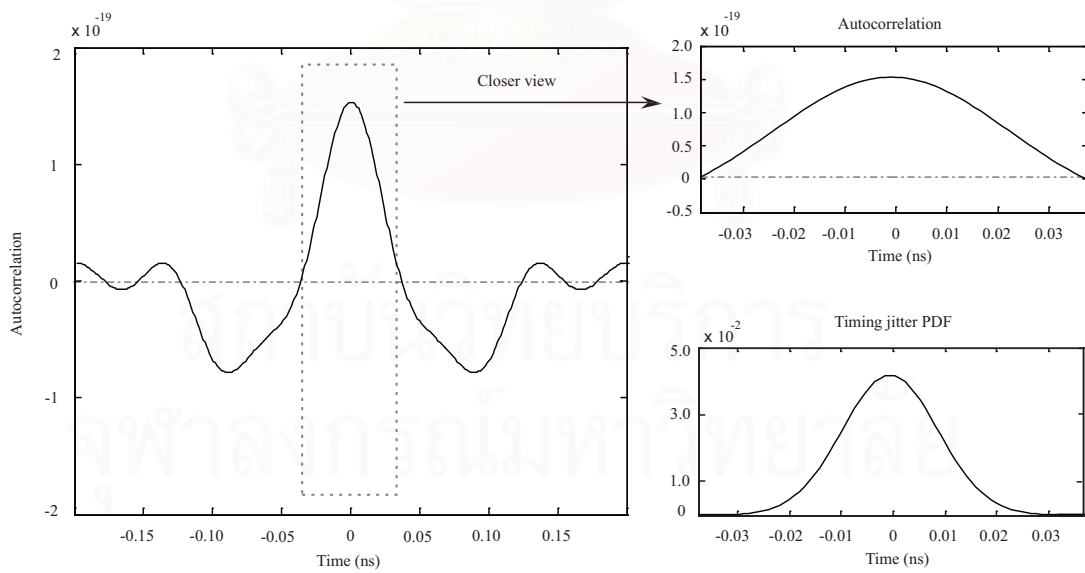


Figure 4.34 The autocorrelation of the 4th orthogonal pulse.

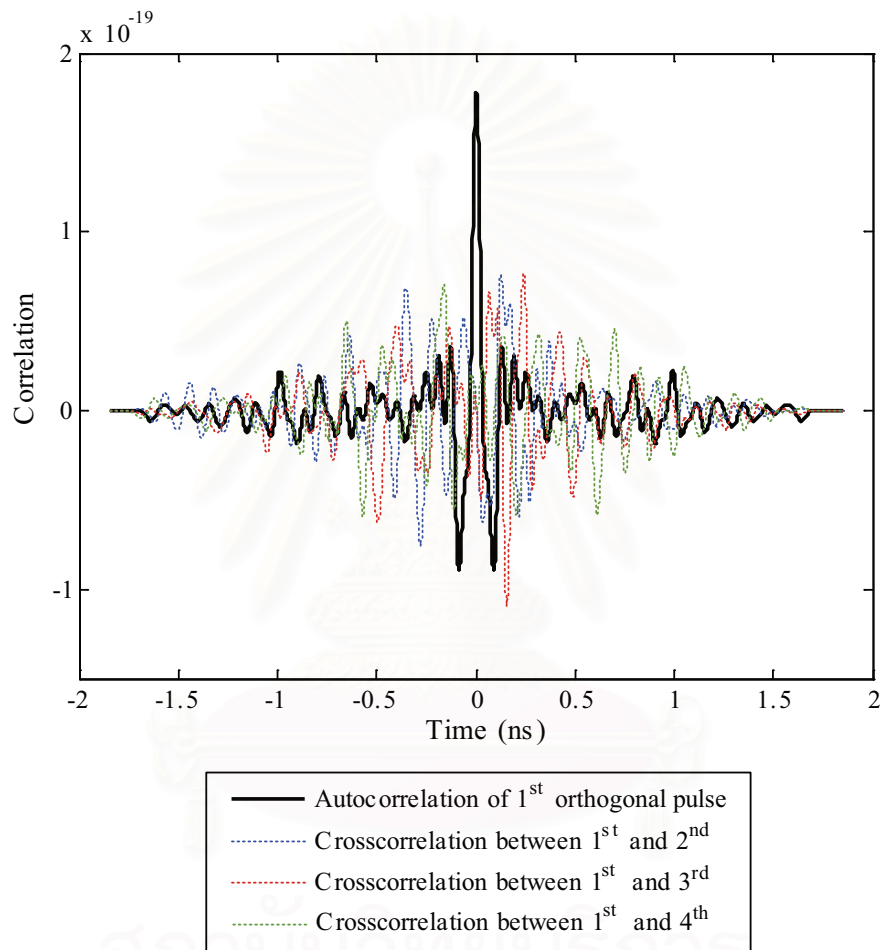


Figure 4.35: The cross-correlation between the 1st orthogonal pulse and the other pulses.

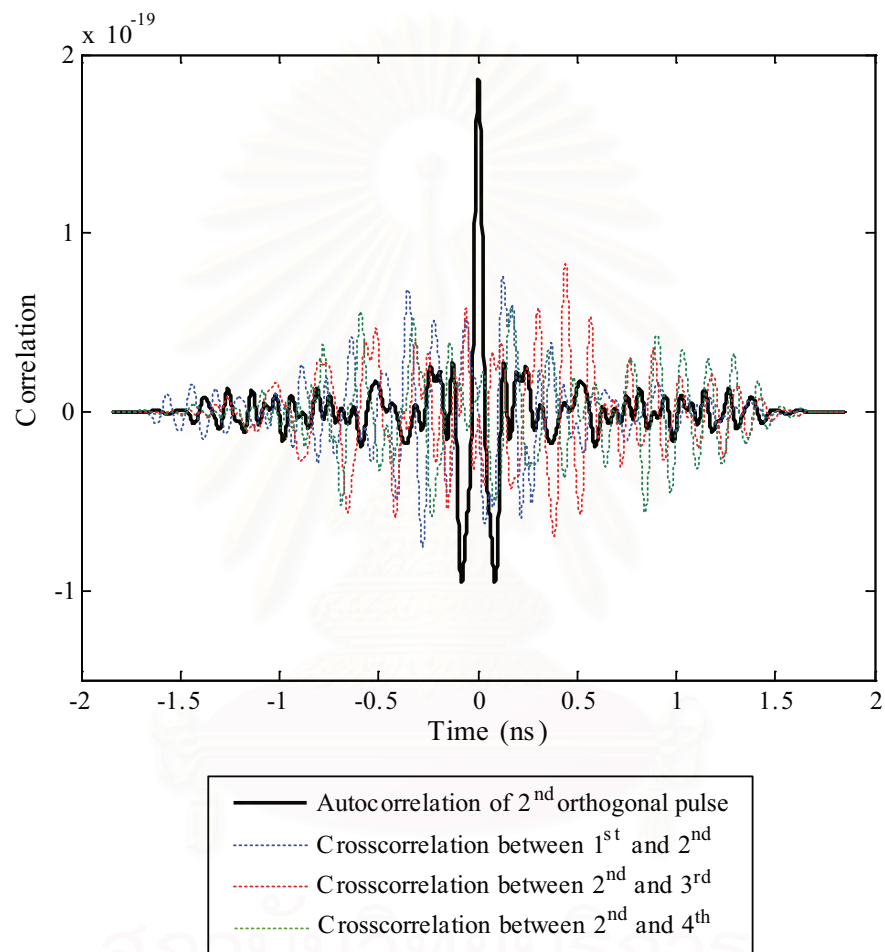


Figure 4.36: The cross-correlation between the 2nd orthogonal pulse and the other pulses.

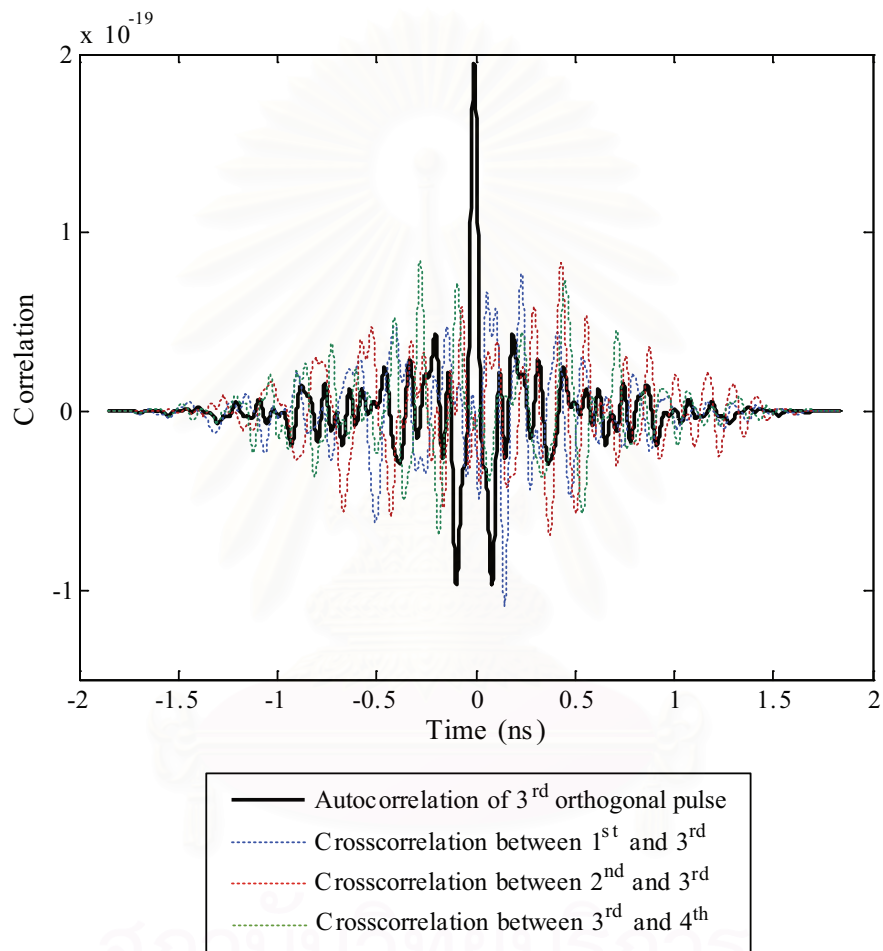


Figure 4.37: The cross-correlation between the 3rd orthogonal pulse and the other pulses.

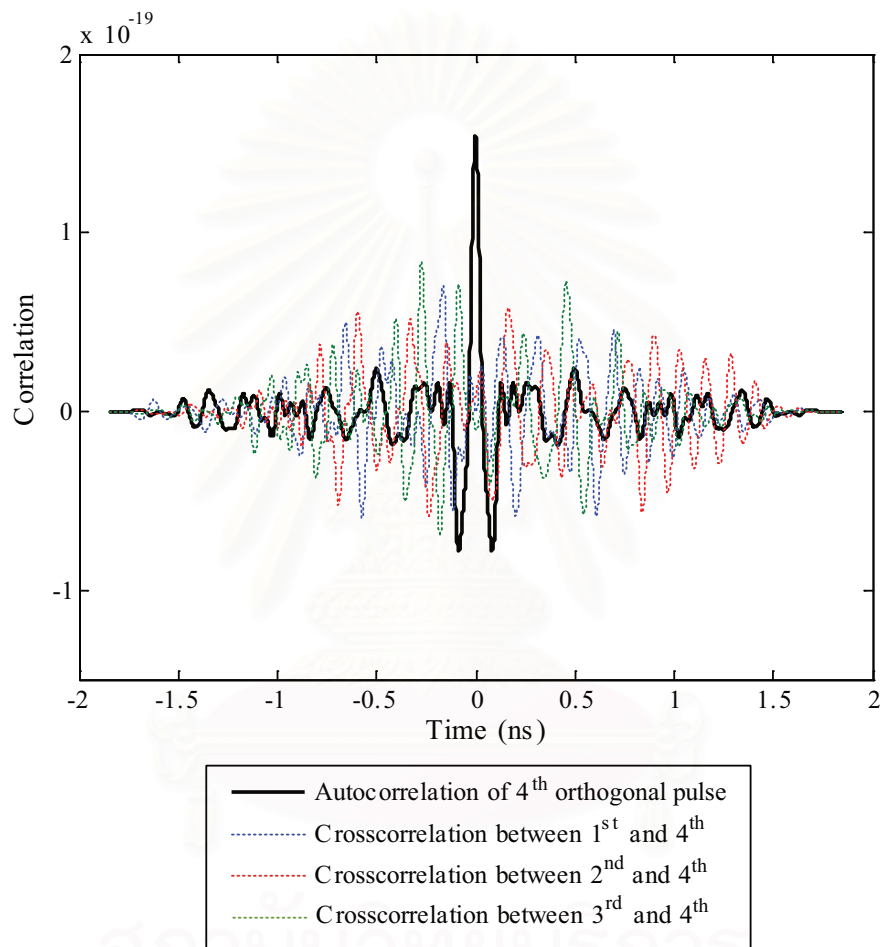


Figure 4.38: The cross-correlation between the 4th orthogonal pulse and the other pulses.

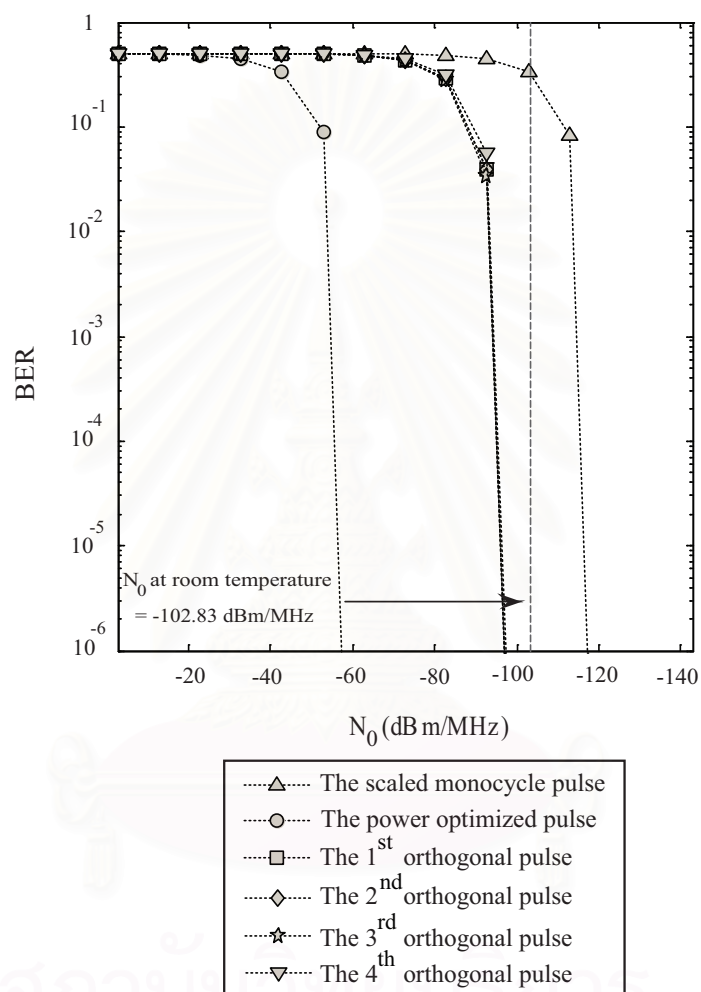


Figure 4.39: The BER comparison of the four orthogonal pulses without timing jitter in AWGN channel.

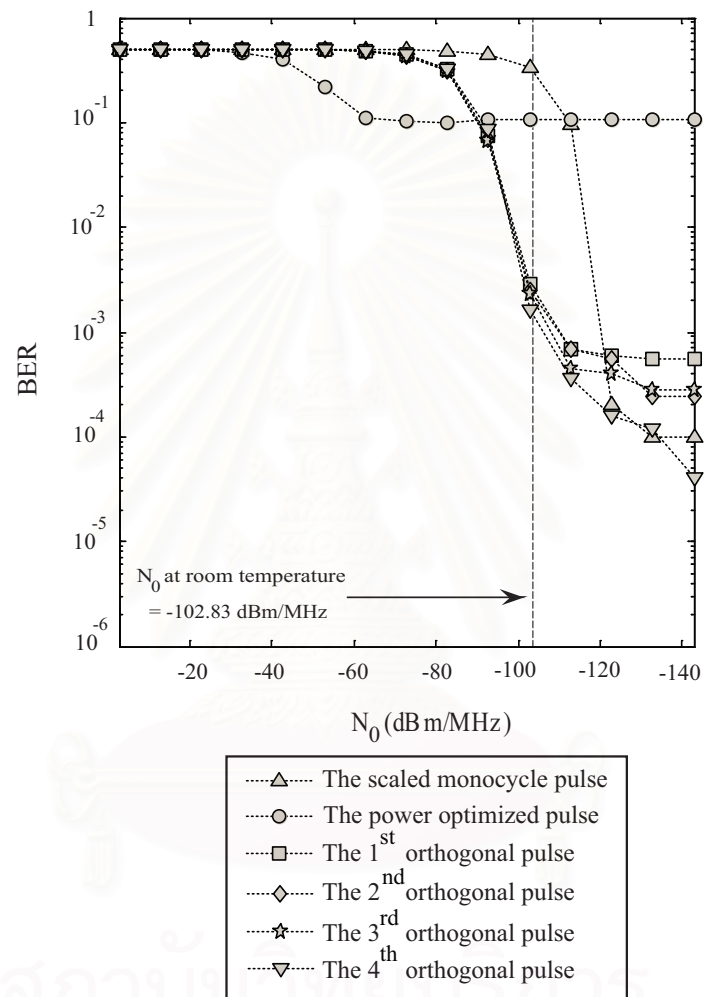


Figure 4.40: The BER comparison of the four orthogonal pulses with timing jitter in AWGN channel.

4.6 Summary

In this chapter, the experimental results of this study are briefly presented. Firstly, we consider the contribution of pulse shapes to the timing error tolerance. The different order of Gaussian pulses has the same probability of error when no timing jitter exists. But if timing jitter occurs in UWB systems, the higher order of Gaussian pulses is more sensitive to timing jitter than the lower order. Hence timing jitter limits the use of pulses with high derivative order. Secondly, we compare 3 UWB pulses that have PSD that meets the FCC spectral masks. Three UWB pulses are the scaled monocycle pulse, the power optimized pulse and the optimum proposed pulse. Two previously known UWB pulses we select to be used for the comparison with our optimum proposed pulse are the scaled monocycle pulse and the power optimized pulse. As a result, we found that the optimum proposed pulse could operate in UWB systems. Especially in the imperfect timing jitter, the performance of the proposed pulses is better than the other previously known pulses. The power optimized pulse achieves the best performance only on a no-timing-jitter condition. For the scaled monocycle pulse, this pulse cannot operate in all environments because of the weak power of the scaled monocycle pulse. To sum up, we come to the conclusion that the scaled monocycle pulse is not suitable for the UWB communications. Table 4.2 demonstrate the BER comparison of all simulation results at room temperature.

Finally, we present four examples of the orthogonal proposed pulses. According to the results, all of the orthogonal proposed pulses have PSD which conforms the FCC spectral masks. In addition, we can observe that the autocorrelation of the orthogonal proposed pulse has less negative values with the PDF of timing jitter range. It means that all of the proposed pulses can resist timing jitter tolerance. Moreover, we show the cross-correlation for confirming the orthogonal properties of the proposed pulses. Furthermore, we also compare the BER performances between the orthogonal proposed pulses and the other previously known pulses. When timing jitter exists, all of the orthogonal pulses have the lower BER values than the other previously known pulses. Therefore, we can conclude that the orthogonal proposed pulses not only have robustness timing jitter properties and PSD that conforms the FCC masks but also are orthogonal to one another. This orthogonality suggests that a variety of design making use of simultaneous pulse transmission can be considered.

Table 4.2 Summary of the BER comparison at room temperature.

Receiver	Tx-Rx duration	Channel	Timing	The scaled monocycle pulse	The power optimized pulse	The proposed pulse
RAKE	10 m	AWGN	without	4.45×10^{-1}	$< 1.0 \times 10^{-6}$	4.62×10^{-3}
			with	4.48×10^{-1}	1×10^{-1}	2.3×10^{-2}
	4 m	AWGN	without	3.31×10^{-1}	$< 1.0 \times 10^{-6}$	$< 1.0 \times 10^{-6}$
			with	3.39×10^{-1}	1.06×10^{-1}	1.6×10^{-3}
		CM2	without	2.04×10^{-1}	$< 1.0 \times 10^{-6}$	$< 1.0 \times 10^{-6}$
			with	2.24×10^{-1}	1×10^{-1}	7.6×10^{-4}
STR	4 m	AWGN	without	4.98×10^{-1}	$< 1.0 \times 10^{-6}$	3.13×10^{-1}
			with	4.99×10^{-1}	1.02×10^{-1}	3.38×10^{-1}
		CM2	without	4.94×10^{-1}	$< 1.0 \times 10^{-6}$	3.17×10^{-2}
			with	4.95×10^{-1}	1.07×10^{-1}	4.85×10^{-2}
ATR	4 m	AWGN	without	4.92×10^{-1}	$< 1.0 \times 10^{-6}$	7.6×10^{-4}
			with	4.99×10^{-1}	1.06×10^{-1}	1.22×10^{-2}
		CM2	without	4.88×10^{-1}	$< 1.0 \times 10^{-6}$	1.64×10^{-3}
			with	4.91×10^{-1}	1.05×10^{-1}	3.96×10^{-3}
R-ATR	4 m	AWGN	without	4.99×10^{-1}	$< 1.0 \times 10^{-6}$	9.6×10^{-4}
			with	4.99×10^{-1}	1.07×10^{-1}	1.33×10^{-2}
		CM2	without	4.91×10^{-1}	$< 1.0 \times 10^{-6}$	2.0×10^{-3}
			with	4.86×10^{-1}	1.03×10^{-1}	3.2×10^{-3}

CHAPTER V

THE CONCLUSIONS

A UWB system has received considerable attention due to its promising potential to provide very high bit rates at low cost. While UWB has many reasons to make it an exciting and useful technology for future wireless communications and many other applications, it also has some problems which must be solved so that it can become a popular and ubiquitous technology.

Since the FCC published its standard for the limitation of EIRP for UWB systems in 2002, the problem of spectrum shaping for UWB systems came to the forefront of scientific discourse. Moreover, the interference of pulse transmission power to and from existing systems operating over the same frequency bands is a crucial key to communications success of UWB systems. This interference may reduce the advantages of UWB systems. The other crucial problem is timing jitter effects. Timing jitter results from the presence of non-ideal sampling clocks in practical receivers. This distortion affects the correlation of signals at the receiver and thus the signal detection ability of UWB systems. Since the UWB pulse duration is very short (in the range of a nanosecond), only small timing misalignment can severely affect the performance of a correlation detector.

This dissertation has proposed a novel pulse design technique for solving the two crucial problems in UWB systems. An optimal pulse design strategy, which simultaneously provides a good match to the FCC spectral masks and robustness to timing jitter. The proposed technique is composed of 2 parts. The first part is the optimum pulse design and the other is the orthogonal pulses design based on a pulse from the previous part. The digital FIR filter technique can be adopted in the proposed algorithm. The model of timing jitter as a normal distributed random variable with zero mean is applied in this dissertation. The proposed pulse is achieved by maximizing a mean weighted correlator output over a PDF of timing jitter. A WFNC is introduced to emphasize the seriousness of a negative correlator output value. In our simulation, we compare 3 UWB families: the scaled monocycle pulse, the power optimized pulse and the optimum proposed pulse. The threshold for considering the operating pulse is the noise power spectral density value at room temperature. Moreover, we show the method we used in finding the parameters of the proposed optimization algorithm. Figure 5.1 shows the summary block diagram of two proposed techniques.

Simulation results of the first part have demonstrated merits of the proposed pulse in various aspects. Firstly, we consider the performance of the proposed pulse in the longest distance which is 10 m Tx-Rx separation of UWB systems and it is workable. In this

case, the proposed pulse can outperform the other previously known pulses in the system with the imperfect timing jitter at room temperature. Additionally, the proposed pulse can outperform the power optimized pulse over a broad range of an actual timing jitter variance although the proposed pulse is generated by an inexact timing jitter variance value. Secondly, we compare the 3 UWB pulses in AWGN and CM2 channel models in 4 m Tx-Rx separation. Two types of receiver including RAKE and TR receivers are used in our simulation. For RAKE receivers, the power optimized pulse demonstrates the best performance when no timing jitter exists in both of the channel models. The pulse obtained from our proposed algorithm is inferior to the power optimized pulse. However, there is no significant difference on the performance between the proposed pulse and the power optimized pulse at the operating temperature. For the imperfect timing jitter, the proposed pulse can outperform the other previously pulses at room temperature. For TR receivers, this type of receivers has drawn significant attention because it has low complexity and it can collect multipath energy without requiring multipath tracking or channel estimation. The performance of the three placement reference pulse including STR, ATR and R-ATR techniques are discussed. STR receivers are the simplest TR receivers. However, the drawback of this type is the noisy reference template. Thus, the only high power transmission pulse can operate with this type. For the other TR receiver types, they are proposed for resolving the drawback of STR receivers. These receivers average all the received reference pulses to reduce the noise in the reference waveform and then data detection proceeds with the reduced noise reference. In these receivers, the proposed pulse at room temperature can operate in with and without timing jitter. Especially, the proposed pulse can outperform the power optimized pulse in the system with the imperfect timing jitter.

The other part of the proposed technique that is the orthogonal pulse design is based on the optimum proposed pulse. Therefore, the advantages of the orthogonal proposed pulses are not only robust against timing jitter effects and of PSD conforming the FCC masks but also orthogonal to one another. Therefore, this technique can improve the capacity of UWB systems. In the simulation results, we show the examples of the orthogonal pulses and compare the performance of these pulses with the other previously known pulses. Simulation results demonstrate the orthogonality properties of each of the proposed pulses. In addition the experimental results show the merits of the proposed pulses compared to the other previously known pulses in AWGN channel by using RAKE receivers in 4 m Tx-Rx separation.

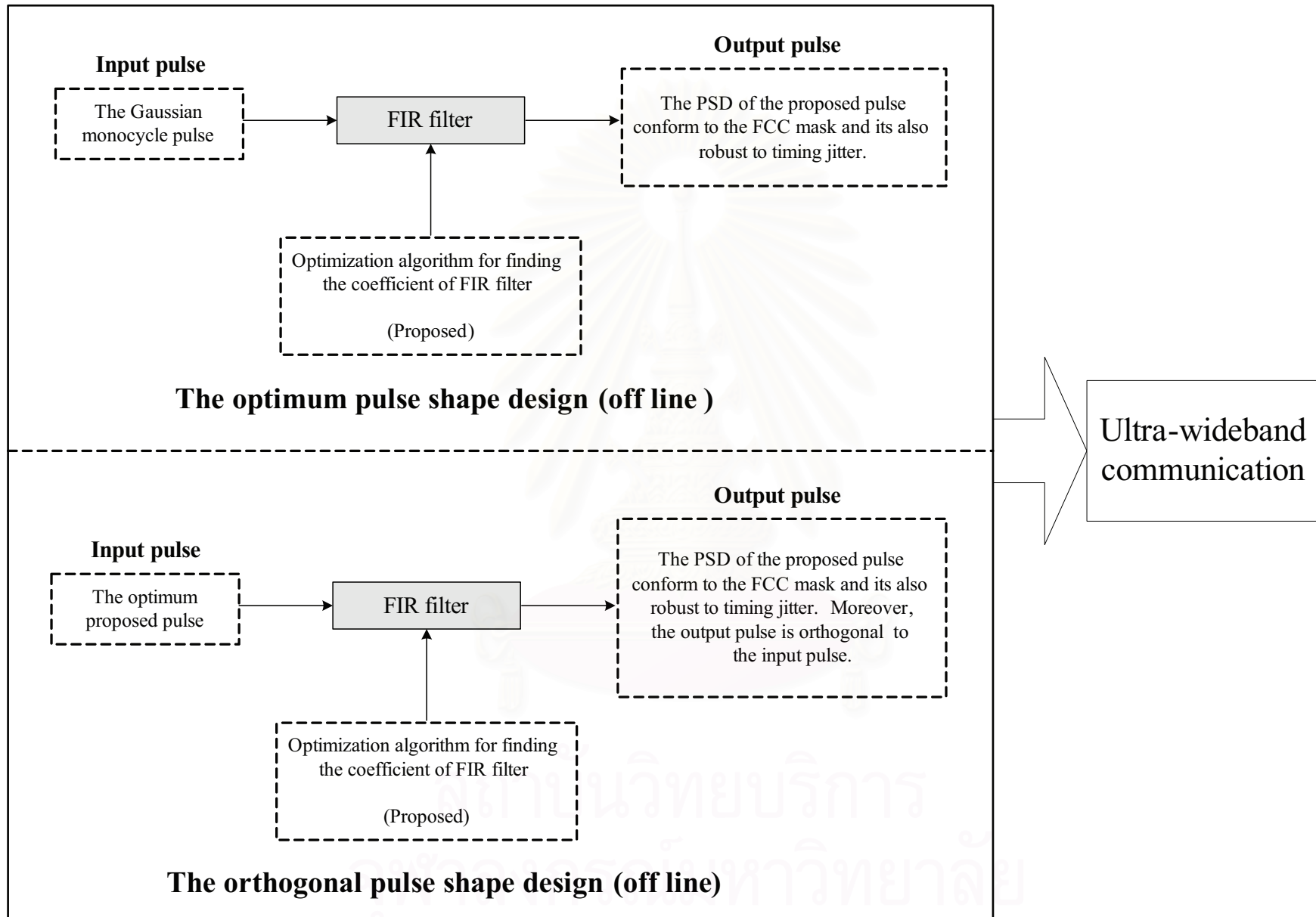


Figure 5.1 The block diagram of two proposed techniques.

5.1 Future Works

Although the concepts of the proposed technique have been developed and it has been extensively studied, there are some interesting issues needed further investigations.

Firstly, the optimization process of the proposed pulse consumes much computation and time. The method to find the new objective function that has a local minimum existence (convex optimization) is the interesting for future research.

Secondly, the automatic optimization algorithm that does not use any parameters are an inspiration for future research because the WFNC parameter has to be implemented in optimization algorithm.

Finally, the advantage of the proposed pulse and the power optimized pulse can be integrated by designing an innovative transmitter. The innovative transmitter should be capable of choosing a pulse between the power optimized and the proposed pulses that provides the best performance under differential noise values. For this reason, the innovative transmitter is one of interesting elements for the better performance of UWB systems in the future.



References

- [1] Federal Communications Commission (FCC), Revision of part 15 of the commission's rules regarding ultra-wideband transmission systems. First Report and Order. FCC Rep. 02-48, February 2002.
- [2] Win, M. Z. and Scholtz, R. A. On the robustness of ultra-wide bandwidth signals in dense multipath environments. IEEE Communication Letters. 2 , 2 (Feb. 1998): 51–53.
- [3] Cassioli, D., Win, M. Z., and Molisch, A. F. The ultra-wide bandwidth indoor channel: From statistical model to simulations. IEEE J. Select. Areas Commun. 20 , 6 (Aug. 2002): 1247–1257.
- [4] Cramer, R. J. M., Scholtz, R. A., and Win, M. Z. Evaluation of an ultra-wideband propagation channel. IEEE Trans. Antennas and Propagation. 50 (May 2002): 561–570.
- [5] Foerster, J. R., The effects of multipath interference on the performance of UWB systems in an indoor wireless channel. Proceedings of the IEEE Vehicular Technology Conference, 2 (May 2001): 1176–1180.
- [6] Reed, J. H. An Introduction to Ultra Wideband Communication Systems. Prentice Hall PTR, 2005.
- [7] Nee, R. V. and Prasad, R. OFDM for Wireless Multimedia Communications. Artech House, 2000.
- [8] Yee, N., Linnartz, J. P., and Fettweis, G., Multi-carrier CDMA in indoor wireless radio networks. IEEE International Symposium on Personal, Indoor, and Mobile Radio Communications, (Sept. 1993): 109–113.
- [9] Barrett, T. W., History of ultrawideband (UWB) radar and communications: Pioneers and innovators. Progress in Electromagnetics Symposium 2000 (PIERS 2000), Cambridge, MA, July, 2000.
- [10] Barrett, T. W., History of ultrawideband (UWB) communications and radar: Part I, UWB communication. Microwave Journal. (Jan. 2001): 22–56.
- [11] Scholtz, R. A., Multiple access with time-hopping impulse modulation, Military Communications Conference, MA, Oct. 11-14, 1993

- [12] Win, M. Z. and Scholtz, R. A. Ultra-wide bandwidth time-hopping spread-spectrum impulse radio for wireless multiple-access communications. IEEE Trans. Commun. 48 (April 2000): 679–691.
- [13] Win, M. Z. and Scholtz, R. A. Impulse radio: How it works. IEEE Communication Letters. 2 (Feb. 1998): 36–38.
- [14] Corral, C. A., Sibecas, S., Emami, S., and Stratis, G., Pulse spectrum optimization for ultra-wideband communication. IEEE Conference on Ultra Wideband Systems and Technology, May 2002.
- [15] Wang, T. and Wang, Y., Capacity of M-ary PAM impulse radio with various derivatives of gaussian pulse subject to FCC spectral masks. International Symposium on Computers and Communications, (July 2004): 696–701.
- [16] Kim, H. and Joo, Y., Fifth-derivative Gaussian pulse generator for UWB system. IEEE Radio Frequency Integrated Circuits , (Nov. 2005): 671–674.
- [17] Phan, T. A., Krizhanovskii, V., Han, S. K., Lee, S., Oh, H. S., and Kim, N., 4.7pj/pulse 7th derivative Gaussian pulse generator for impulse radio UWB. International Symposium on Circuits and Systems, New Orleans, Louisiana, USA, May 2007.
- [18] Nardis, L. D. and Giancola, G., Power limits fulfilment and MUI reduction based on pulse shaping in uwb networks. IEEE International Conference on Communications, 6 (June 2004): 3576–3580.
- [19] Gao, W., Venkatesan, R., and Li, C., A pulse shape design method for Ultra-Wideband communications. IEEE Wireless Communications and Networking Conference, (March 2007): 2802–2807.
- [20] Lewis, T. P. and Scholtz, R. A., An ultrawideband signal design with power spectral density constraints. IEEE 38th Asilomar Conference on Signal, System and Computer, (Nov. 2004): 1521–1525.
- [21] Maddula, S. and Chakrabarti, S., Synthesis of UWB pulse following FCC mask. 23th General Assembly of International Union of Radio Science (URSI), New Delhi, October, 2005.
- [22] Maddula, S. and Chakrabarti, S., A new UWB pulse generator for FCC spectral masks. Proc. IEEE Veh. Techn. Conf. (VTC-Spring 2003), Jeju, South Korea, April 2003.
- [23] Parr, B., Cho, B., Wallace, K., and Ding, Z. A novel ultra-wideband pulse design algorithm. IEEE Communication Letters. 7 (May 2003): 219–221.

- [24] Wallace, K. P., Parr, A. B., Byung, L. C., and Ding, Z. Performance analysis of a spectrally compliant ultra-wideband pulse design. IEEE Trans. Wireless Commun. 4 , 5 (2005): 2172–2181.
- [25] Yin, L. and Hongbo, Z., UWB pulse design using the approximate prolate spheroidal wave functions. Microwave, Antenna, Propagation and EMC Technologies for Wireless Communications, 1 (Aug. 2005): 450–453.
- [26] Yin, L. and Hongbo, Z., Interference mitigation in UWB communications through pulse waveform design. 4th Asia Pacific Conference on Environmental Electromagnetics, (Aug. 2006): 569–572.
- [27] Zimmer, R. and Waldow, P., A simple method of generating UWB pulses. IEEE International Symposium on Spread Spectrum Techniques and Applications, (Aug. 2004): 112–114.
- [28] Zhang, L. and Zhou, Z., A novel synthesis design and implementation for generating UWB narrow pulse based on wavelet. International Symposium on Communications and Information Technologies, (Oct. 2004): 1228–1231.
- [29] Kim, Y., Jang, B., Shin, C., and Womack, B. F. Orthonormal pulses for high data rate communications in indoor UWB systems. IEEE Communications Letters. 9 (May 2005): 405–407.
- [30] Cilolino, S., Ghavami, M., and Aghvami, H. On the use of wavelet packets in Ultra Wideband pulse shape modulation systems. IEICE Trans. Fundamentals. 9 (2005): 2310–2317.
- [31] Abreu, G. T. F., Mitchell, C. J., and Kohno, R. On the design of orthogonal pulse-shape modulation for UWB systems using Hermite pulse. IEEE Trans. Commun. 5 , 4 (2003): 1–17.
- [32] Wu, D., Spsojevic, P., and Seskar, I., Ternary complementary sets for orthogonal pulse based UWB. 37th Asilomar Conference on Signals, Systems and Computers, (Nov. 2003): 1776–1780.
- [33] Hu, W. and Zheng, G., Orthogonal hermite pulses used for UWB M-ary communication. International Conference on Information Technology: Coding and Computing, (Apr. 2005): 97–101.
- [34] Xing, J. G., Bo, Z. H., and Wei, C., A novel pulse design based on Hermite functions for UWB communications. Journal of China universities of posts and telecommunications. 13 , 1 (March 2006): 49–52.
- [35] Dotlic, I. and Kohno, R., Design of the family of orthogonal and spectrally efficient UWB waveforms. IEEE Trans. Signal Process. 1 , 1 (2007): 313–322.

- [36] Wenke, L. and Yu, W., Pulse shaping for ultra-wideband communications. Wireless Communications, Networking and Mobile Computing, (Sept. 2007): 586–589.
- [37] Liang, C. S., Xin, Z. H., Hua, L. Y., and Fei, H. P., Generation of orthogonal UWB shaping pulses based on compressed chirp signal. Journal of China universities of posts and telecommunications. 14, 2 (June 2007): 99–102.
- [38] Wu, X. L., Sha, X. J., and Zhang, N. T., Modified hermite function based pulse shaping algorithm for ultra-wideband communications. Radio and wireless symposium, (Jan. 2007): 395–398.
- [39] Silva, J. A. N. and Campos, M. L. R., Spectrally efficient UWB pulse shaping with application in orthogonal PSM. IEEE Trans. Commun. 55 , 2 (Feb. 2007): 313–322.
- [40] Jang, W. M., Pulse design in UWB communications using Nyquist Criterion. International Conference on Advanced Communication Technology, (Feb. 2006): 559–564.
- [41] Matsuo, M., Kamada, M., and Habuchi, H., Design of UWB pulses based on b-splines. International Symposium on Circuits and Systems, Kobe, Japan, May 2005.
- [42] Matsuo, M., Kamada, M., and Habuchi, H., Design of UWB pulses by spline approximation. IEEE Wireless and Communications and Networking Conference, New orlens, LA, USA, March 2005.
- [43] Matsuo, M., Kamada, M., and Habuchi, H. Design of UWB pulses terms of B-splines. IEICE Trans. Fundamentals, 9 (2005): 2287–2298.
- [44] Wu, Y., Molisch, A. F., Kung, S. Y., and Zhang, J., Impulse radio pulse shaping for ultra-wide bandwidth (UWB) systems. 14th IEEE International Symposium on Personal, Indoor and Mobile Radio Communications, (2003): 877–881.
- [45] Zeng, D., A. Annamalai, J., and Zaghoul, A. I., Pulse shaping filter design in UWB system. IEEE Conference on Ultra Wideband Systems and Technologies, (2003): 66–70.
- [46] Luo, X., Yang, L., and Giannakis, G. B., Designing optimal pulse-shapers for ultra-wideband radios. IEEE Conference on Ultra Wideband Systems and Technologies, (2003): 349–353.
- [47] Luo, X., Yang, L., and Giannakis, G. B. Designing optimal pulse-shapers for ultra-wideband radios. J. Commun. Netw. 5 , 4 (2003): 344–353.

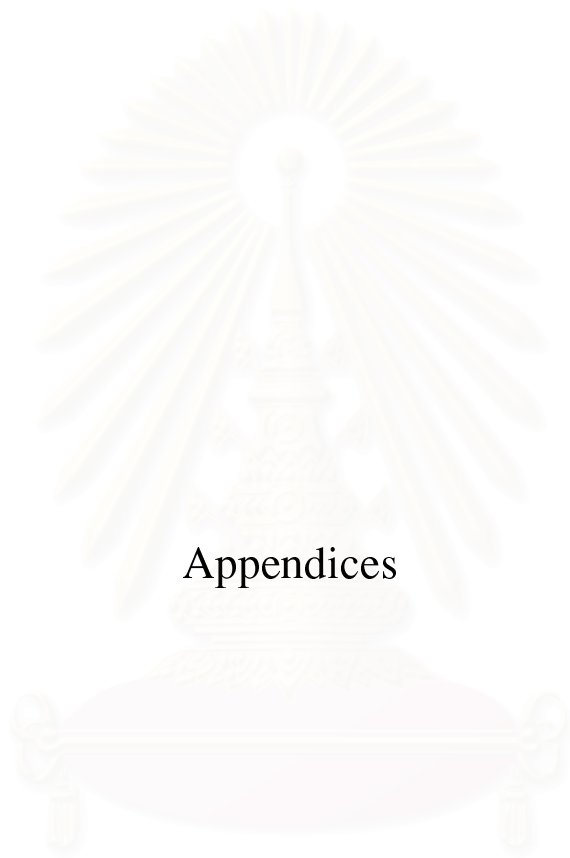
- [48] Wu, X., Tian, Z., Davidson, T. N., and Giannakis, G. B., Optimal waveform design for UWB radios. IEEE International Conference on Acoustics, Speech, and Signal Processing, 4 (May 2004): 521–524.
- [49] Wu, X., Tian, Z., Davidson, T. N., and Giannakis, G. B. Optimal waveform design for UWB radios. IEEE Trans. Signal Process. 54 , 6 (2006): 2009–2021.
- [50] Wu, X., Tian, Z., Davidson, T. N., and Giannakis, G. B., Orthogonal waveform design for UWB radios. IEEE Workshop on Signal Processing Advances in Wireless Communications, (2004): 150–154.
- [51] Abreu, G. T. F. and Kohno, R., Design of jitter-robust orthogonal pulses for UWB systems. IEEE Global Communications Conference, 2 (Dec. 2003): 739–743.
- [52] Abreu, G. T. F., Mitchell, C. J., and Kohno, R. Jitter-robust orthogonal hermite pulses for ultra-wideband impulse radio communications. EURASIP J. Appl. Signal Process. 2005, 1 (2005): 369–381.
- [53] Chen, Y., Chen, J., and Lv, T., A high order biphasic modulation scheme for UWB transmission. Proc. IEEE Veh. Techn. Conf. (VTC-Fall 2004), (2004): 5209–5213.
- [54] Chen, J., Chen, Y., and Lv, T., A timing-jitter robust UWB modulation scheme. IEEE Signal Processing Letter. 13 , 10 (2006): 593–596.
- [55] Xin, L., Premkumar, A. B., and Madhukumar, A. S., Jitter resistant Ultra Wideband pulse generation based on wavelet. IEEE Conference on Ultra Wideband Systems and Technologies, (Sept. 2007): 349–353.
- [56] Hu, B. and Beaulieu, N. C. Pulse shapes for ultrawideband communication systems. IEEE Trans. Wireless Commun. 4 (July 2005): 1536–1276.
- [57] Lovelace, W. M. and Townsend, J. K. The effects of timing jitter and tracking on the performance of impulse radio. IEEE J. Select Areas Communication. 20 , 9 (2002): 1646–1651.
- [58] Lovelace, W. M. and Townsend, J. K. The effects of timing jitter on the performance of impulse radio. IEEE Conference on Ultra Wideband Systems and Technologies, (May 2002): 251–254.
- [59] Guvenc, I. and Arslan, H., Performance evaluation of UWB systems in the presence of timing jitter. IEEE Conference on Ultra Wideband Systems and Technologies, (2003): 136–141.

- [60] Guvenc, I. and Arslan, H., On the modulation options for UWB systems. Military Communications Conference, (2003): 892–897.
- [61] Mucchi, L., Marabissi, D., Ranaldi, M., Re, E. D., and Fantacci, R., Impact of synchronization error and multiple access interference to the performance of UWB impulse radio systems. IEEE International Symposium on Spread Spectrum Techniques and Applications, (2004): 477–482.
- [62] Liang, Z., Du, H., and Zhou, Z., The effects of synchronization timing error on the performance of UWB systems using different monocycle shapes. International Symposium on Communications and Information Technologies, (2004): 1033–1038.
- [63] Park, K., Joo, J., Sung, S., and Kim, K., Effects of timing jitter in low-band DS-BPSK UWB system under Nakagami-M fading channels. IEEE TENCON, (2004): 149–152.
- [64] Sum, C. S., Rahman, M. A., Sasaki, S., Zhou, J., and Kikuchi, H., Impact of timing jitter on RAKE reception of DS-UWB signal over AWGN and multipath environment. International conference on Wireless Networks, Communications and Mobile Computing, (2005): 1225–1230.
- [65] Tian, Z. and Giannakis, G. B. BER sensitivity to mistiming in ultra-wideband impulse radios—Part I: Nonrandom channels. IEEE Trans. Signal Process. 54 (Apr. 2005): 1550–1560.
- [66] Tian, Z. and Giannakis, G. B. BER sensitivity to mistiming in ultra-wideband impulse radios—Part II: Fading channels. IEEE Trans. Signal Process. 54 (May 2005): 1897–1907.
- [67] Kokkalis, N. V., Mathiopoulos, P. T., Karagiannidis, G. K., and Koukourlis, C. S. Performance analysis of M-ary PPM TH-UWB systems in the presence of MUI and timing jitter. IEEE J. Select Areas Communication. 24 (Apr. 2006): 822–828.
- [68] Lee, W., Kunaruttanapruk, S., and Jitapunkul, S., Performance evaluation of UWB systems using different order of gaussian pulses. The International Conference on Signal Processing, Gunlin, China, 2006.
- [69] Hor, P. B., Ko, C. C., and Zhi, W., BER performance of pulsed UWB system in the presence of colored timing jitter. IEEE Conference on Ultra Wideband Systems and Technologies, Kyoto, Japan, 2004.
- [70] Ko, C. C., Huang, L., and Poh, B. H. Effect and compensation of colored timing jitter in pulsed uwb systems. Wirel. Pers. Commun. 40 , 1 (2007): 19–33.

- [71] Onunkwo, U., Li, Y., and Swami, A. Effect of timing jitter on OFDM-based UWB systems. IEEE J. Select Areas Communication. 24 (Apr. 2006): 787–793.
- [72] Onunkwo, U., Timing jitter in Ultra-Wideband (UWB) systems. Ph.D. dissertation. Georgia Institute of Technology, 2006.
- [73] Zhang, W., Bail, Z., Shen, H., Liu, W., and Kwak, K. S., A novel timing jitter resist method in UWB systems. International Symposium on Communications and Information Technologies, 2 (2005): 833–836.
- [74] Li, Q. and Wong, W. S., A novel timing jitter robust UWB impulse radio system. Military Communications Conference, 2 (2005): 1252–1257.
- [75] Kamoun, M., Buzenac, V., Courville, M., and Duhamel, P., A digital jitter canceling algorithm for PPM impulse radio ultra-wide-band systems. International Conference on Communications, 1 (May 2005): 412–416.
- [76] Oh, M. K., Jung, B., Harjani, R., and Park, D. J., A new noncoherent UWB impulse radio receiver. IEEE Communication Letters. (Feb. 2005): 151–153.
- [77] Nejad, M. B. and Zheng, L. R., An innovative receiver architecture for autonomous detection of ultra-wideband signals. International Symposium on Circuits and Systems, (May 2006): 2589–2592.
- [78] Gezici, S., Sahinoglu, Z., Kobayashi, H., and Poor, H. V. Ultra-wideband impulse radio systems with multiple pulse types. IEEE J. Select Areas Communication. 24 (Apr. 2006): 892–898.
- [79] Gezici, S., Molisch, A. F., Poor, H. V., and Kobayashi, H., The trade-off between processing gains of impulse radio system in the presence of timing jitter. International Conference on Communications, (2004): 3596–3600.
- [80] Gezici, S., Molisch, A. F., Poor, H. V., and Kobayashi, H. The trade-off between processing gains of an impulse radio UWB system in the presence of timing jitter. IEEE J. Select Areas Communication. 55 , 8 (2007): 1504–1515.
- [81] Merz, R., Botteron, C., and Farine, P. A., Performance of an impulse radio communication system in the presence of Gaussian jitter. IEEE International Conference on Ultra-Wideband, Marina Mandarin, Singapore, 2007.
- [82] Ghavami, M., Michael, L. B., and Kohno, R. Ultra Wideband Signals and Systems in Communication Engineering. West Sussex, England : John Wiley & Sons, Inc., 2004.

- [83] Durisi, G. and Benedetto, S., Performance evaluation and comparison of different modulation schemes for UWB multiaccess systems. International Conference on Communications, 3, (May 2003): 2187–2191.
- [84] Hamalainen, M., Tesi, R., Inatti, J., and Hovinen, V., On the performance comparison of different UWB data modulation schemes in AWGN channel in the presence of jamming. IEEE Radio and Wireless Conference, (2002): 83–86.
- [85] Laney, D. C., Maggio, G. M., Lehmann, F., and Larson, L. Multiple access for UWB impulse radio with pseudochaotic time hopping. IEEE J. Select Areas Communication. 20 , 9 (2002): 1692–1700.
- [86] Weisenhorn, M. and Hirt, W. Uncoordinated rate-division multiple-access scheme for pulsed UWB signals. IEEE Trans. Vehicular Technology. 5 (2005): 1646–1662.
- [87] Somayazulu, V. S., Multiple access performance in UWB systems using time hopping vs. direct sequence spreading. IEEE Wireless and Communications and Networking Conference, (2002): 522–525.
- [88] Zhao, J. and Ugweje, O. C., Performance of UWB TH-PPM multiple access schemes in dense multipath fading environment. 37th Southeastern Symposium on System Theory (SSST), (2005): 15–19.
- [89] Nasiri-Kenari, M. and Shayesteh, M. G., Performance analysis and comparison of different multirate TH-UWB systems: uncoded and coded schemes. IEE ip-com. 152, (Dec. 2005): 833–844.
- [90] Tan, S. S., Nallanathan, A., and Kannan, B. Performance of DS-UWB multiple-access systems with diversity reception in dense multipath environme. IEEE Trans. Vehicular Technology. 4 (2006): 1269–1280.
- [91] Hingorani, G. D. and Hancock, J., A transmitted reference system for communication in random or unknown channels. IEEE Trans. Commun. 13 , 3 (1965): 293–301.
- [92] Foerster, J. R., The performance of a direct-sequence spread ultra-wideband system in the presence of multipath, narrowband interference, and multiuser interference. IEEE Conference on Ultra Wideband Systems and Technologies, (May 2002): 87–92.
- [93] Time variance for UWB Wireless Channels. IEEE P802.15 Working Group for WPANs, Nov. 2002.
- [94] Saleh, A. A. M. and Valenzuela, R. A. A statistical model for indoor multipath propagation. IEEE J. Select Areas Communication. 5 , 2 (1987): 128–137.

- [95] Zhao, S., Pulsed Ultra-Wideband: Transmission, Detection, and Performance. Ph.D. dissertation. Oregon State University, 2006.
- [96] Win, M. Z. and Scholtz, R. A. On the energy capture of ultrawide bandwidth signals in dense multipath environments. IEEE Communications Letters. 9 (1998): 245–247.
- [97] Gaur, S. and Annamalai, A., Improving the range of UWB transmission using RAKE receivers. Proc. IEEE Veh. Techn. Conf. (VTC-Spring 2003), 1 (2003): 597–601.
- [98] Molisch, A. F., Foerster, J. R., and Pendergrass, M., Channel models for ultrawideband personal area networks. IEEE Wireless Communications, 10, 6 (2003): 14–21.
- [99] Quek, T. Q. S. and Win, M.Z. Analysis of uwb transmitted-reference communication systems in dense multipath channels. IEEE J. Select Areas Communication. (2005): 1863–1874.
- [100] Choi, J. D. and Stark, W. E. Performance of ultra-wideband communications with suboptimal receiver in multipath channels. IEEE J. Select Areas Communication. 9 (2002): 1754–1766.
- [101] Lee, W., Kunaruttanapruk, S., and Jitapunkul, S. Optimum pulse shape design for uwb systems with timing jitter. IEICE communication. 3 (2008): xx-xx.
- [102] Optimization Toolbox For Use with MATLAB, Version 3.1 (Release 2006b). The MathWorks, Inc. Mass., 2006.
- [103] Gassezadeh, S. S. and Tarokh, V. The ultra-wideband indoor path loss model. IEEE 802.15-02/278rl-SG3a.
- [104] Sumethnapi, J. and Araki, K. TR-UWB systems with pulse-position multi-pulse modulation for ECC's and Japan's radiation masks. IEICE Transactions on communication , 10 (2007): 2969–2972.
- [105] Chao, Y. L. and Scholtz, R. A., Optimal and suboptimal receivers for ultra-wideband transmitted reference systems. IEEE Global Communications Conference, (2003): 759–763.



Appendices

สถาบันวิทยบริการ
จุฬาลงกรณ์มหาวิทยาลัย

Appendix A

List of Abbreviations

AWGN	Additive White Gaussian Noise
BER	Bit Error Rate
BPM	Biphase Modulation
BW	Bandwidth
CDMA	Code Division Multiple Access
CM	Channel Model
DS	Direct Sequence
EIRP	Equivalent Isotropic Radiated Power
FB	Fractional Bandwidth
FCC	Federal Communications Commission
FIR	Finite-duration Impulse Response
IR-UWB	Impulse Radio Ultra-Wideband
LOS	Line Of Sight
MA	Multiple Access
MAI	Multiple Access Interference
MC-UWB	Multi-Carrier Ultra-Wideband
NBI	Narrow Band Interference
NLOS	Non Line Of Sight
OFDM	Orthogonal Frequency Division Multiplexing
OOK	On-Off Keying
PAM	Pulse-Amplitude Modulation
PDF	Probability Density Function
PN	Pseudo Noise
PPM	Pulse-Position Modulation
PSD	Power Spectrum Density
RF	Radio Frequency
RMS	Root Mean Square
SNR	Signal-to-Noise Ratio
TH	Time Hopping
TR	Transmitted Reference
UWB	Ultra-Wideband
WFNC	Weight Factor for Negative Correlation

Appendix B

Publications and Presentations

Wilaiporn Lee, Suwich Kunaruttanapruk and Somchai Jitapunkul,

“Optimum Pulse Shape Design for UWB Systems with Timing Jitter,” IEICE Transaction on Communication, Vol. E91-B, No. 3, pp. 772–783, March. 2008.

Wilaiporn Lee, Suwich Kunaruttanapruk and Somchai Jitapunkul,

“Performance evaluation of UWB systems using different order of Gaussian pulses,” Proceeding on IEEE International Conference on Signal Processing (ICSP 2006), Guilin, CHINA, 16 - 20 November 2006.



สถาบันวิทยบริการ
จุฬาลงกรณ์มหาวิทยาลัย

Vitae

Wilaiporn Lee was born in Sisaket, Thailand, in 1979. She earned the B.Eng. degree in electrical engineering from the Department of Electrical Engineering at the Khonkhan University, Thailand, in 2001 and the M.Eng. degree in electrical engineering from the Department of Electrical Engineering at the Chulalongkorn University, Thailand, in 2004. She is now working toward the Ph.D. degree in electrical engineering from Chulalongkorn University, Thailand. Her research areas are digital signal processing in wireless communication systems including MC-CDMA, UWB, etc.



สถาบันวิทยบริการ
จุฬาลงกรณ์มหาวิทยาลัย